中国科学技术大学
University of Science and Technology of China

Higgs combinations and EFT interpretations

Nan Lu
on behalf of ATLAS and CMS Collaborations

University of Science and Technology of China

Extended Scalar Sectors From All Angles Workshop

CERN Oct 21-25, 2024

Standard Model Higgs production at LHC

Gluon-fusion ggF (~87%)
48.5 pb

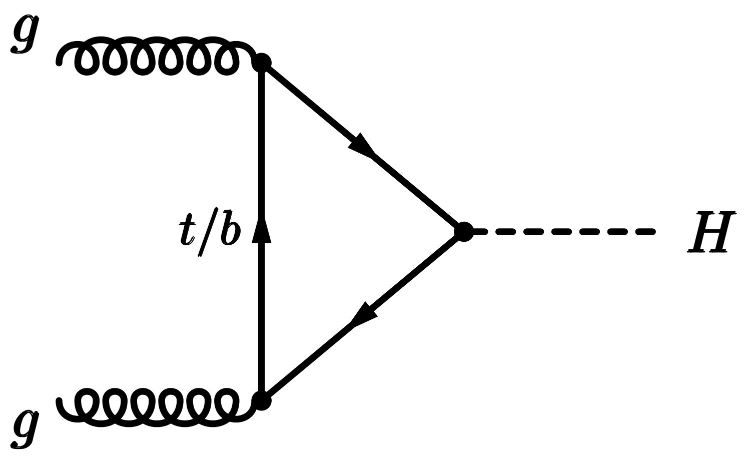

Vector boson fusion VBF (~7%):
3.78 pb

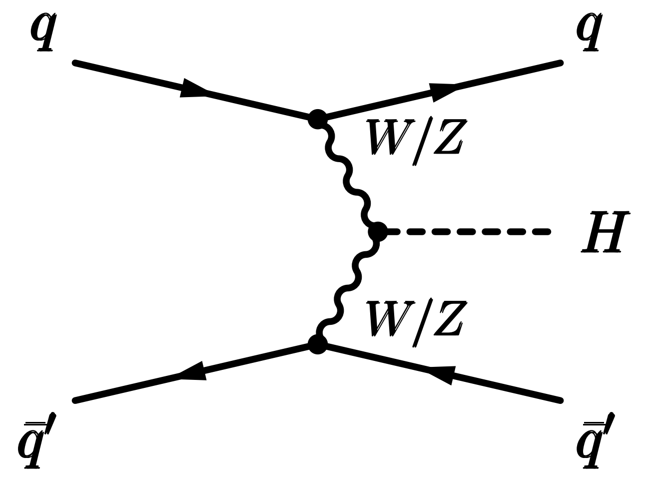

VH (~4%) ZH: 0.88 pb
WH: 1.37 pb

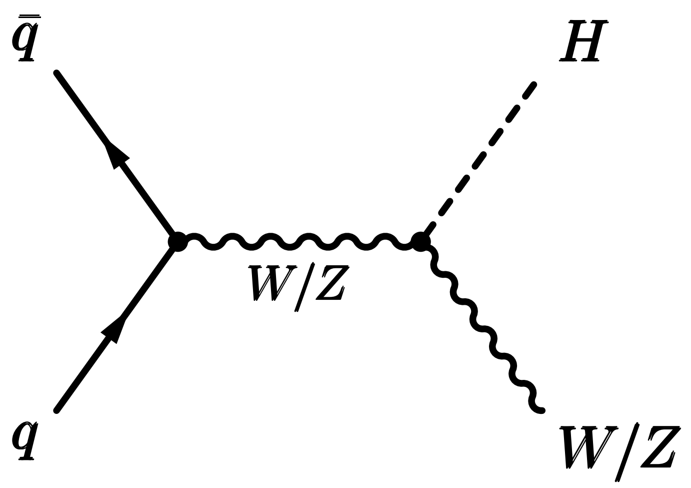

ttH (~1%), 0.51 pb

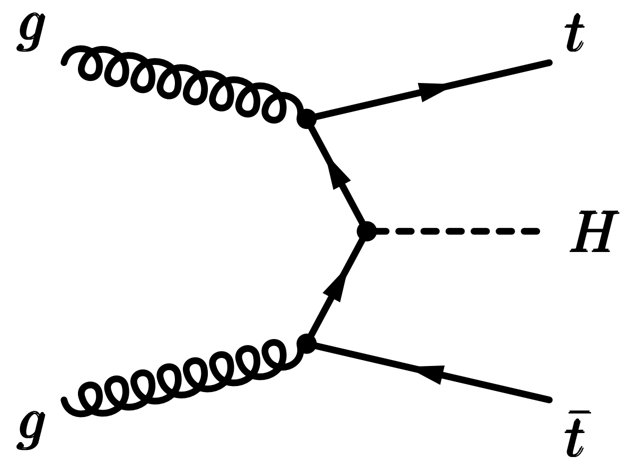

bbH (~1%), 0.49 pb

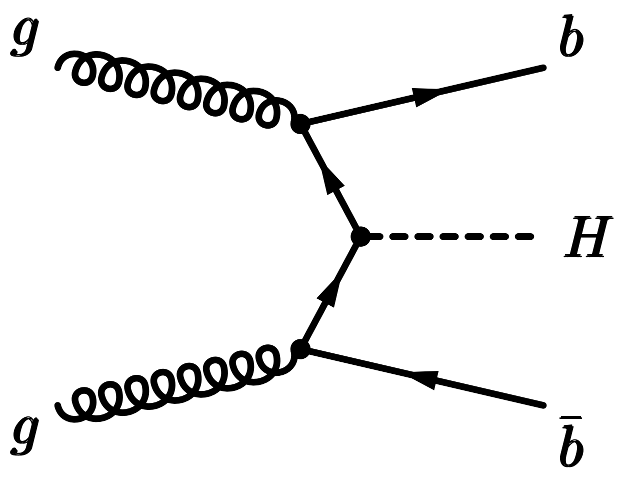

single top tH (~0.1%), 0.09 pb

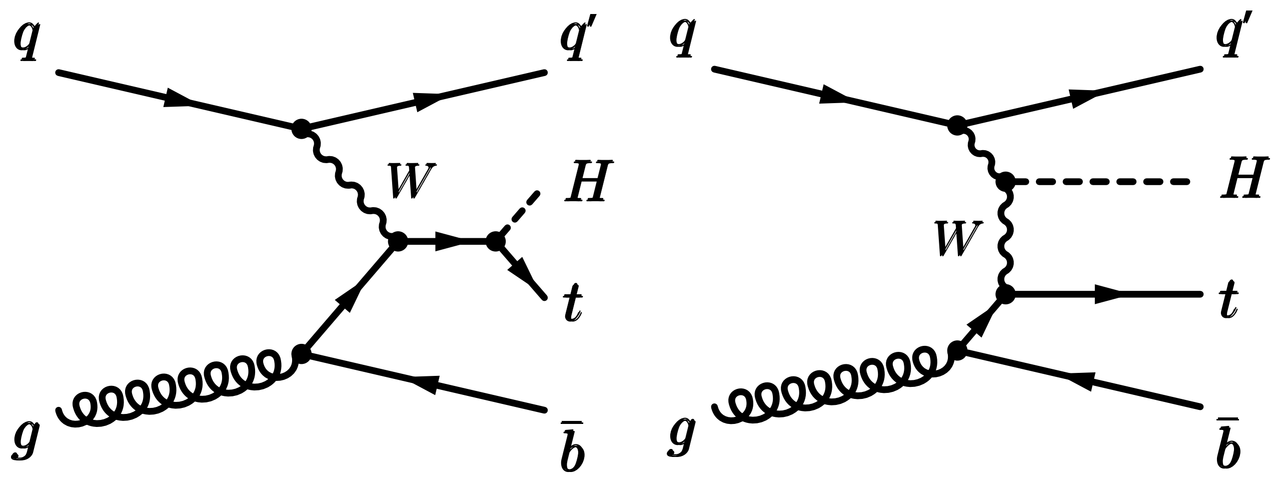

* Cross-sections @ $\sqrt{s} = 13$ TeV

Run 1: 7-8 TeV
pp collisions
Run 3: 13.6 TeV
Run 2: 13 TeV

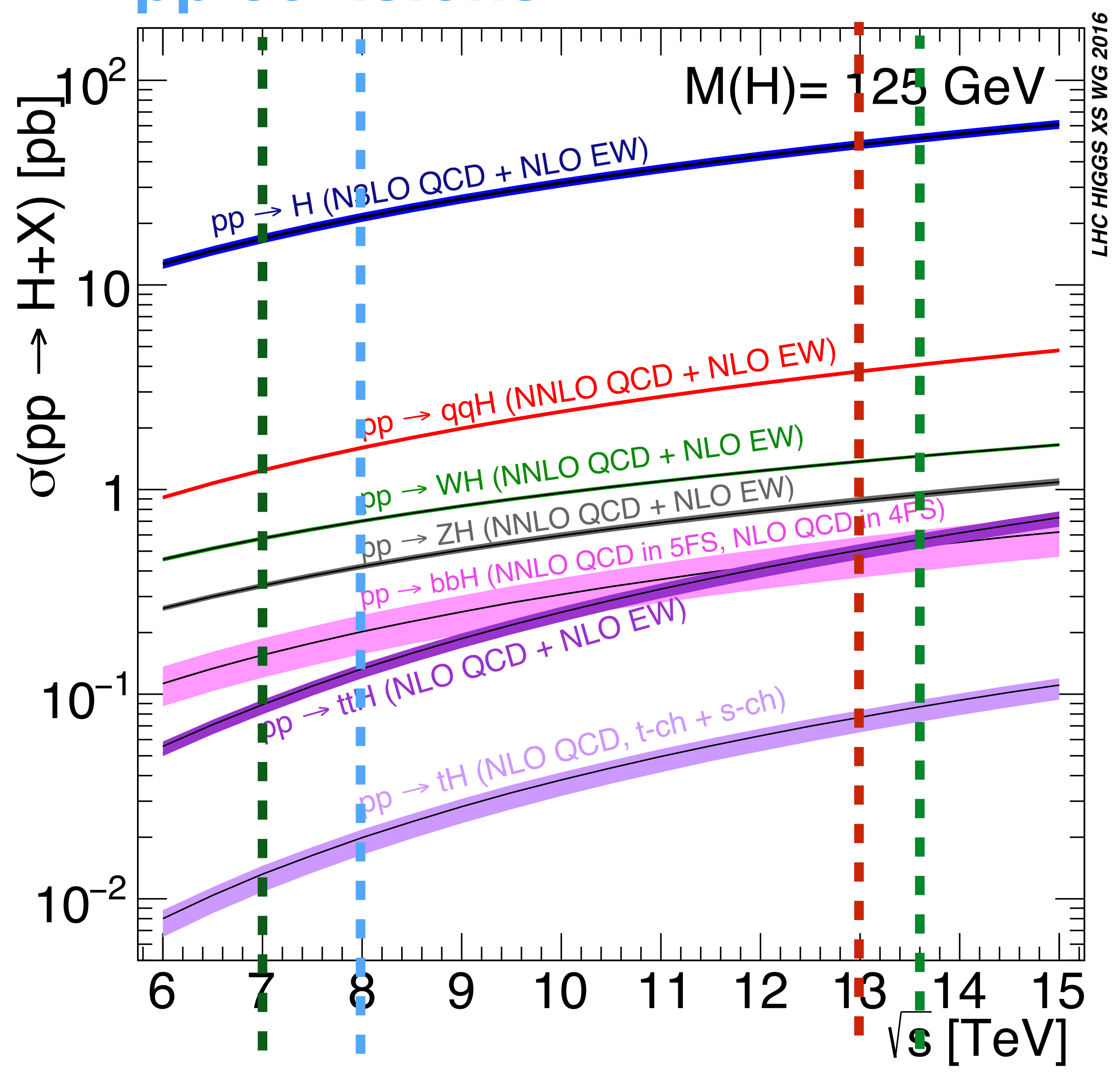

Yellow Report 4

- Distinct topology in each production mechanism

Higgs boson decays

- **"Big five"**: **γγ, ZZ, WW, ττ, bb**
  - γγ and ZZ→4l: high resolution and S/B: precise mass and differential measurement
  - WW→μνeν: high BR, low S/B, low resolution due to neutrinos
  - **ττ, bb:** high BR, low S/B, **directly probe Higgs couplings to fermions**
- **Rare decay channels to be observed: μμ, Zγ, cc, …**

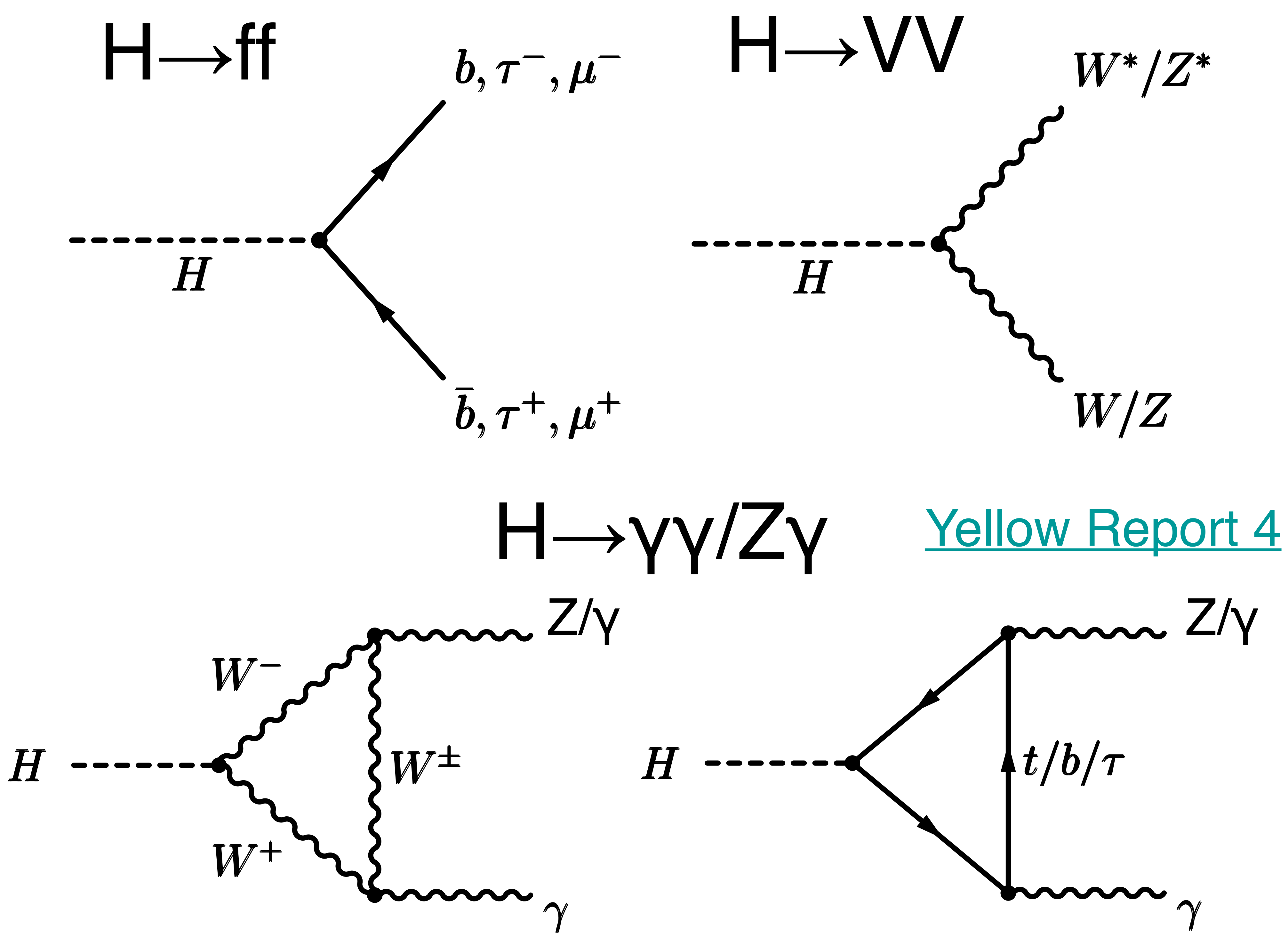

[Yellow Report 4]

Decay channel	SM BR [%] with m_H=125.09 GeV
H→bb	58.1
H→WW	21.5
H→ττ	6.26
H→ZZ	2.64
H→γγ	0.23
H→μμ	0.022
H→Zγ	0.154
H→cc	2.88
H→gg	8.18

Measurement of Higgs boson mass

Phys. Lett. B 847 (2023) 138315

- H→ZZ*→4l and H→γγ are used to measure Higgs boson mass: fully reconstructed with high resolution

H→ZZ*→4l mass distribution

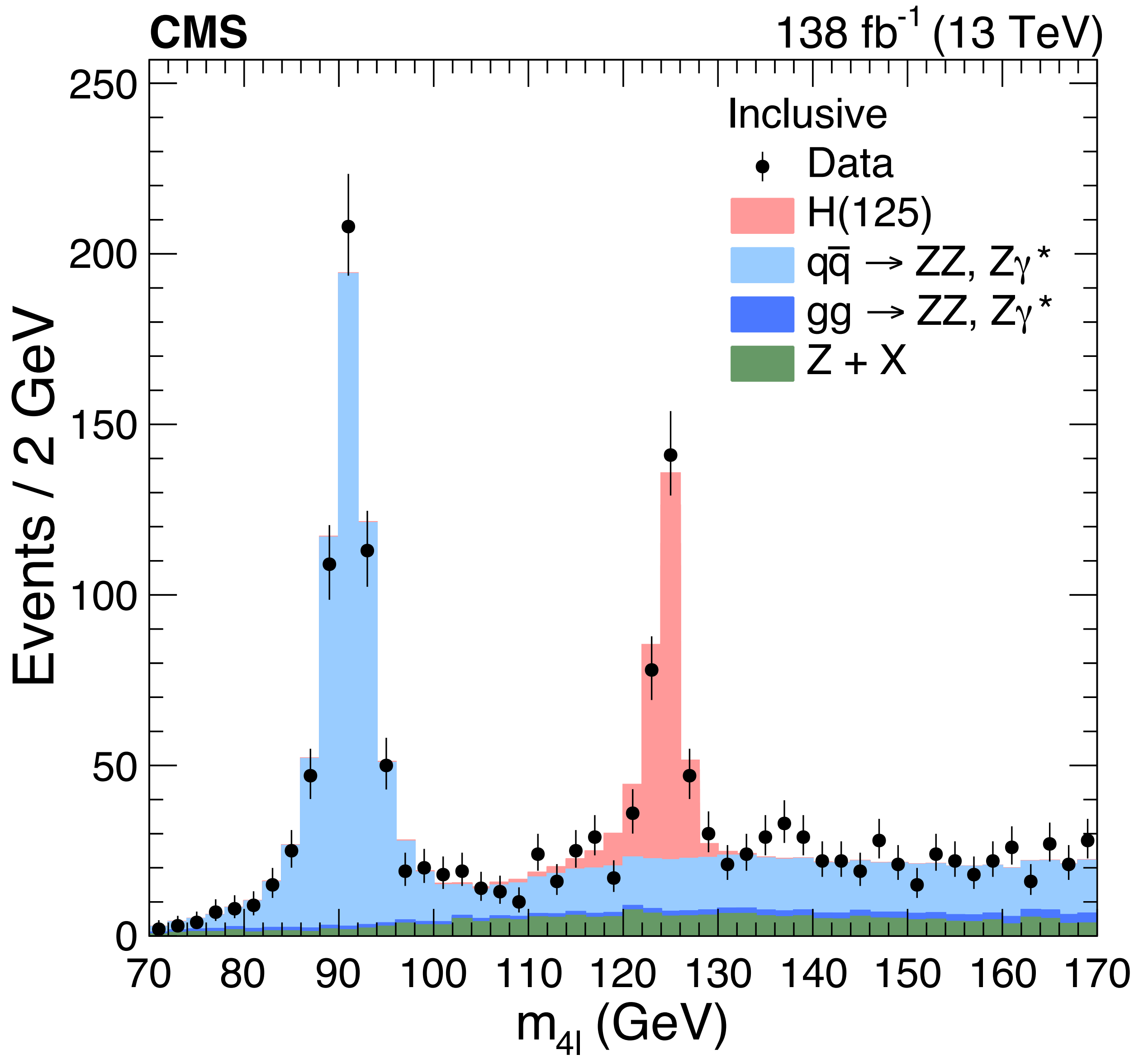

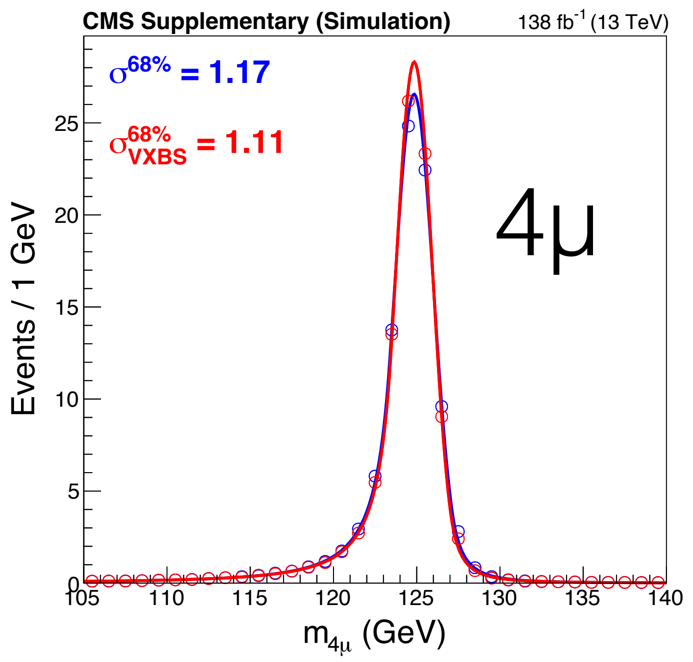

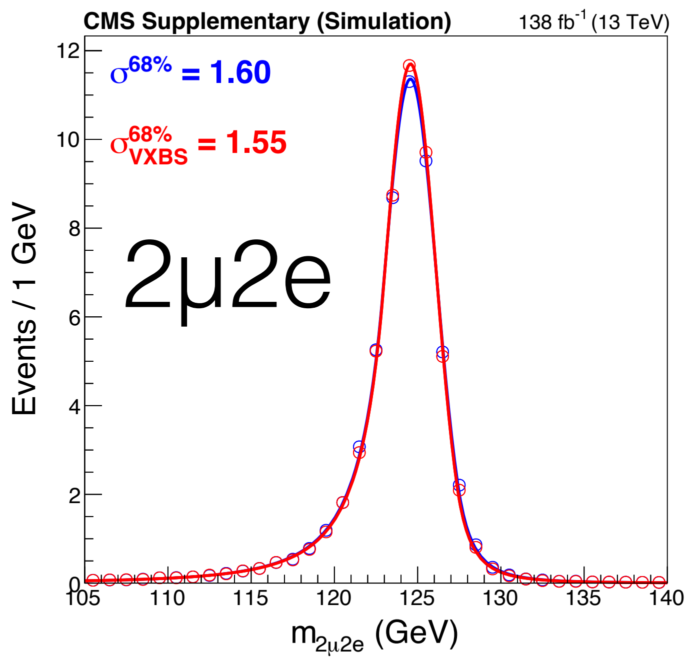

H→γγ mass distribution

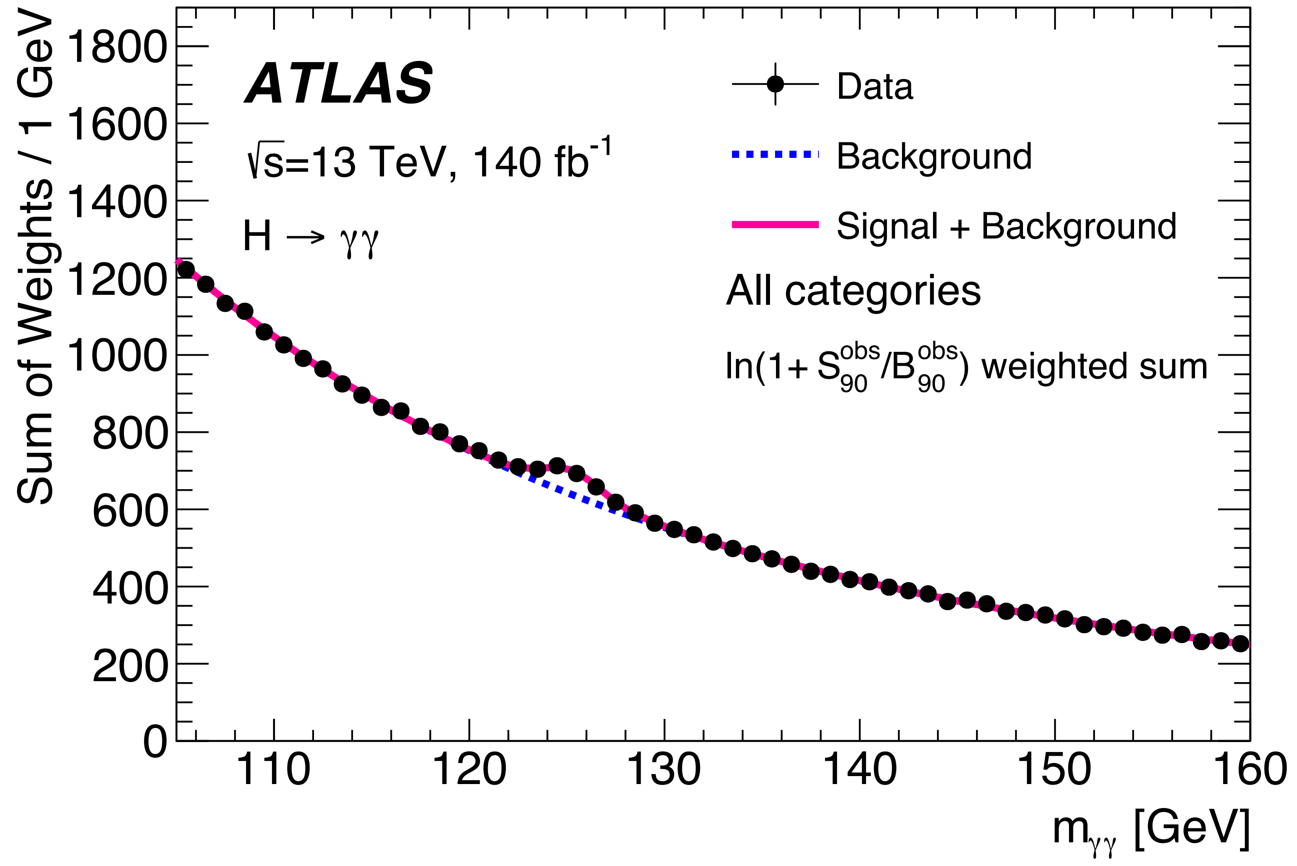

$m_{\gamma\gamma}$ in categories with the best and worst experimental resolutions categories

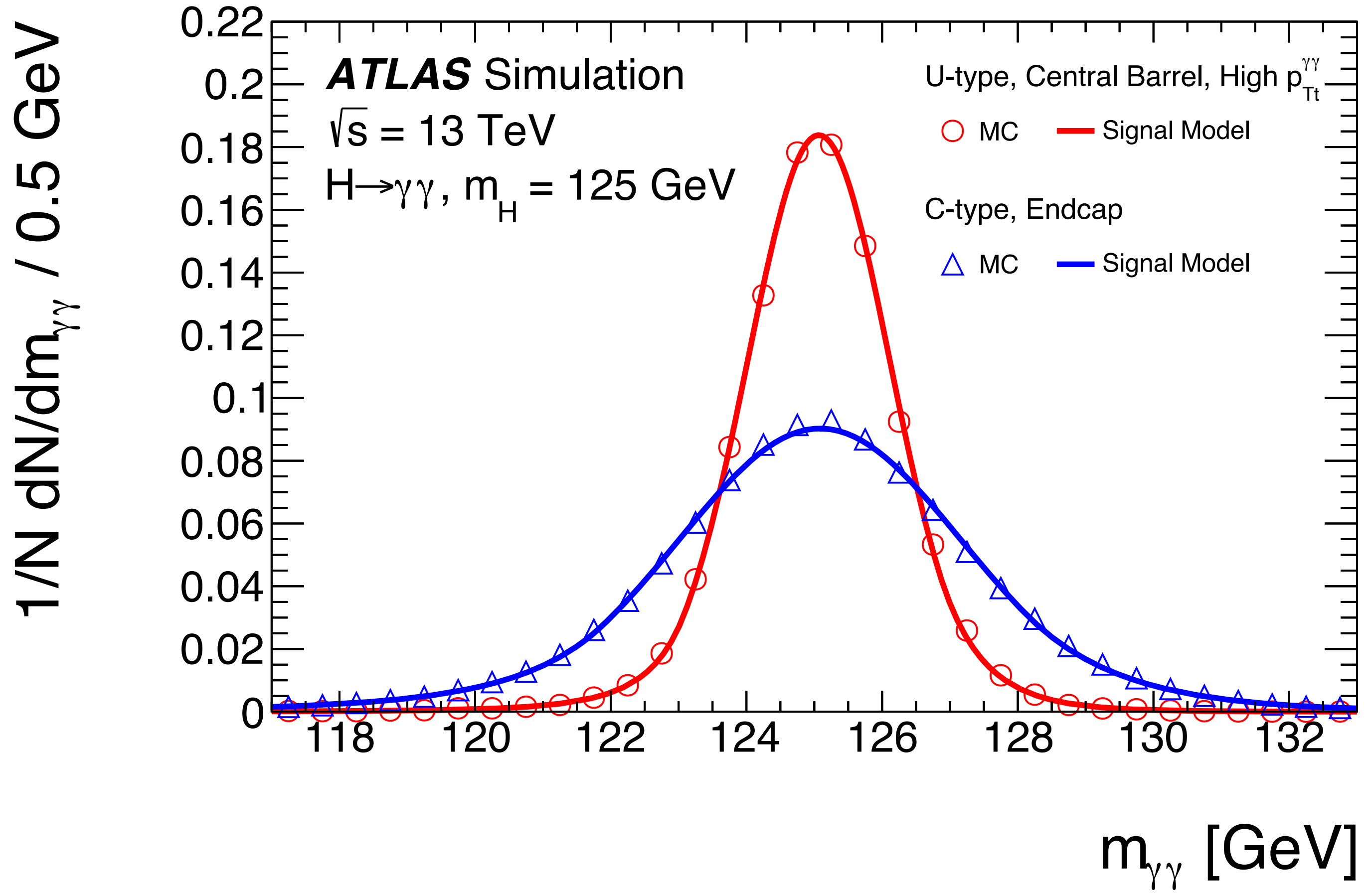

Measurement of Higgs boson mass

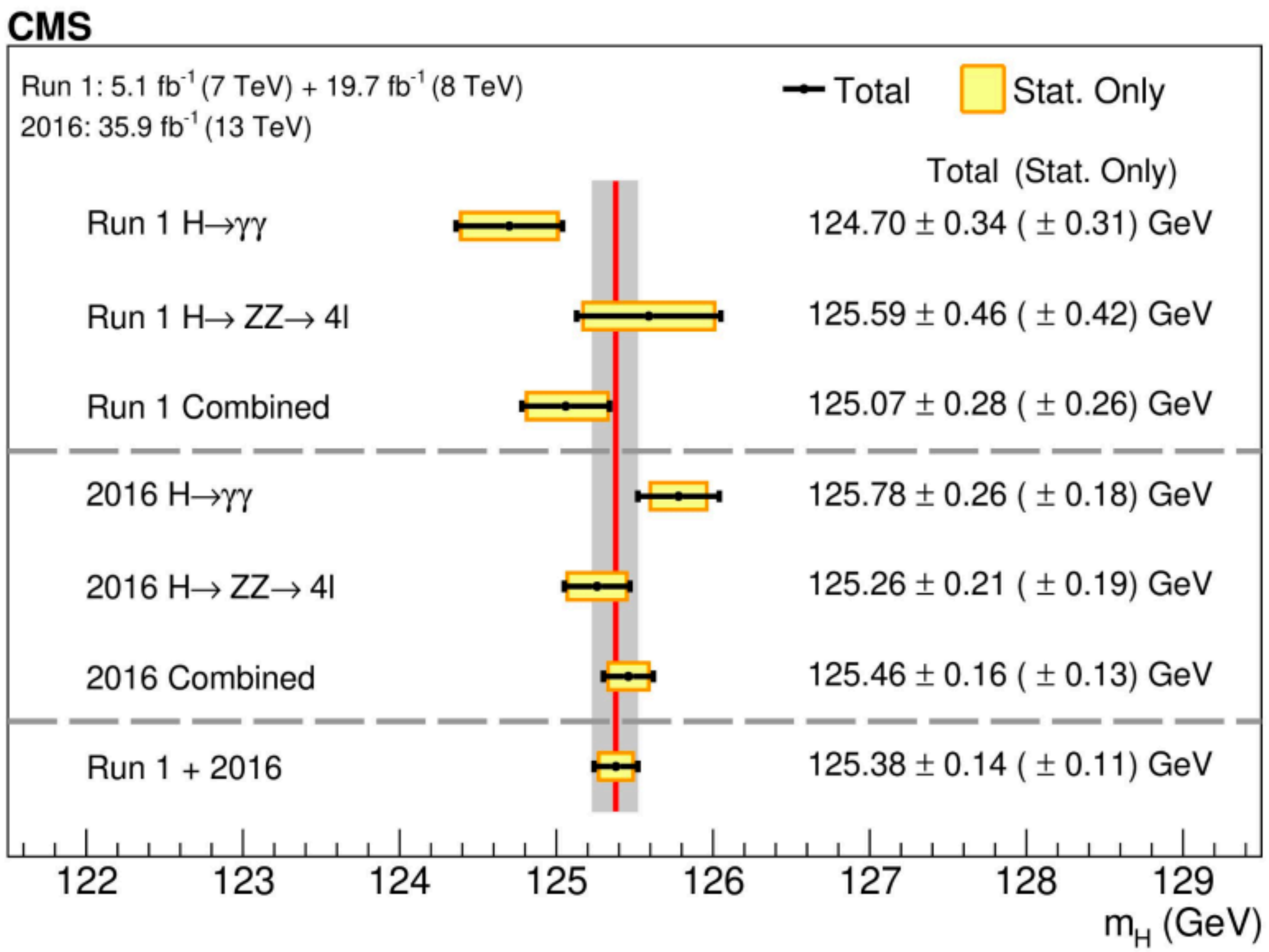

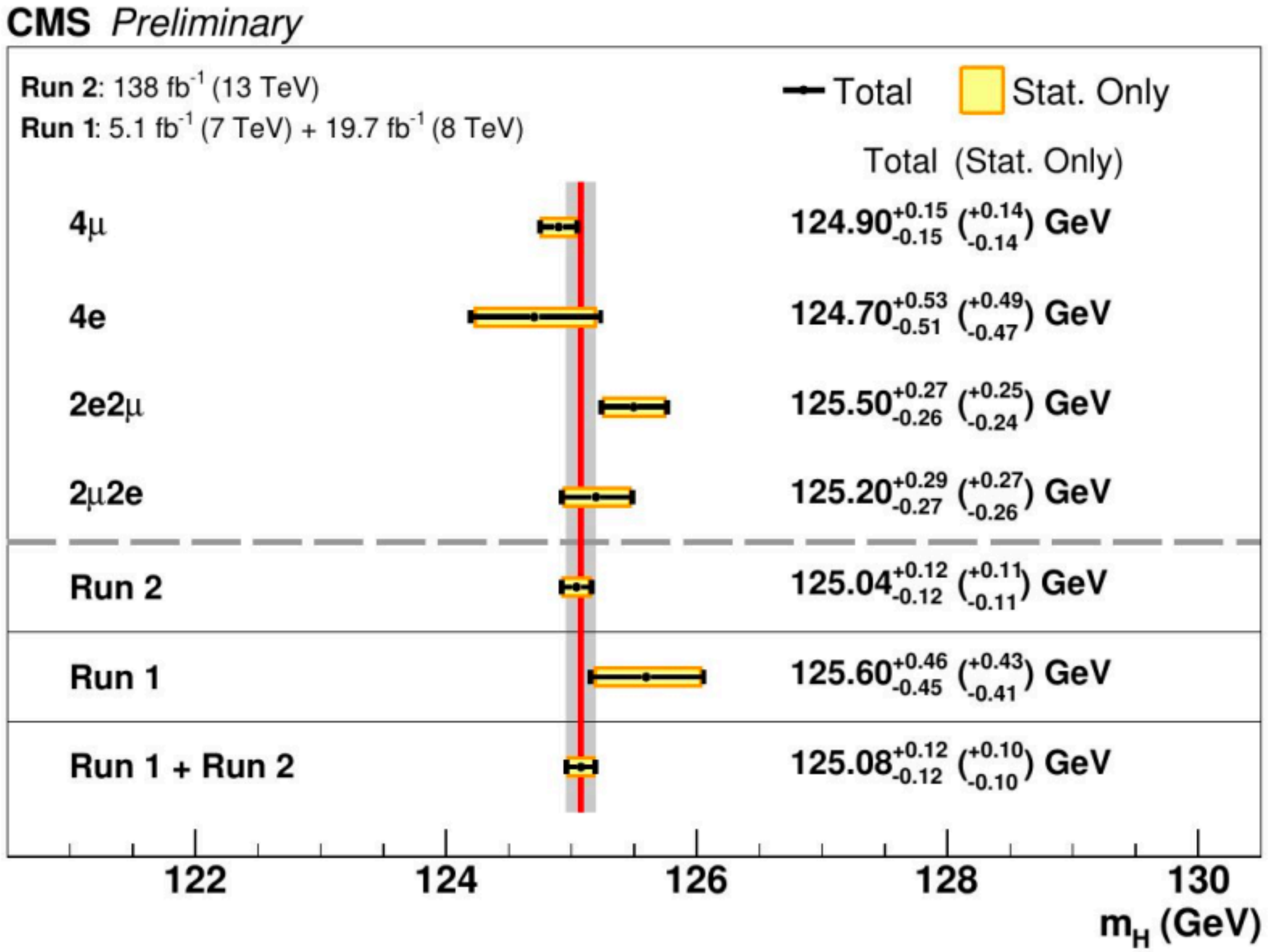

- Using two high resolution channels: $H\to\gamma\gamma$ & $H\to ZZ^*\to 4l$
  - CMS+ATLAS Run1 combination: **m_H = 125.09 ± 0.24 GeV**
  - CMS: $H\to\gamma\gamma$ & $H\to ZZ^*\to 4l$ Run1 + 2016 data: **m_H = 125.38 ± 0.12 (±0.10 Stat. only) GeV**
  - CMS: $H\to ZZ^*\to 4l$ Run 1+ Run 2 data: **m_H = 125.08 ± 0.14 (±0.11 Stat. only) GeV**
- Combined measurement still dominated by statistical uncertainty

Phys. Lett. B 805 (2020) 135425
Phys. Rev. Letters 131 (2023) 251802
Phys. Lett. B 843 (2023) 137880
HIG-21-019, submitted to PRD

Measurement of Higgs boson mass

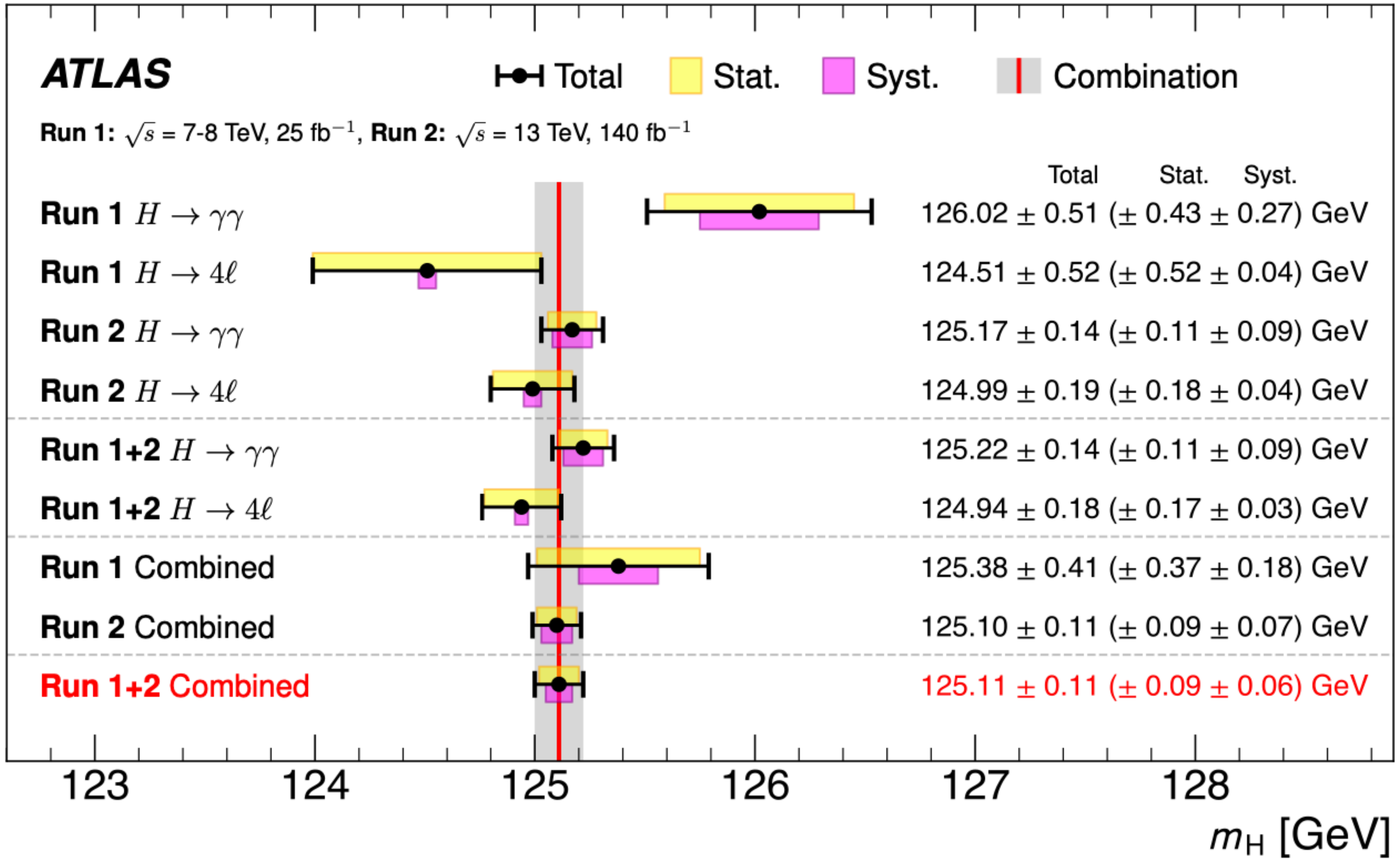

Phys. Lett. B 805 (2020) 135425
Phys. Rev. Letters 131 (2023) 251802
Phys. Lett. B 843 (2023) 137880
HIG-21-019, submitted to PRD

- Using two high resolution channels: H→γγ & H→ZZ*→4l
  - CMS+ATLAS Run1 combination: **m_H = 125.09 ± 0.24 GeV**
  - ATLAS Run 1 + Run 2 data: $m_H = 125.11 \pm 0.09(Stats.) \pm 0.06(Sys.)$ **GeV**
- Combined measurement still dominated by statistical uncertainty

Input channels to ATLAS and CMS combined measurements of Higgs boson couplings in Run 2

ATLAS: Nature 607, 52–59 (2022)

Decay mode	Targeted production processes	$\mathcal{L}$ [fb^{-1}]	Ref.	Fits deployed in
$H \to \gamma\gamma$	ggF, VBF, $WH, ZH, t\bar{t}H, tH$	139	[31]	All
$H \to ZZ$	ggF, VBF, $WH+ZH, t\bar{t}H+tH$	139	[28]	All
	$t\bar{t}H+tH$ (multilepton)	36.1	[39]	All but fit of kinematics
$H \to WW$	ggF, VBF	139	[29]	All
	WH, ZH	36.1	[30]	All but fit of kinematics
	$t\bar{t}H+tH$ (multilepton)	36.1	[39]	All but fit of kinematics
$H \to Z\gamma$	inclusive	139	[32]	All but fit of kinematics
$H \to b\bar{b}$	WH, ZH	139	[33, 34]	All
	VBF	126	[35]	All
	$t\bar{t}H+tH$	139	[36]	All
	inclusive	139	[37]	Only for fit of kinematics
$H \to \tau\tau$	ggF, VBF, $WH+ZH, t\bar{t}H+tH$	139	[38]	All
	$t\bar{t}H+tH$ (multilepton)	36.1	[39]	All but fit of kinematics
$H \to \mu\mu$	ggF + $t\bar{t}H+tH$, VBF + $WH+ZH$	139	[40]	All but fit of kinematics
$H \to c\bar{c}$	$WH+ZH$	139	[41]	Only for free-floating κ_c
$H \to$ invisible	VBF	139	[42]	κ models with $B_{u.}$ & $B_{inv.}$
	ZH	139	[43]	κ models with $B_{u.}$ & $B_{inv.}$

CMS: Nature 607, 60–68 (2022)

Analysis	Decay tags	Production tags
Single Higgs boson production		
$H \to \gamma\gamma$ [42]	$\gamma\gamma$	ggH, $p_T(H) \times N_j$ bins VBF/VH hadronic, $p_T(Hjj)$ bins WH leptonic, $p_T(V)$ bins ZH leptonic ttH $p_T(H)$ bins, tH
$H \to ZZ \to 4\ell$ [43]	4μ, $2e2\mu$, 4e	ggH, $p_T(H) \times N_j$ bins VBF, m_{jj} bins VH hadronic VH leptonic, $p_T(V)$ bins ttH
$H \to WW \to \ell\nu\ell\nu$ [44]	$e\mu/ee/\mu\mu$ $\mu\mu$+jj/ee+jj/$e\mu$+jj 3ℓ 4ℓ	ggH $\leq$ 2-jets VBF VH hadronic WH leptonic ZH leptonic
$H \to Z\gamma$ [45]	$Z\gamma$	ggH VBF
$H \to \tau\tau$ [46]	$e\mu, e\tau_h, \mu\tau_h, \tau_h\tau_h$	ggH, $p_T(H) \times N_j$ bins VH hadronic VBF
$H \to bb$ [47–51]	$W(\ell\nu)H(bb)$ $Z(\nu\nu)H(bb)$, $Z(\ell\ell)H(bb)$ bb	VH, high-$p_T(V)$ WH leptonic ZH leptonic ttH, $\to 0, 1, 2\ell$ + jets ggH, high-$p_T(H)$ bins
$H \to \mu\mu$ [52]	$\mu\mu$	ggH VBF
ttH production with $H \to$ leptons [53]	2ℓSS, 3ℓ, 4ℓ, $1\ell+\tau_h$, 2ℓSS+$1\tau_h$, $3\ell+1\tau_h$	ttH
$H \to$ Inv. [71, 72]	p_T^{miss}	ggH VBF VH hadronic ZH leptonic
Higgs boson pair production		
$HH \to bbbb$ [57, 58]	H(bb)H(bb)	ggHH, VBFHH (resolved, boosted)
$HH \to bb\tau\tau$ [59]	$H(bb)H(\tau\tau)$	ggHH, VBFHH
$HH \to$ leptons [60]	H(WW)H(WW), $H(WW)H(\tau\tau)$, $H(\tau\tau)H(\tau\tau)$	ggHH, VBFHH
$HH \to bb\gamma\gamma$ [61]	$H(bb)H(\gamma\gamma)$	ggHH, VBFHH
$HH \to bbZZ$ [62]	H(bb)H(ZZ)	ggHH

Input channels for couplings and STXS combination

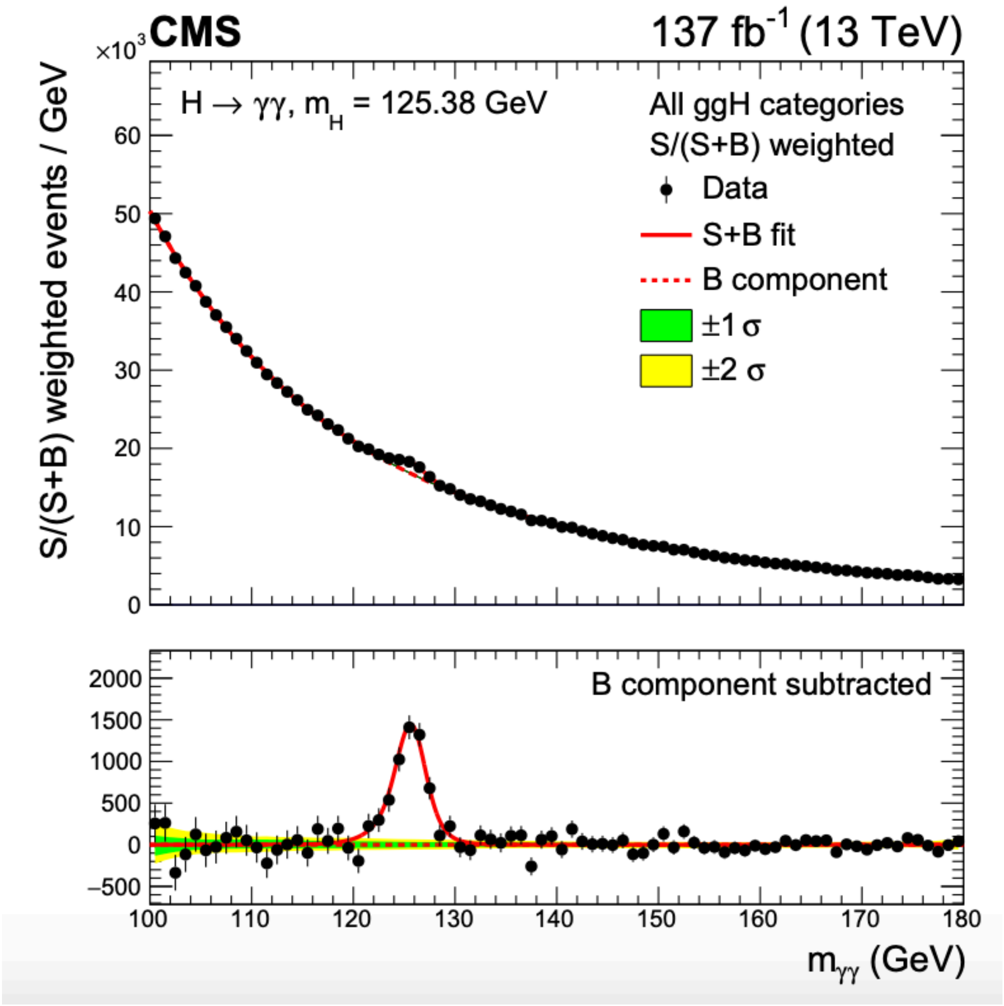

H→γγ

JHEP 07 027(2021)

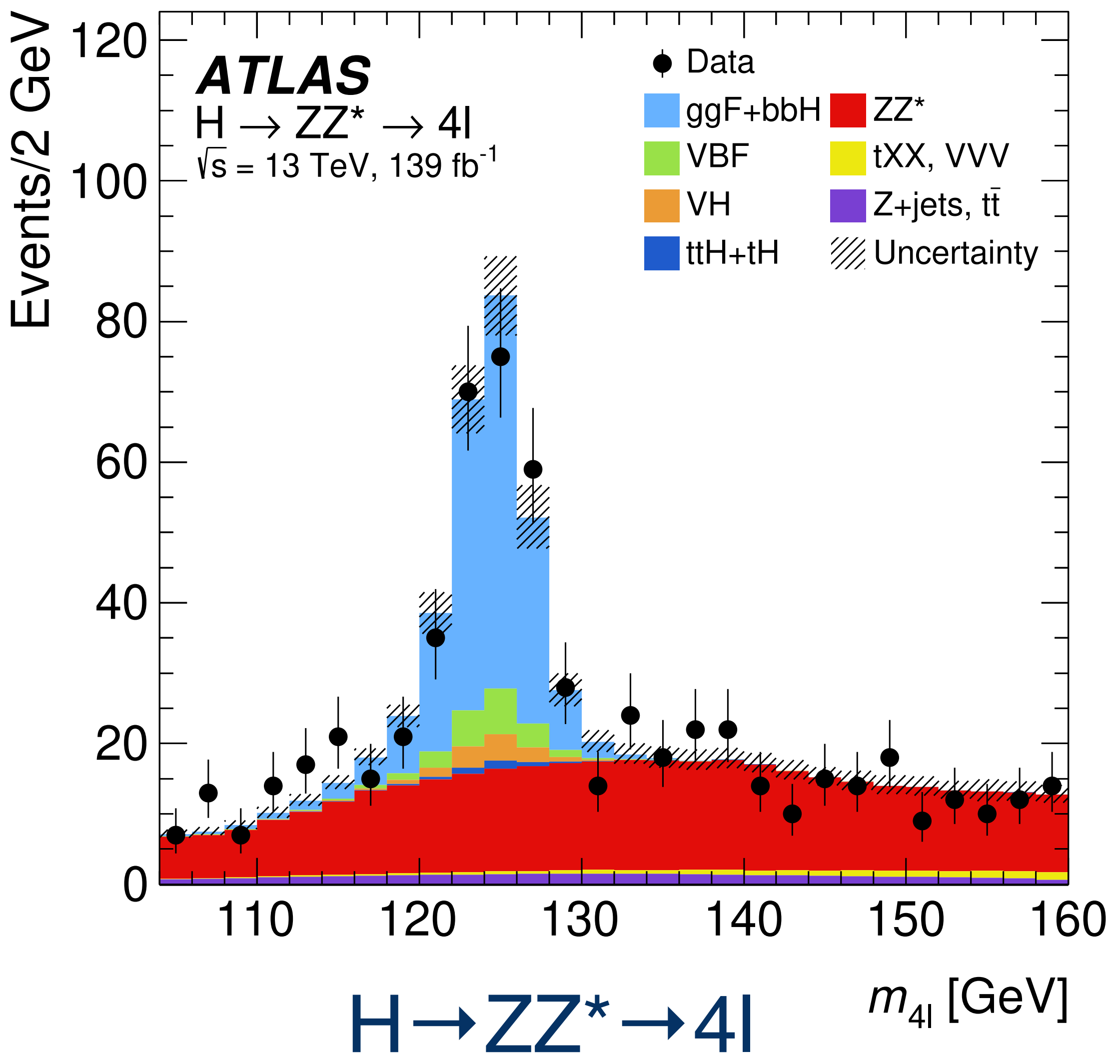

H→ZZ*→4l

EPJC 80 (2020) 957

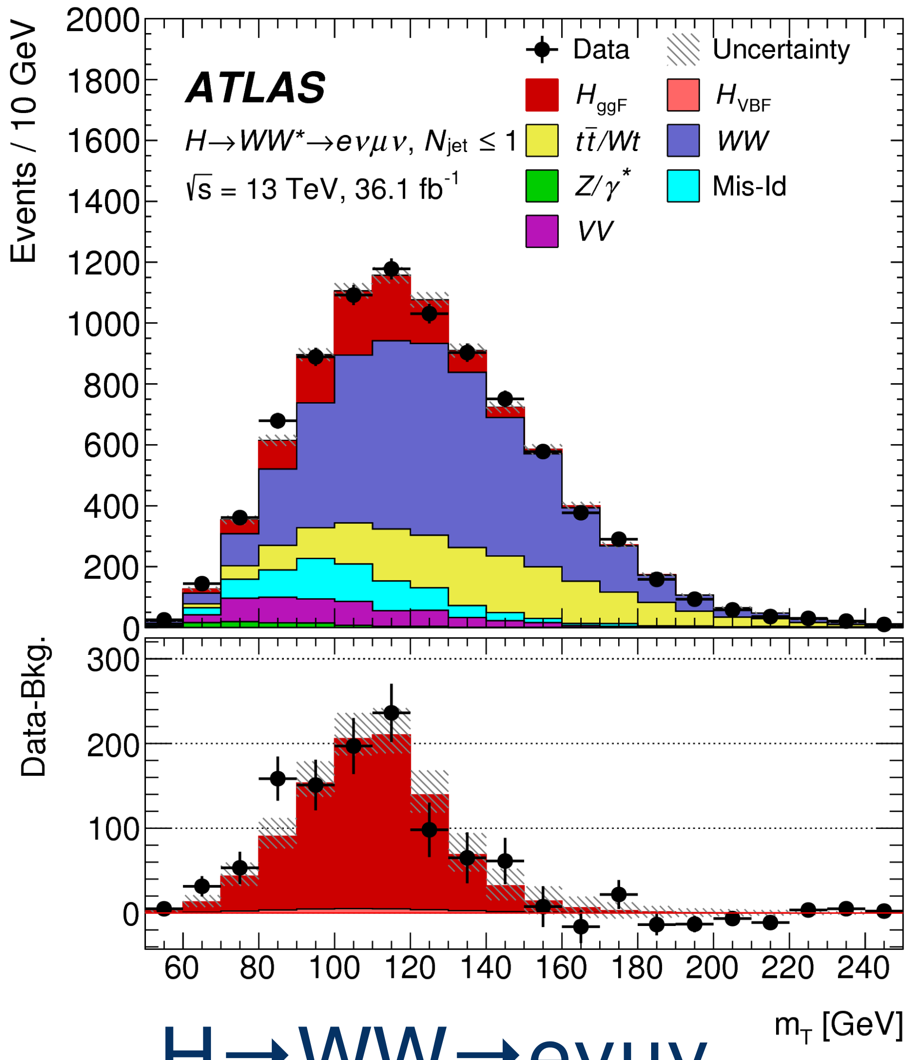

H→WW→eνμν

PLB 789 (2019) 508

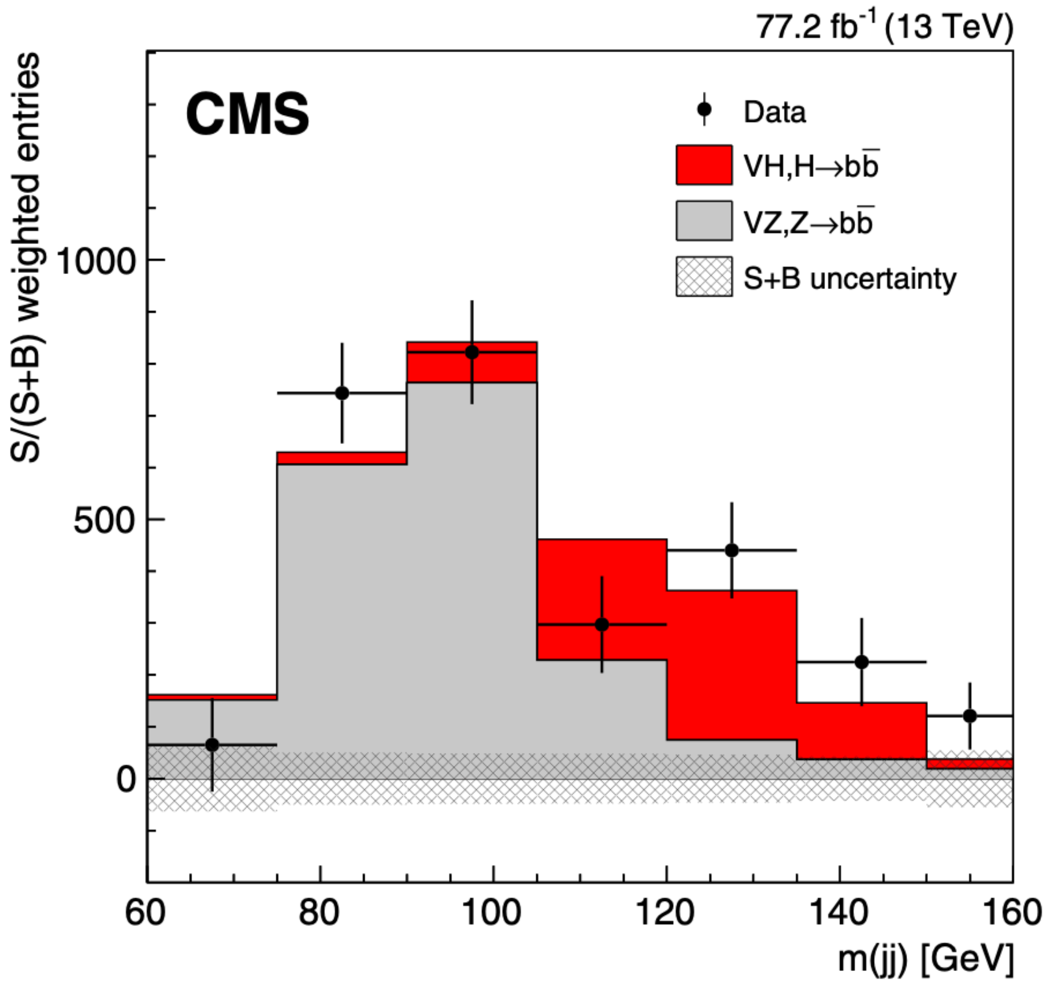

VH, H→bb

PRL 121 121801

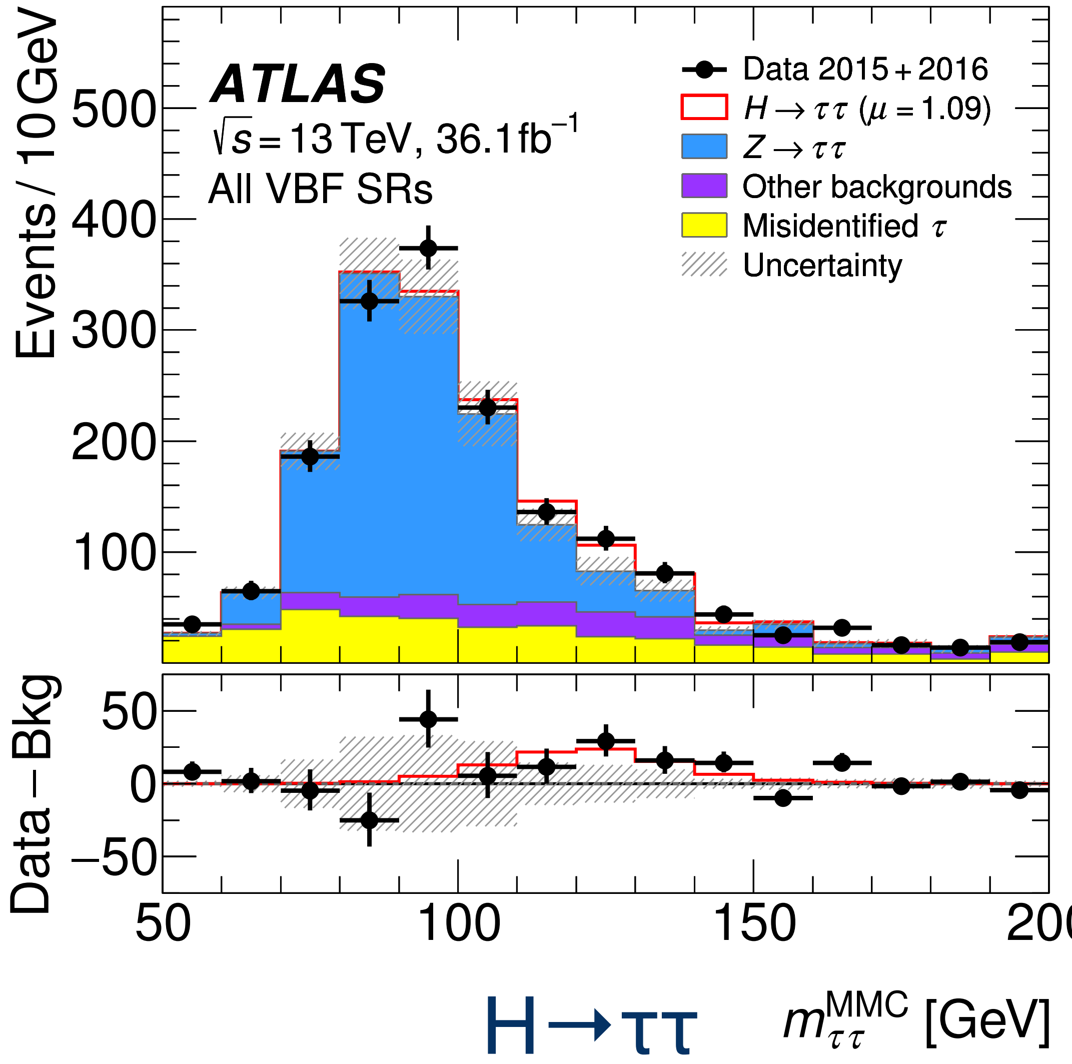

H→ττ

PRD 99 (2019) 072001

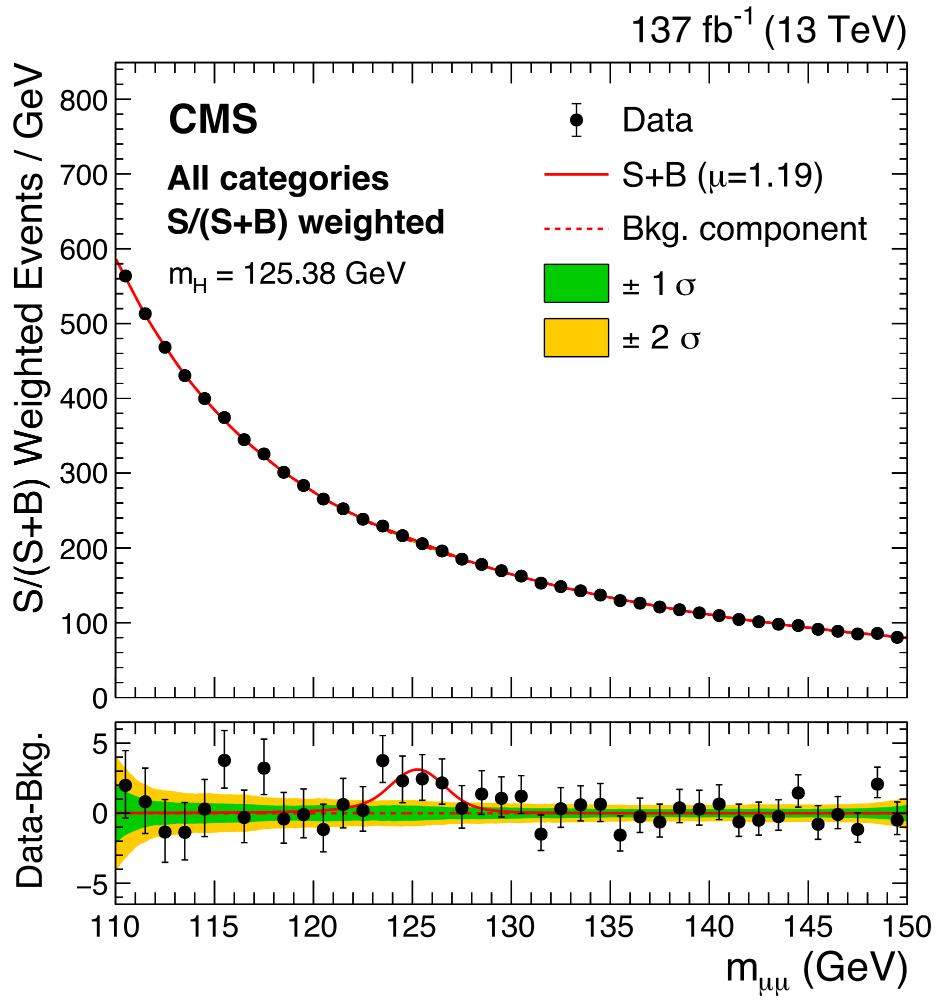

H→μμ

JHEP 01 (2021) 148

Input channels for couplings and STXS combination

ttH multi-lepton (H→ZZ, WW, ττ)
PRD 97 (2018) 072003

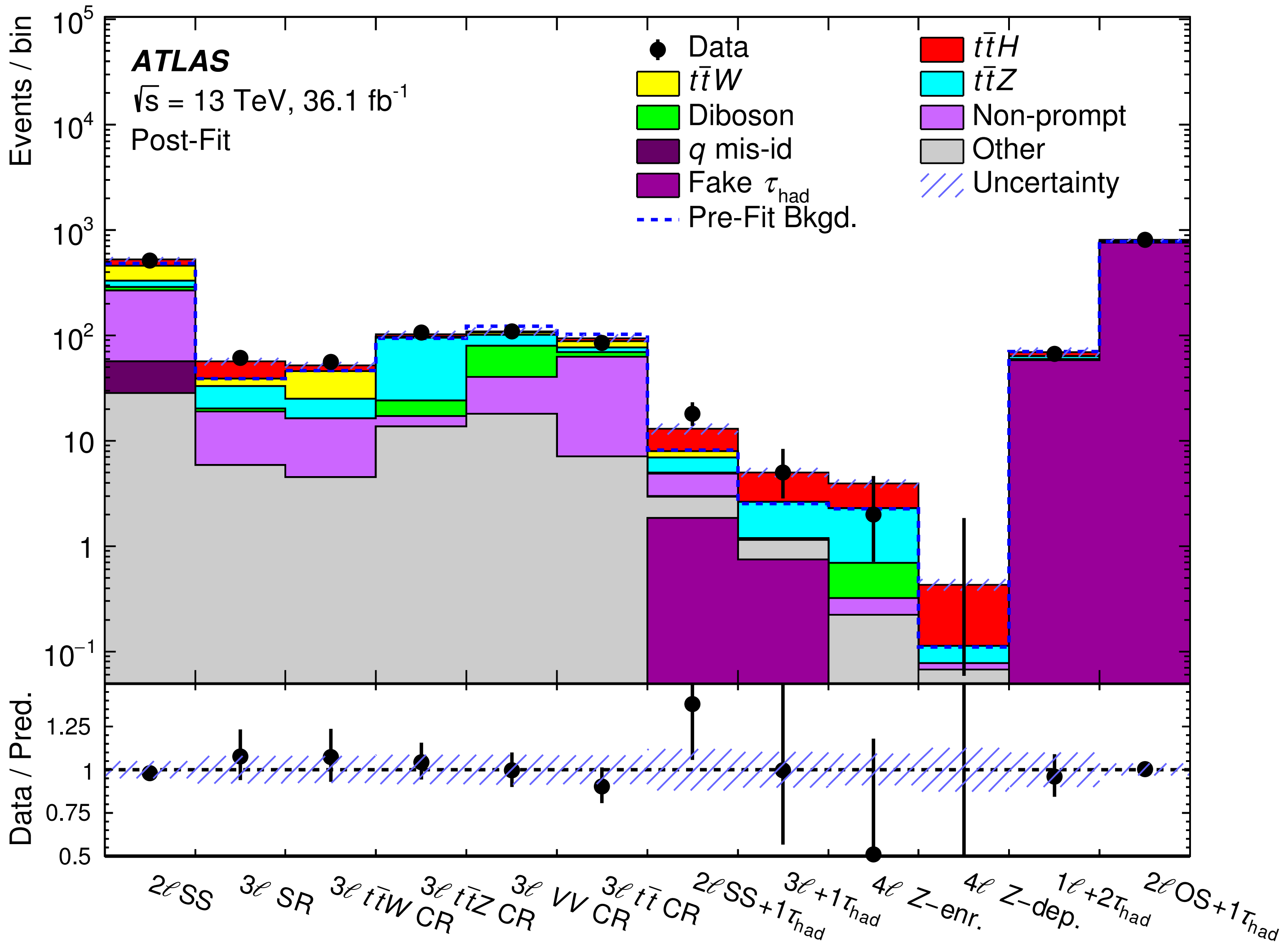

ttH, H→bb
PRD 97 (2018) 072016

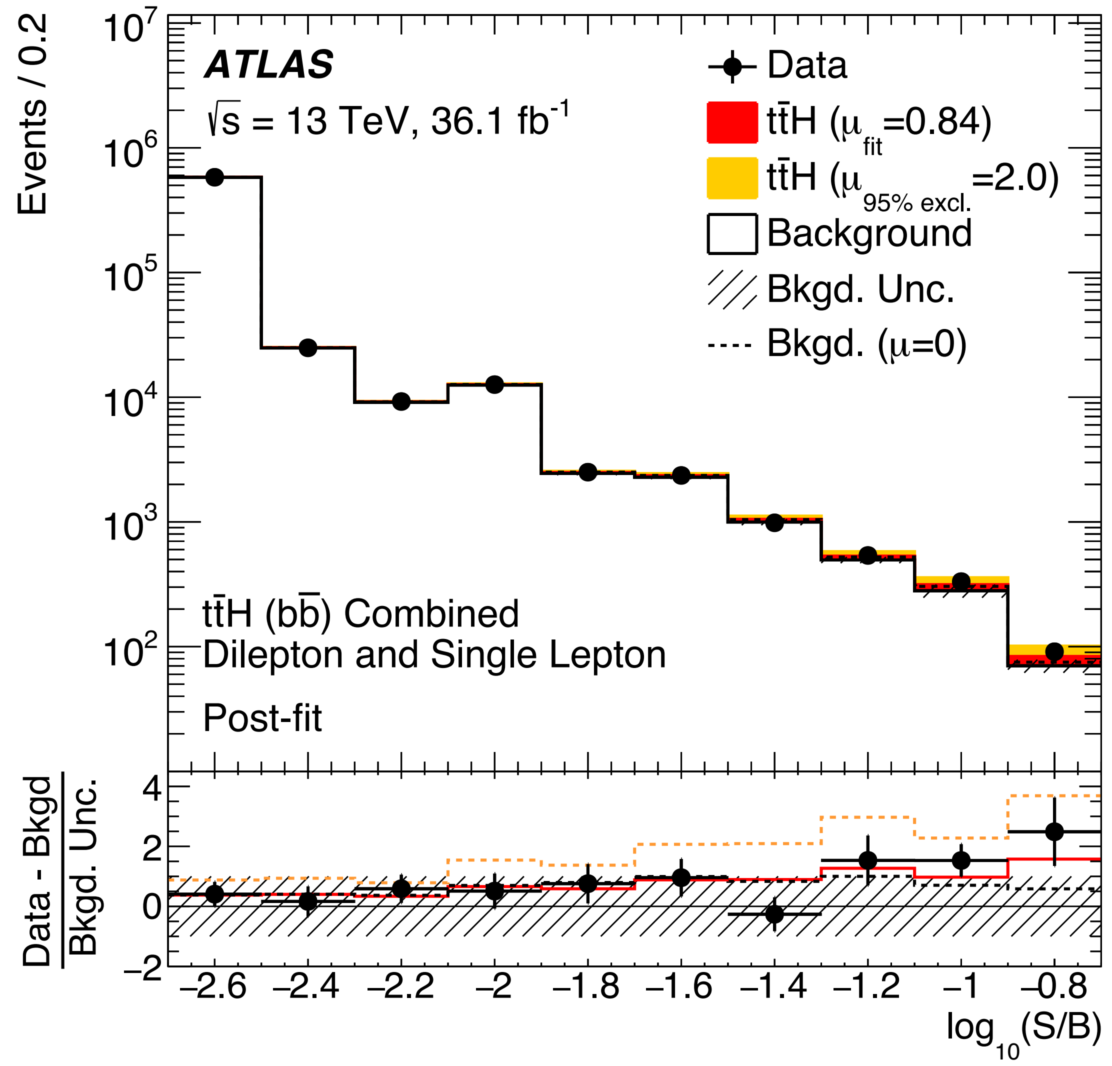

H→Zγ
JHEP 01 (2021) 148

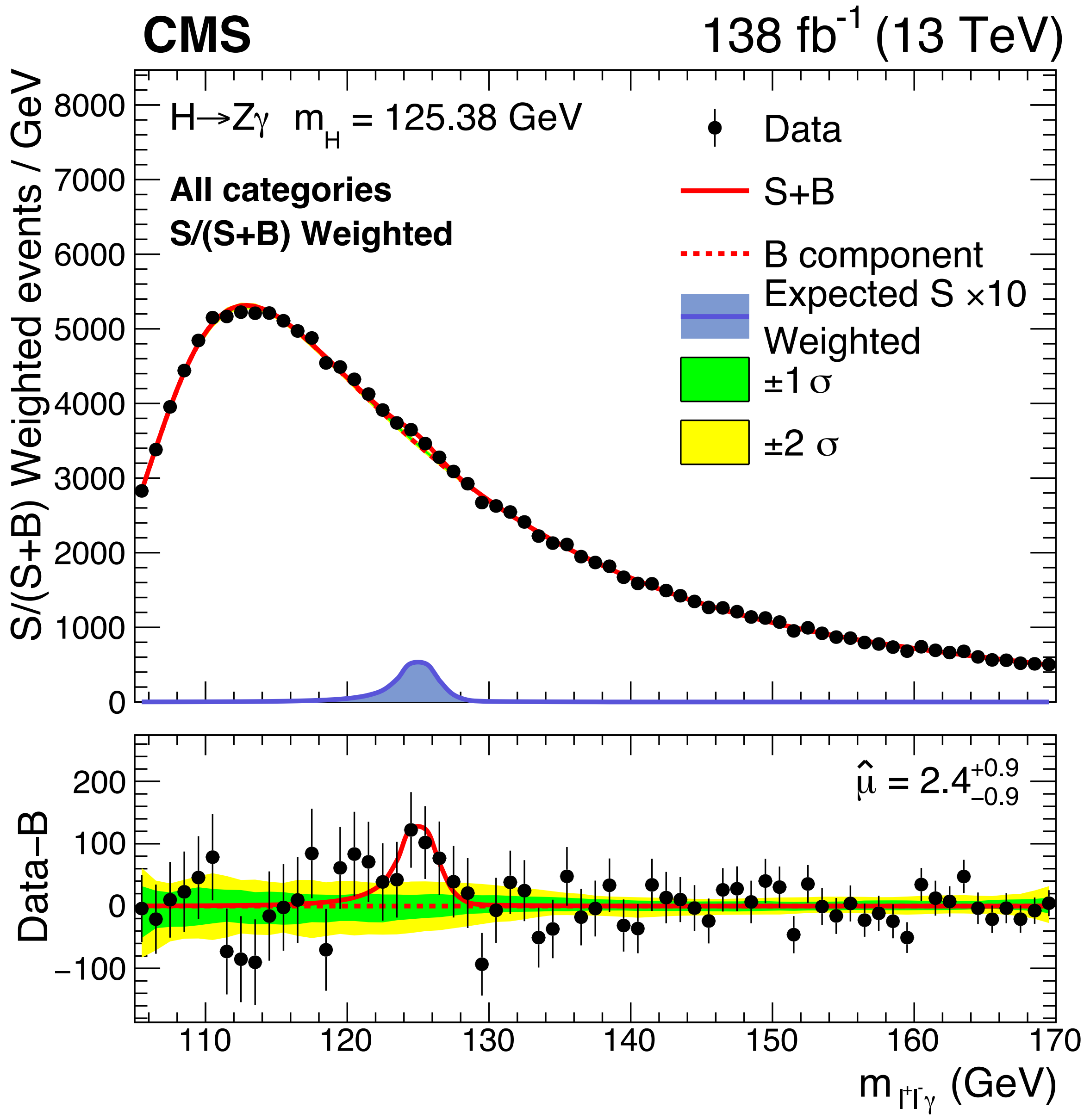

boosted H→bb
Phys. Rev. Lett. 120, 071802

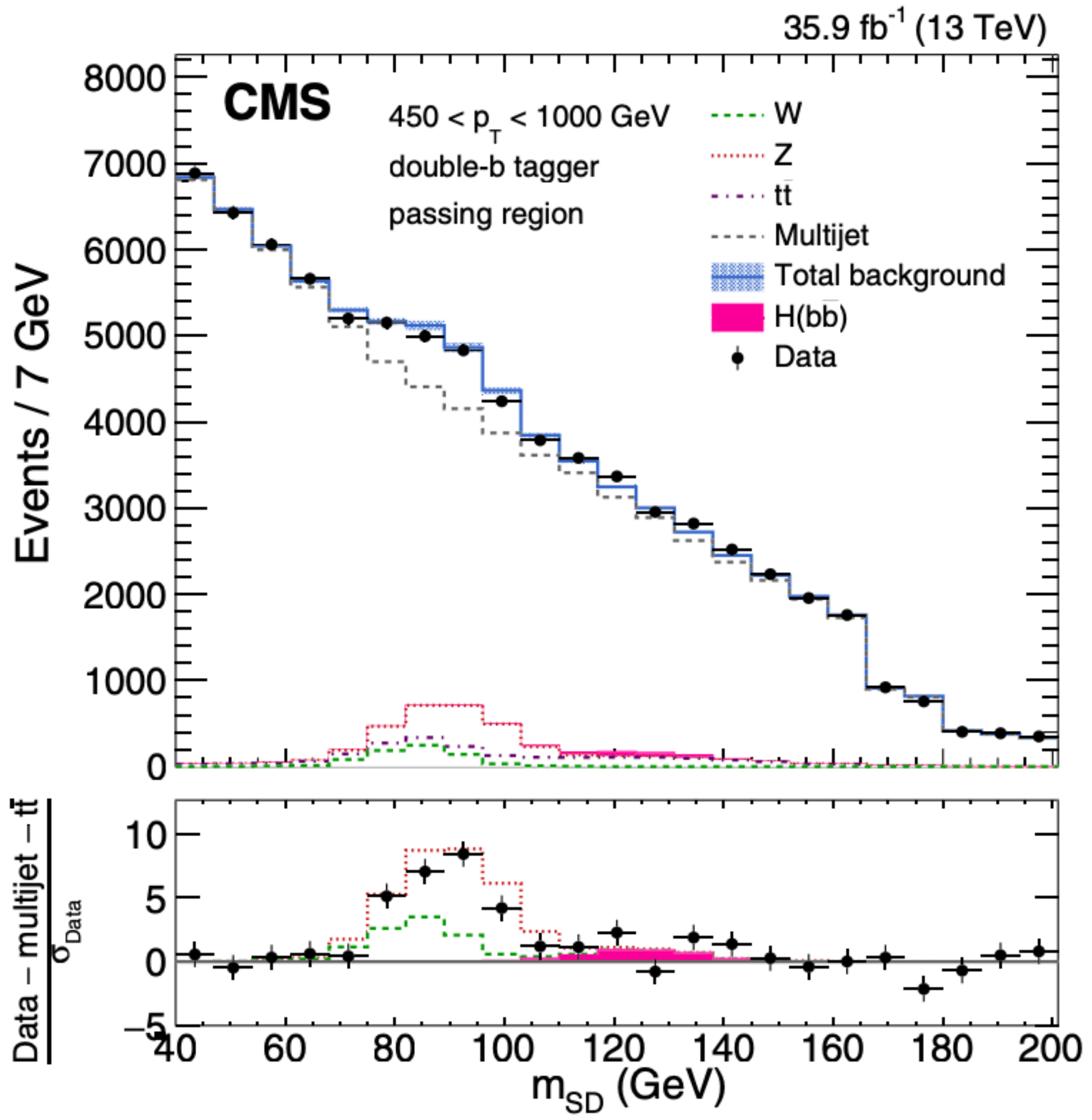

Higgs boson production and decay rates

Signal strength: **μ = N$_{signal}$(obs.)/N$_{signal}$(exp.)**

Nature 607, 52–59 (2022)

Inclusive signal strength:

$$\mu = 1.05 \pm 0.06 = 1.05 \pm 0.03(\text{stat.}) \pm 0.03(\text{exp.}) \pm 0.04(\text{sig. th.}) \pm 0.02(\text{bkg. th.})$$

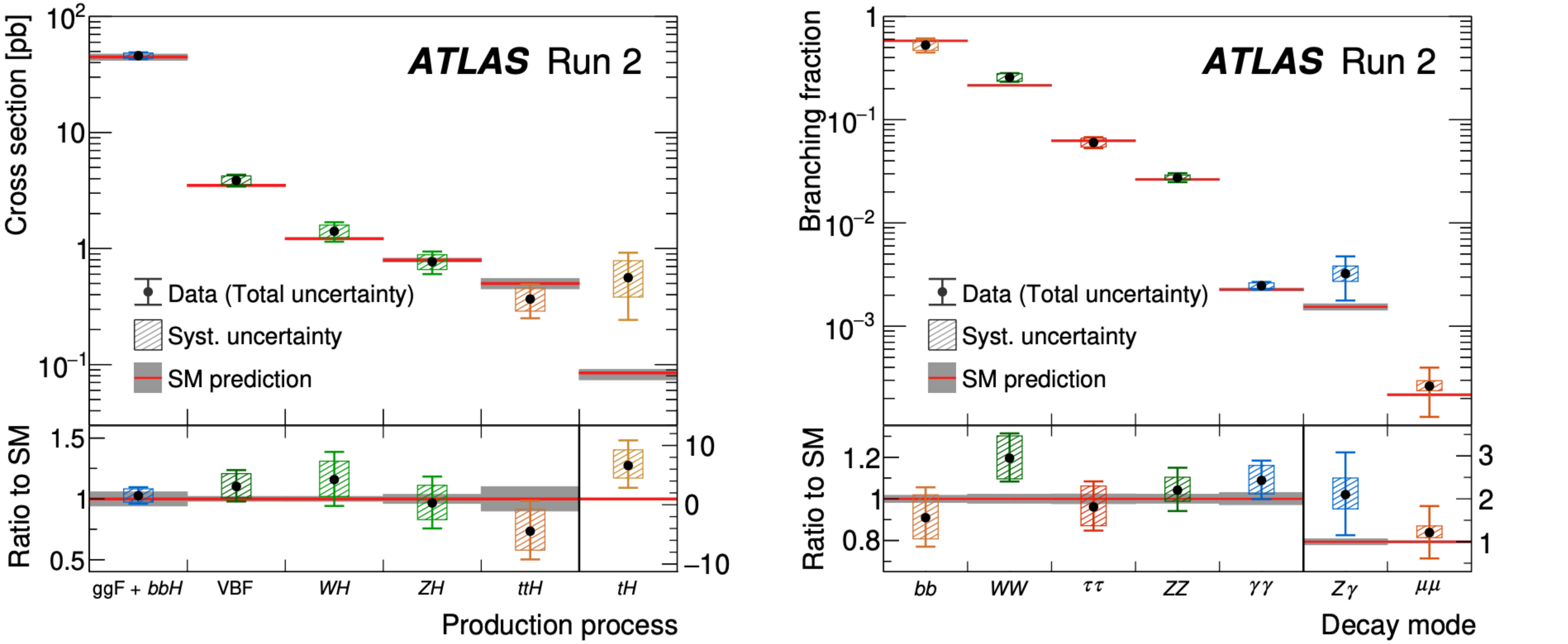

Good compatibility among decay channels and with SM

Higgs boson production and decay rates

Inclusive signal strength: $\mu = 1.002 \pm 0.057$ Nature 607, 60–68 (2022)

- Good compatibility among decay channels and with SM

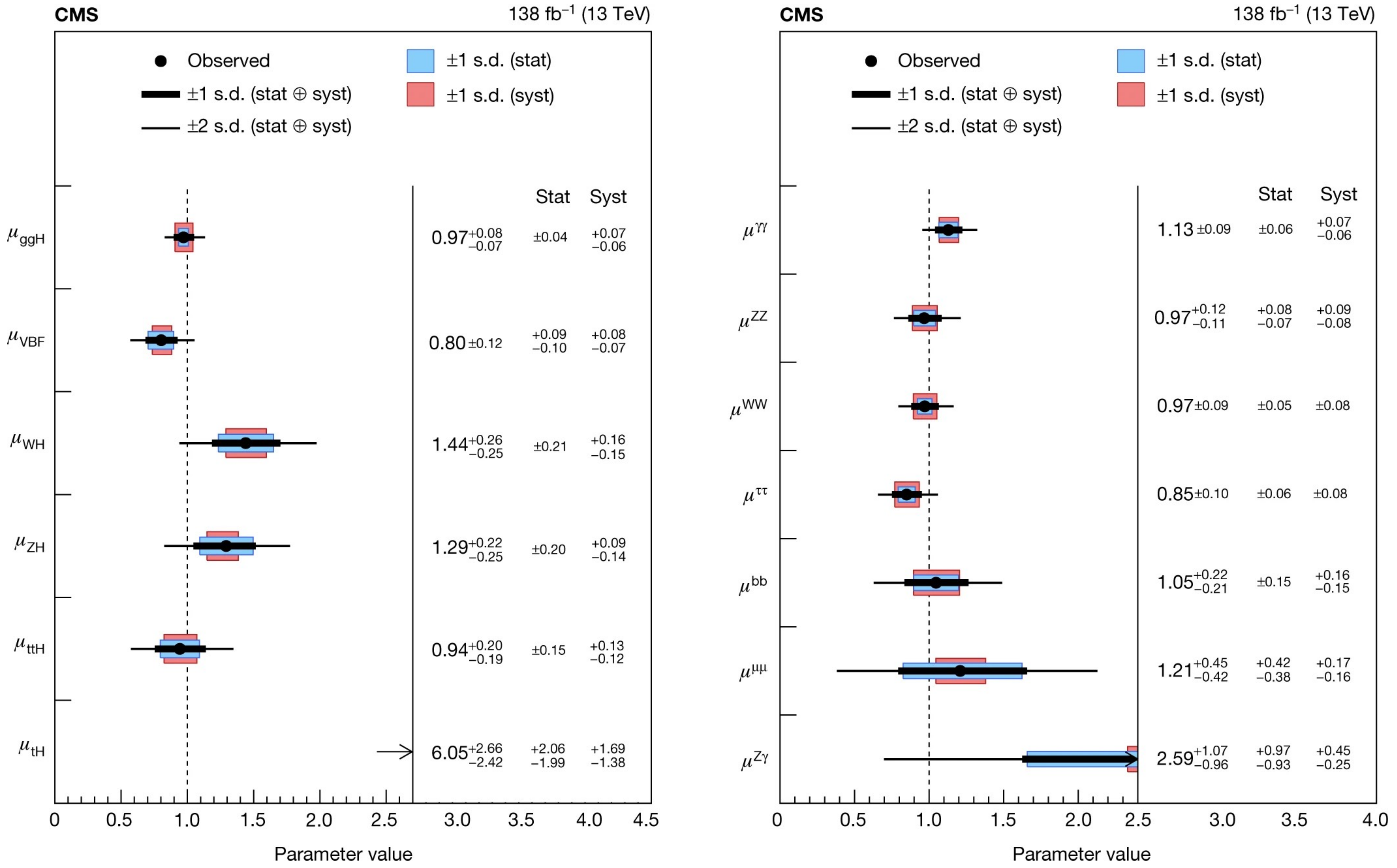

Higgs boson couplings: κ-framework

- Leading order framework to characterize possible deviations from the SM: assign coupling modifier to each (effective) interaction vertex (e.g. κ_W, κ_Z, κ_t…) and total width (κ_H)
- Assumptions: single resonance, zero width, SM tensor structure $J^P = 0^+$
- Coupling Compatibility Tests using κ and their ratios

Cross section for production and decay i→H→f parametrized as
SM cross sections and widths scaled by coupling modifiers

$$\sigma \cdot B(i \to H \to f) = \frac{\sigma_i \cdot \Gamma_f}{\Gamma_H} = \frac{\sigma_i^{SM} \cdot \Gamma_f^{SM}}{\Gamma_H^{SM}} \cdot \left(\frac{\kappa_i^2 \kappa_f^2}{\kappa_H^2}\right)$$

coupling modifiers: $\kappa_i^2 = \frac{\sigma_i}{\sigma_i^{SM}}$ Production; $\kappa_f^2 = \frac{\Gamma_f}{\Gamma_f^{SM}}$ Decay; $\kappa_H^2 = \frac{\sum \Gamma_f}{\sum \Gamma_f^{SM}}$ Total width

https://doi.org/10.5170/CERN-2013-004

Example: $gg \to H \to \gamma\gamma$

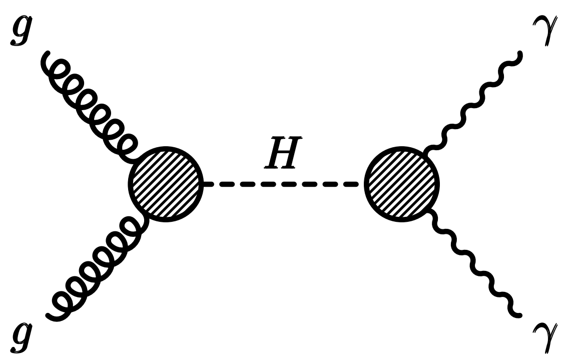

Assume only SM particles contribute in the loops

Nature 607, 52–59 (2022)

$$\frac{\sigma \times BR(gg \to H \to \gamma\gamma)}{\sigma \times BR(gg \to H \to \gamma\gamma)_{SM}} = \kappa_g^2 \frac{\kappa_\gamma^2}{\kappa_H^2} = (1.040\kappa_t^2 + 0.002\kappa_b^2 - 0.038\kappa_t\kappa_b - 0.005\kappa_t\kappa_c)\frac{1.589\kappa_W^2 + 0.072\kappa_t^2 - 0.674\kappa_W\kappa_t + 0.009\kappa_W\kappa_\tau + 0.008\kappa_W\kappa_b - 0.002\kappa_t\kappa_b - 0.002\kappa_t\kappa_\tau}{\kappa_H^2(\kappa_b, \kappa_W, \kappa_\tau, \ldots)}$$

Higgs boson couplings to massive gauge bosons vs fermions

- κ_V and κ_F, scaling the Higgs boson couplings to massive gauge bosons and to fermions
- κ_V and κ_F measured to be in agreement with SM prediction, within ~10% uncertainty

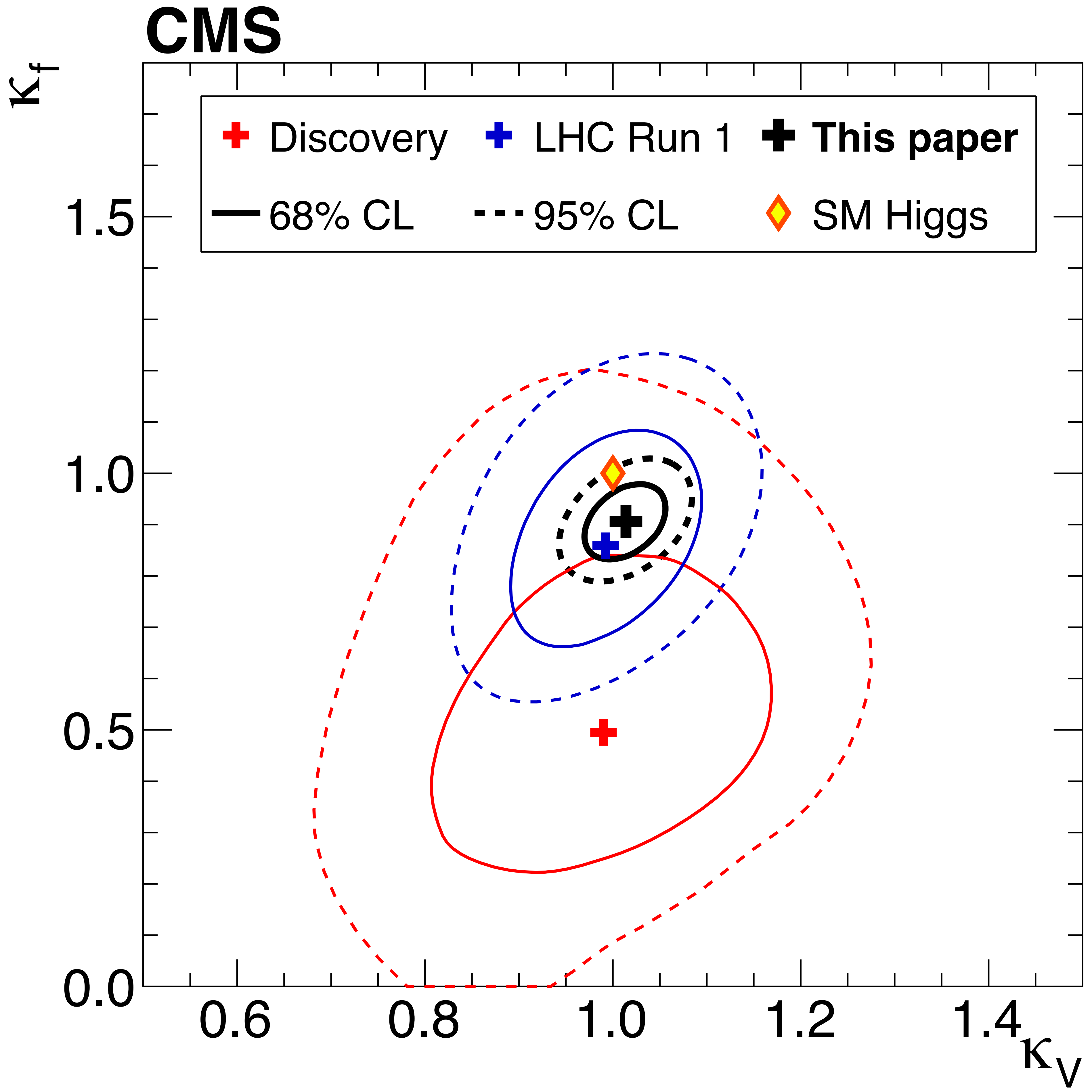

Nature 607, 60–68 (2022)

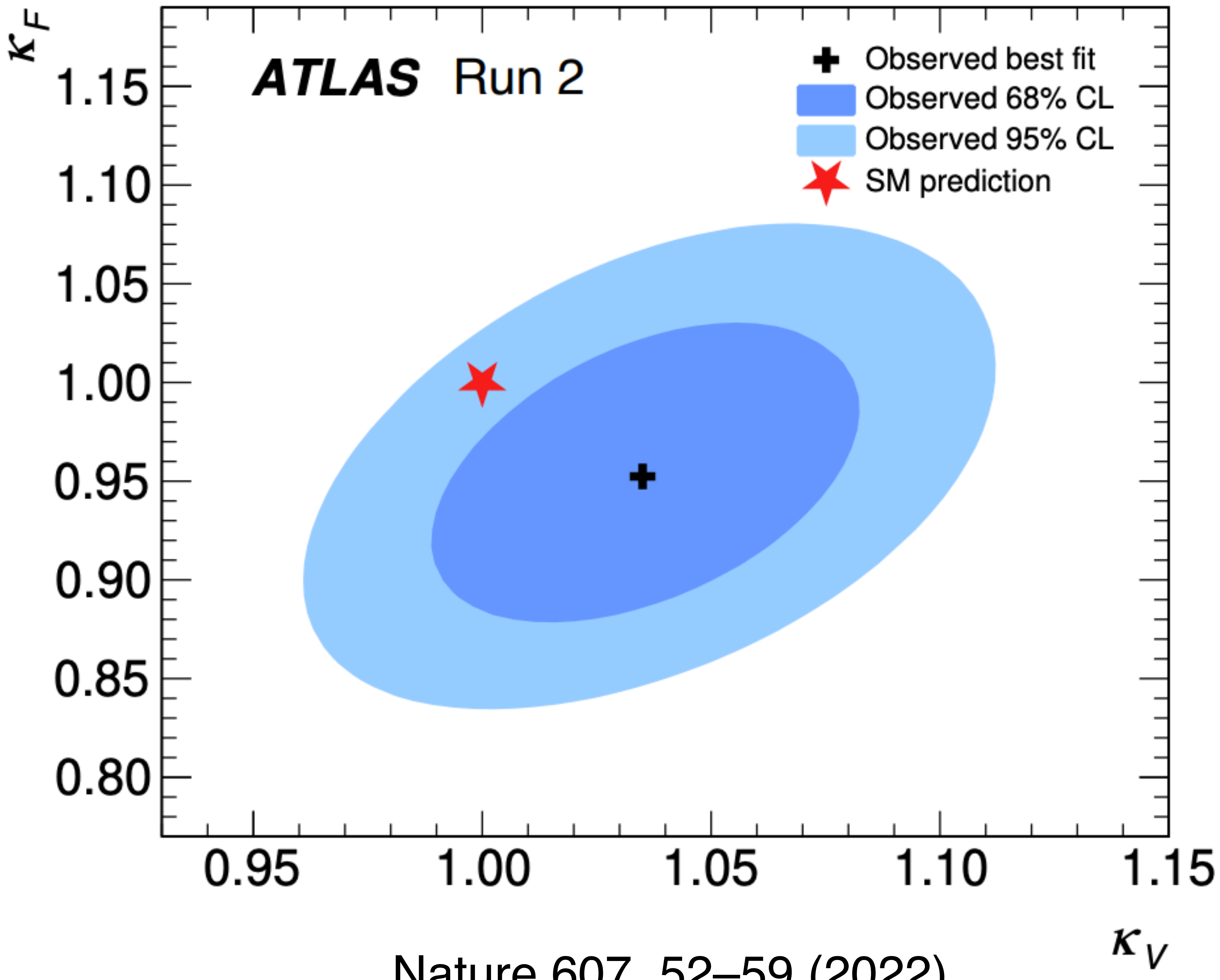

Nature 607, 52–59 (2022)

Higgs boson couplings vs particle mass

- Measure coupling modifiers κ for the massive gauge bosons (κ_W and κ_Z) and fermions probed in the present analyses (κ_t, κ_b, κ_τ, κ_μ and κ_c)
- Predictions for processes in SM occur via loops of intermediate virtual particles computed in terms of κ_i

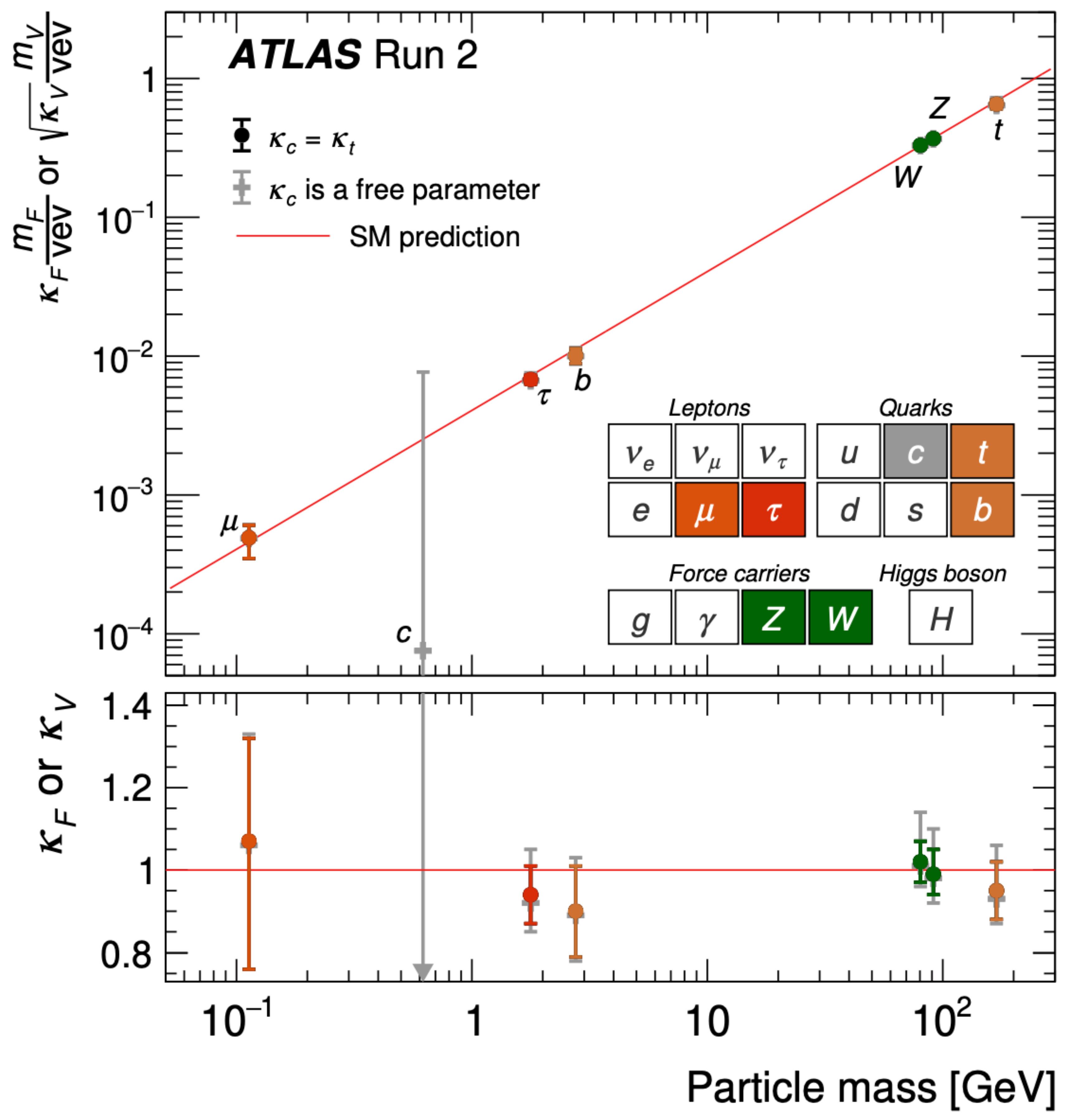

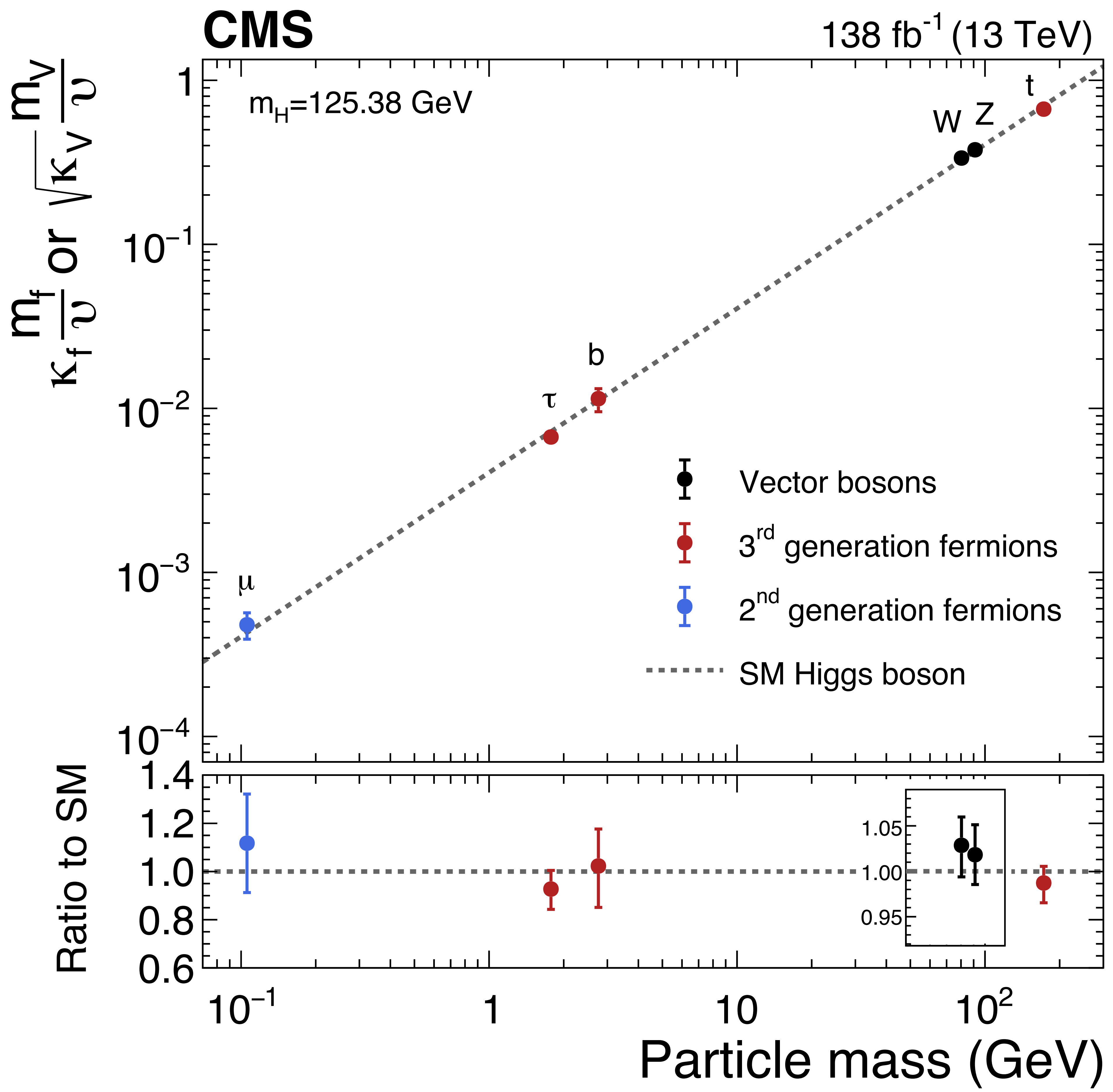

Higgs Boson coupling results

- Presence of non-SM particles in loop-induced process with effective coupling modifiers **$\kappa_g, \kappa_\gamma, \kappa_{Z\gamma}$**

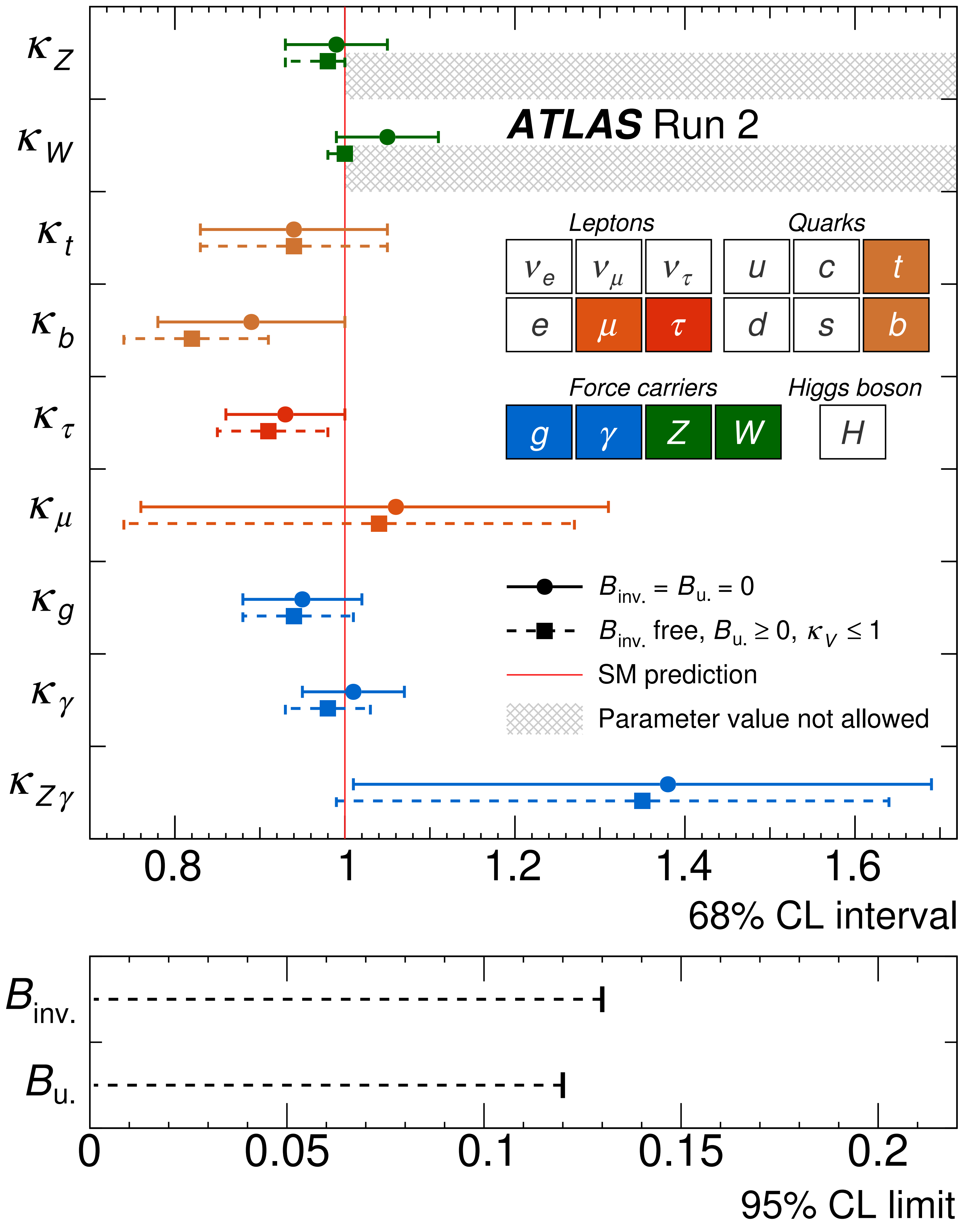

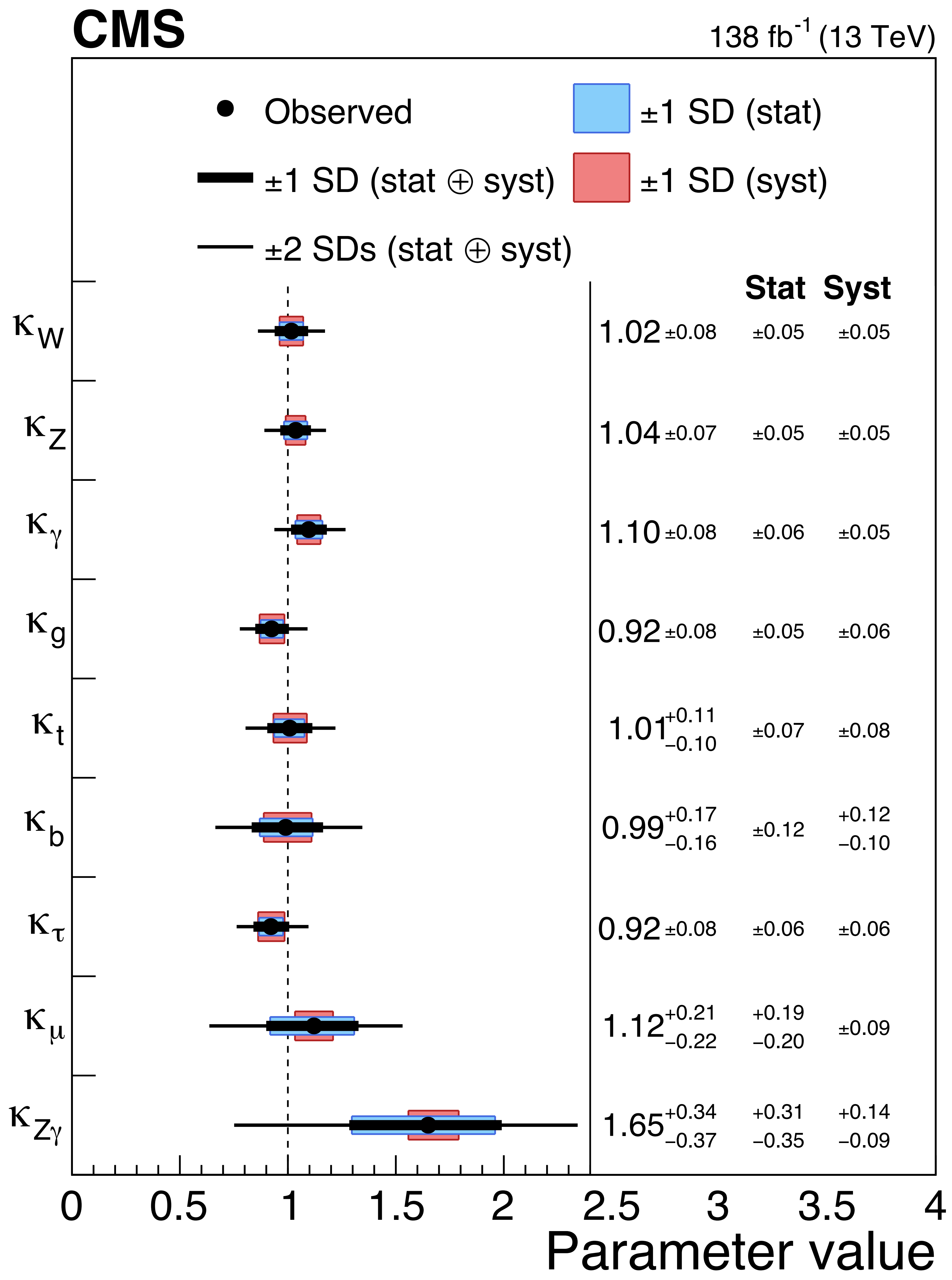

Simplified Template Cross Sections (STXS)

STXS: a natural evolution from Run 1 signal strength measurements

- Measure **production mode cross sections** in **exclusive phase space regions**
  - reduce theory dependence comparing to signal strength measurements
  - provide more finely-grained measurements
  - isolate BSM sensitive phase space
- Benefitting from **global combination**
  - Significant progress from ATLAS and CMS across accessible Higgs decays

Development initiated at Les Houches 2015

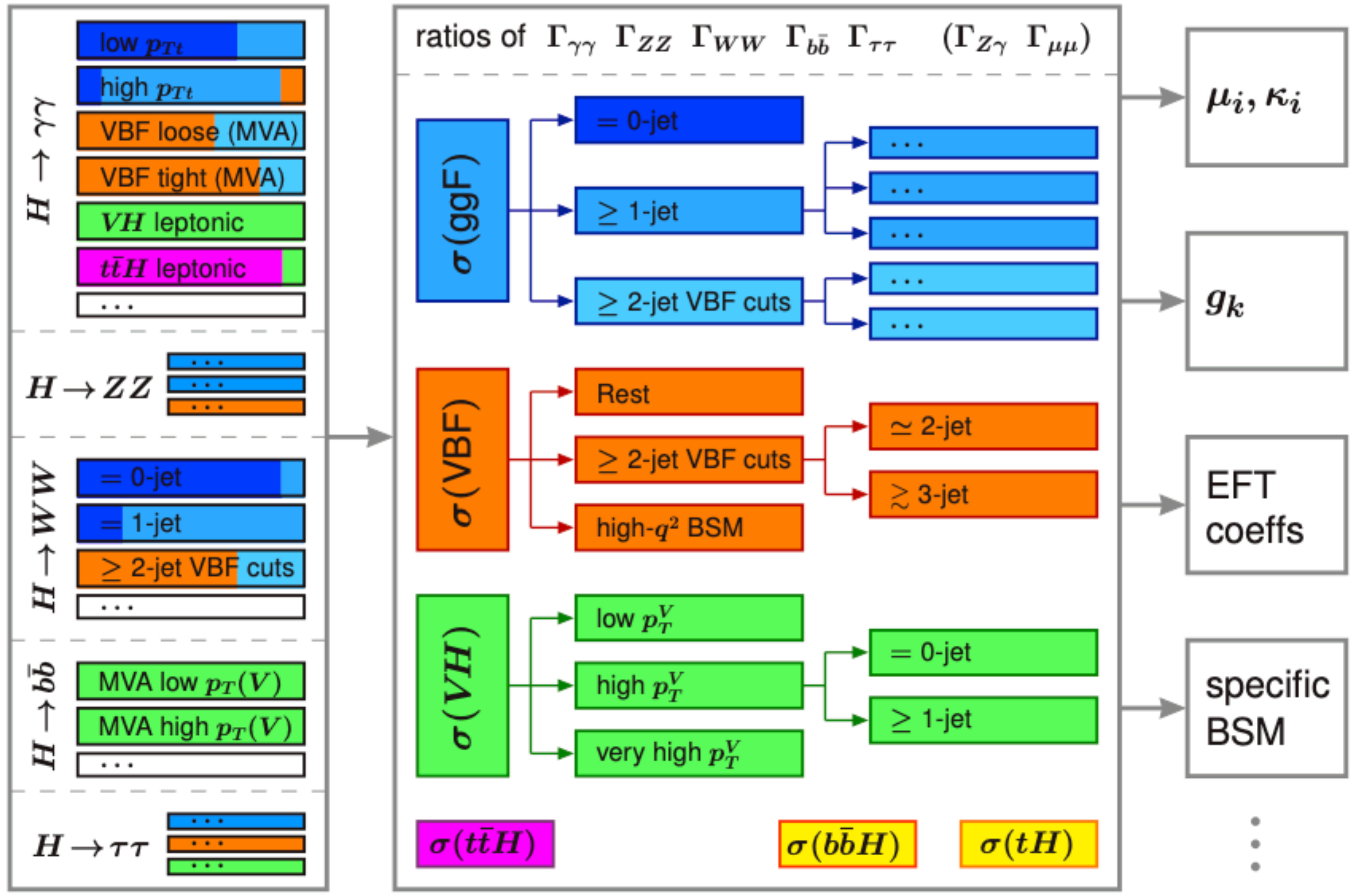

STXS stage 1.2 ggH production mode bins

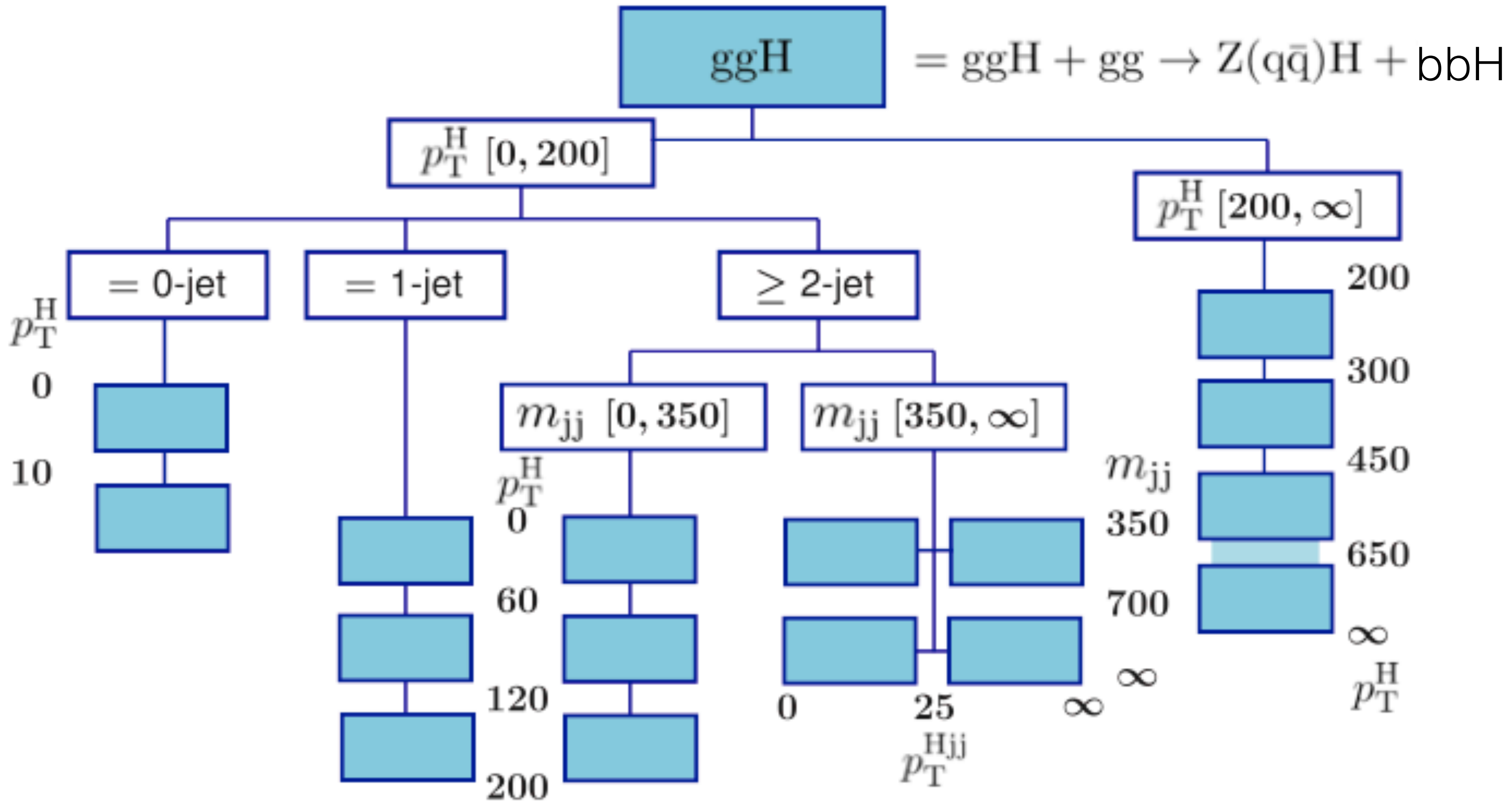

CMS STXS: recent result H→bb

Phys. Rev. D 109 (2024) 092011

- Full Run 2 measurement targeting VH production mechanism
- Dedicated category:
  - resolved topology: 2 b-tagged jets
  - boosted topology: large-radius H→bb jet

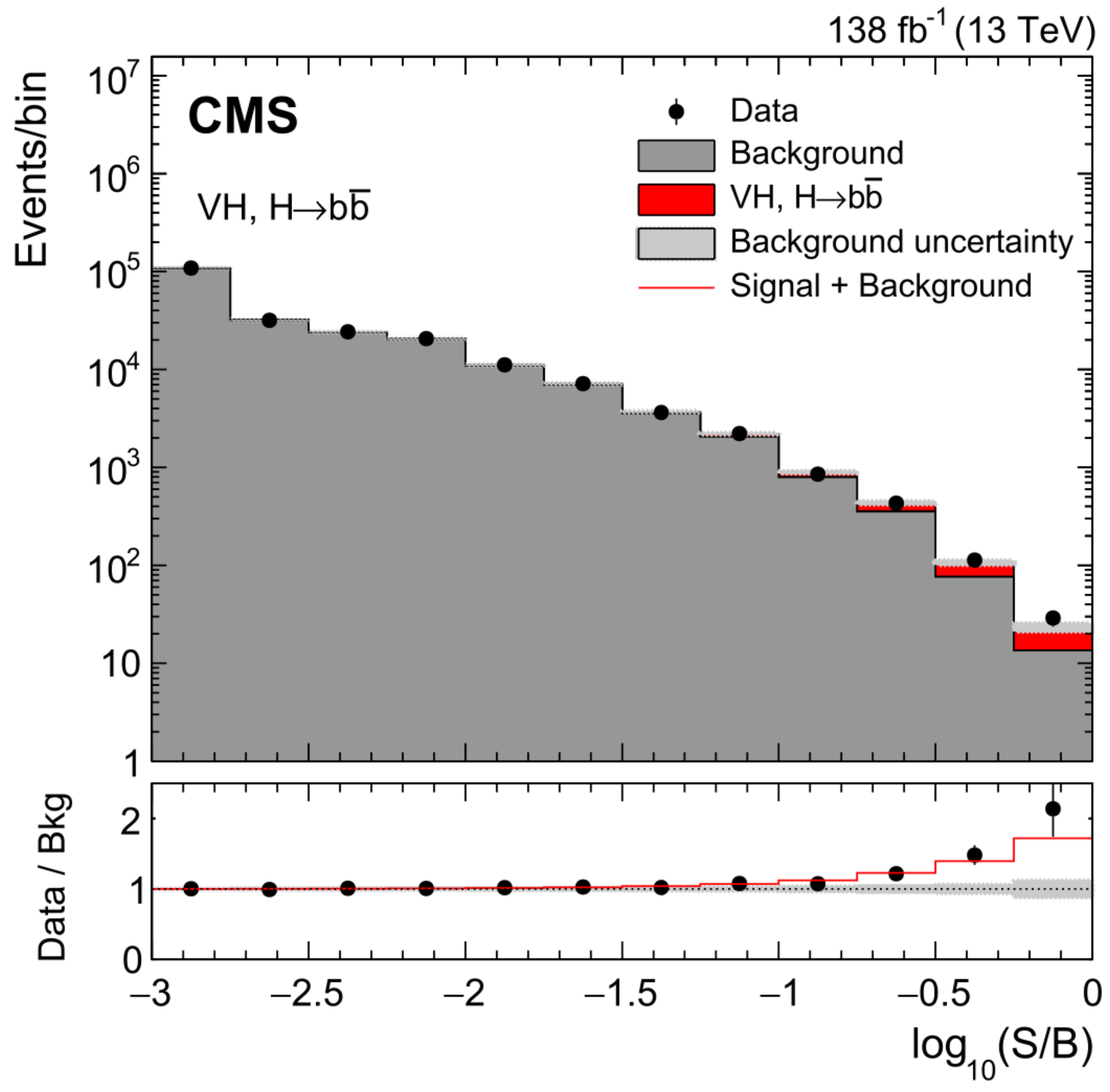

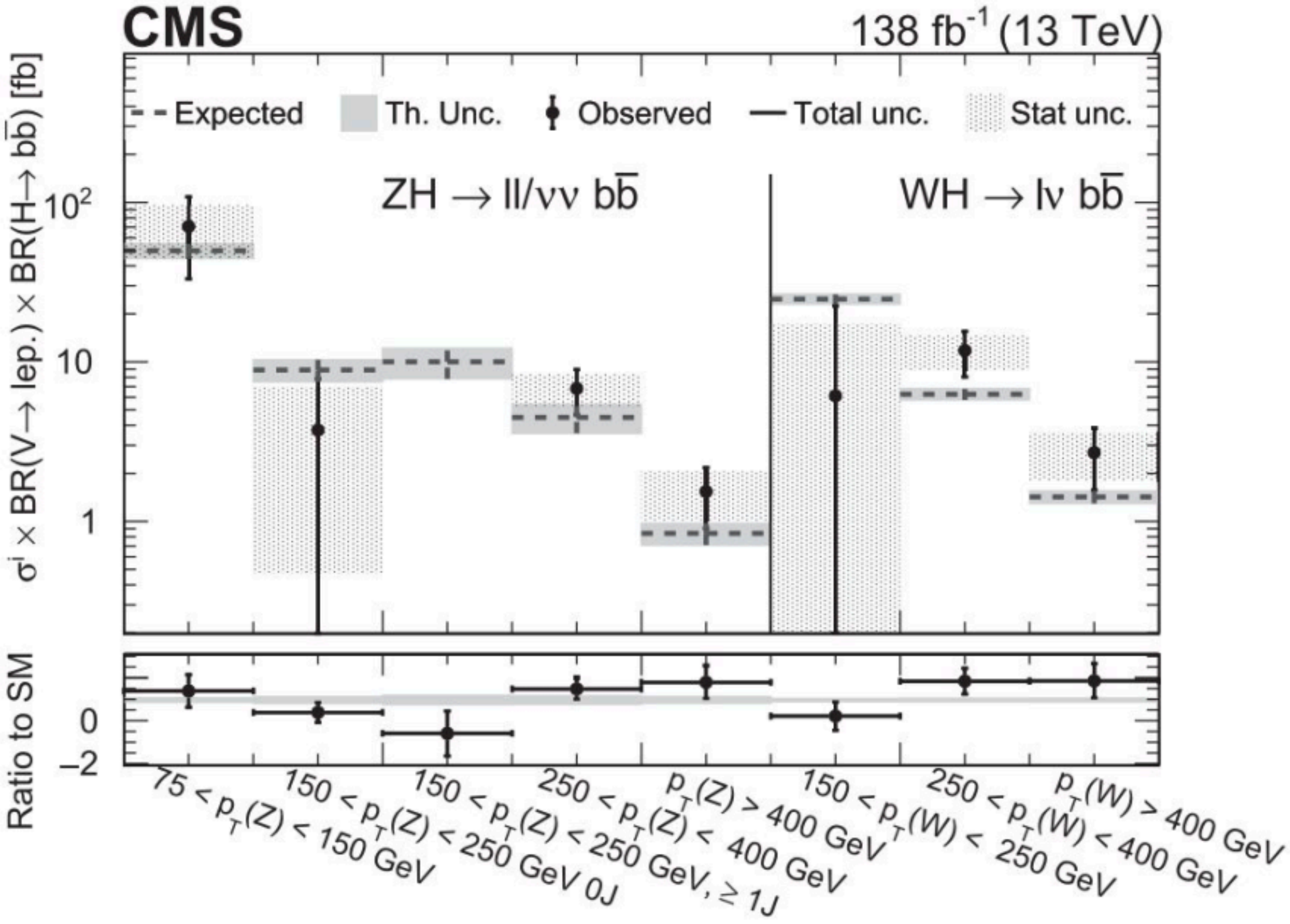

STXS Combination

Most precise measurements and interpretations obtained from statistical combination of STXS measurements in production modes and decay channels:

- Statistical precision, in particular in most BSM-sensitive regions is still limited: more data will help! [Nature volume 607, 52–59 (2022)]
- Provide an indirect constraint of the Higgs boson self-coupling through NLO EW corrections [PLB 843(2023)137745, CMS HIG-19-005]
- Measurements interpreted using EFT framework and BSM models: [arXiv:2402.05742, CMS-PAS-HIG-23-013]

- Example: STXS measurements in H→ZZ*, H→WW* decay channels, overall good compatibility with SM

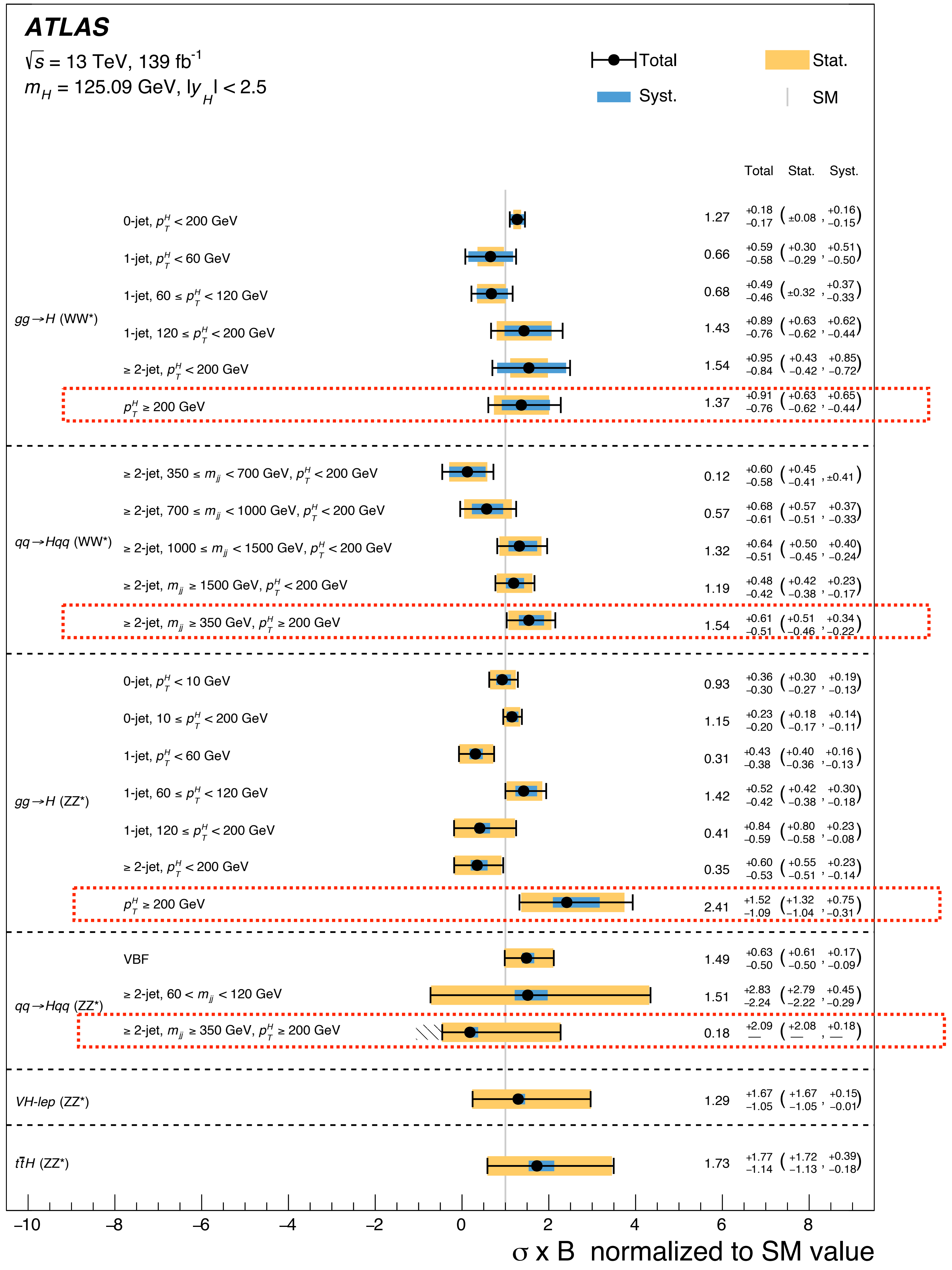

arXiv:2402.05742

ATLAS STXS Combination - ggH production

- ATLAS full Run 2 STXS combination [Nature volume 607, 52–59 (2022)]
- Input channels: H→$\gamma\gamma$, H→ZZ*, H→WW*, H→Zγ, H→bb, H→$\tau\tau$ and H→μμ

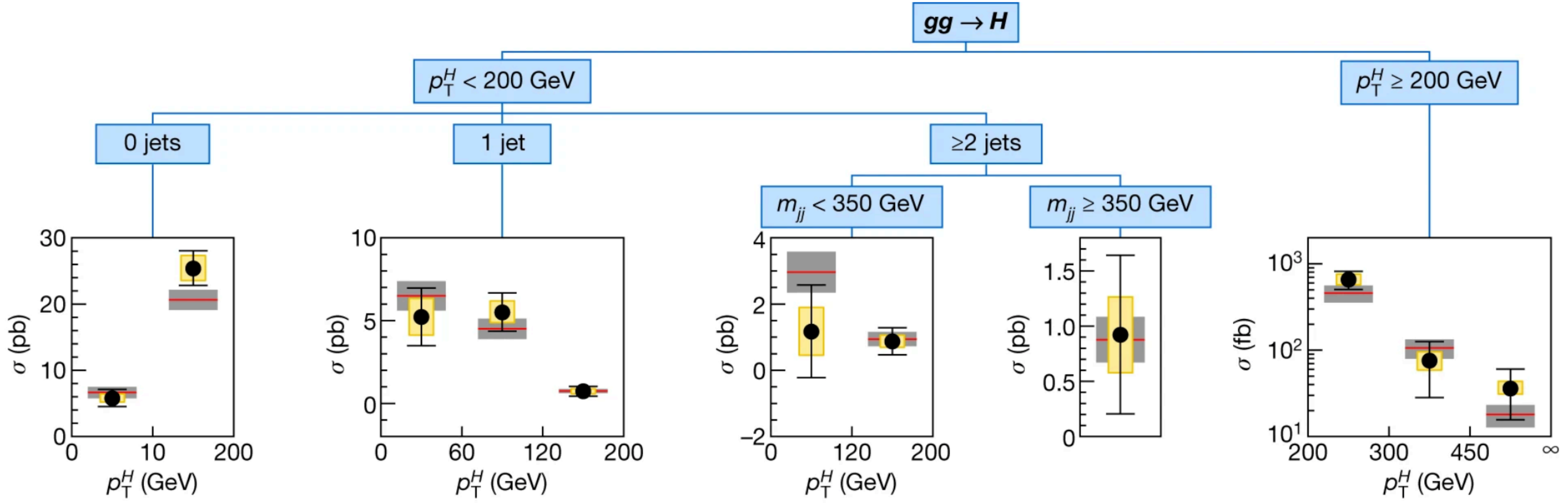

ATLAS STXS Combination: VBFH, VH, tt/tH

- ATLAS full Run 2 STXS combination [Nature volume 607, 52–59 (2022)]

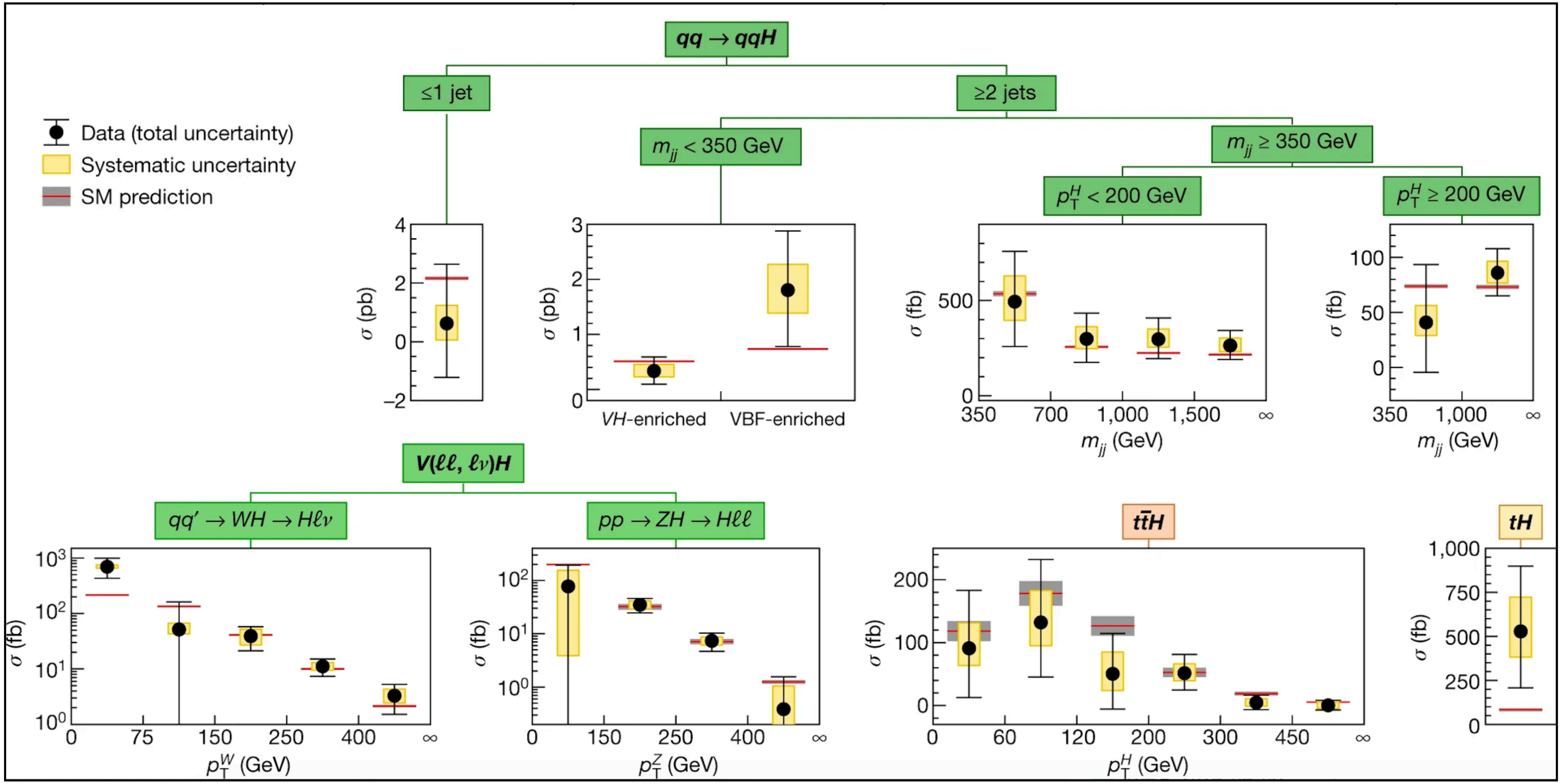

SMEFT and 2HDM and (h)MSSM interpretation of ATLAS STXS combination

arXiv:2402.05742 submitted to JHEP

Decay channel	Analysis Production mode	$\mathcal{L}$ [fb^{-1}]	Reference	Binning	SMEFT	2HDM and (h)MSSM
$H \to \gamma\gamma$	(ggF, VBF, WH, ZH, $t\bar{t}H$, tH)	139	[38] [19]	STXS-1.2 differential	✓ ✓(subset)	✓
$H \to ZZ^*$	($ZZ^* \to 4\ell$: ggF, VBF, $WH+ZH$, $t\bar{t}H+tH$)	139	[22] [18]	STXS-1.2 differential	✓ ✓(subset)	✓
	($ZZ^* \to \ell\ell\nu\bar{\nu}/\ell\ell q\bar{q}$: $t\bar{t}H$ multileptons)	36.1	[27]	STXS-0*		✓
$H \to \tau\tau$	(ggF, VBF, $WH+ZH$, $t\bar{t}H+tH$)	139	[39]	STXS-1.2	✓	✓
	($t\bar{t}H$ multileptons)	36.1	[27]	STXS-0*		✓
$H \to WW^*$	(ggF, VBF)	139	[40]	STXS-1.2	✓	✓
	(WH, ZH)	36.1	[41]	STXS-0*		✓
	($t\bar{t}H$ multileptons)	36.1	[27]	STXS-0*		✓
$H \to bb$	(WH, ZH)	139	[42,25]	STXS-1.2	✓	✓
	(VBF)	126	[43]	STXS-1.2	✓	✓
	($t\bar{t}H+tH$)	139	[44]	STXS-1.2	✓	✓
	(boosted Higgs bosons: inclusive production)	139	[45]	STXS-1.2	✓	✓
$H \to Z\gamma$	(inclusive production)	139	[46]	STXS-0*	✓	✓
$H \to \mu\mu$	(ggF $+ t\bar{t}H + tH$, VBF $+ WH + ZH$)	139	[47]	STXS-0*	✓	✓

SMEFT interpretation of STXS combination

arXiv:2402.05742 submitted to JHEP

- Standard Model Effective Field Theory (**SMEFT**) Effective Lagrangian :

$$\mathscr{L}_{\mathrm{SMEFT}} = \mathscr{L}_{\mathrm{SM}} + \sum_i^{N_{d=6}} \frac{c_i}{\Lambda^2}\mathcal{O}_i^{(6)} + \sum_j^{N_{d=8}} \frac{b_j}{\Lambda^4}\mathcal{O}_j^{(8)} + \ldots$$

Only $d = 6$ operators are considered, impact of $d = 8$ operators might be non-negligible.

- Ratio of SMEFT cross section wrt SM prediction

$$\frac{\sigma_{\mathrm{EFT}}}{\sigma_{\mathrm{SM}}} = 1 + \sum_i A_i c_i + \sum_{ij} B_{ij} c_i c_j$$

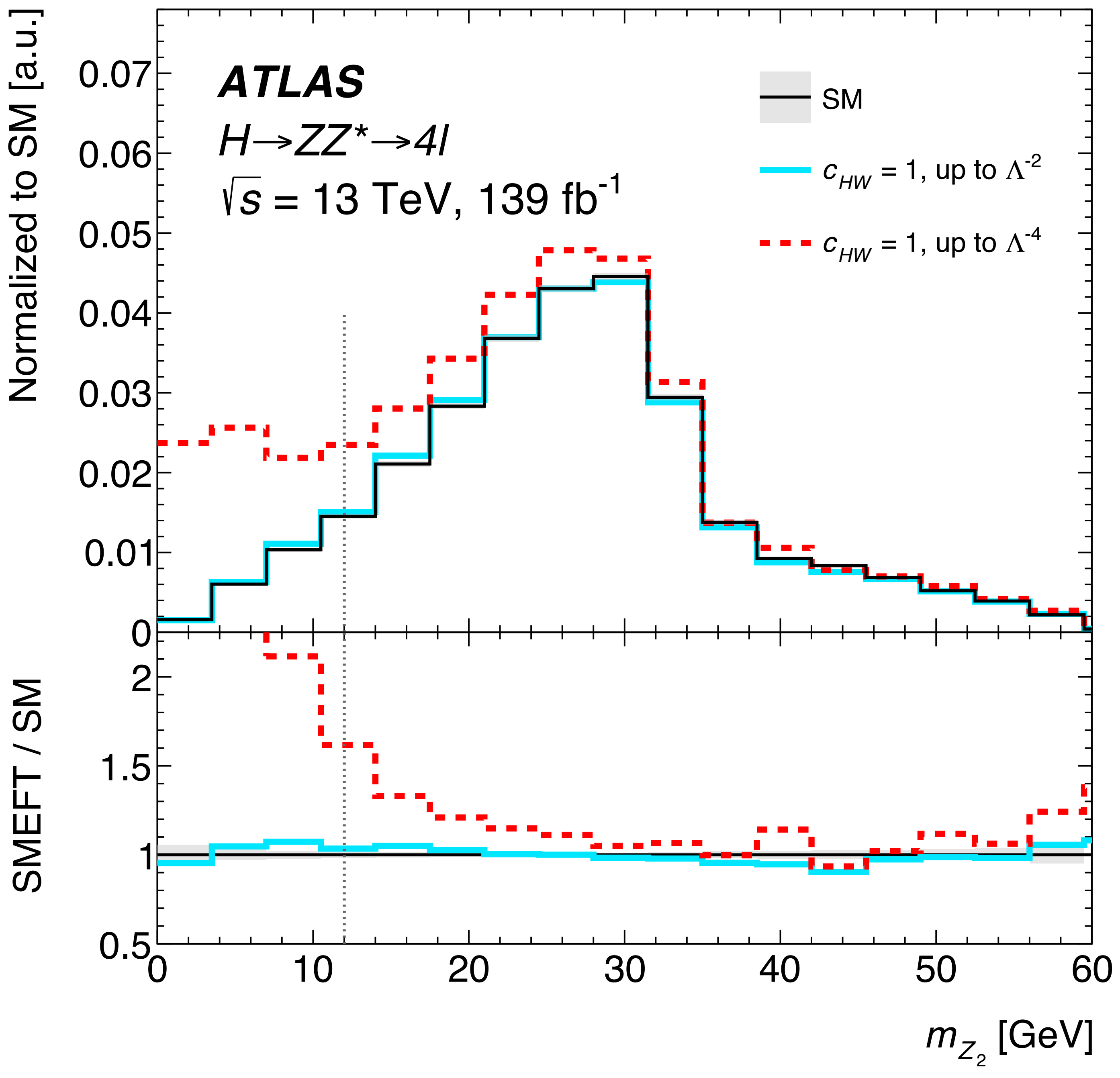

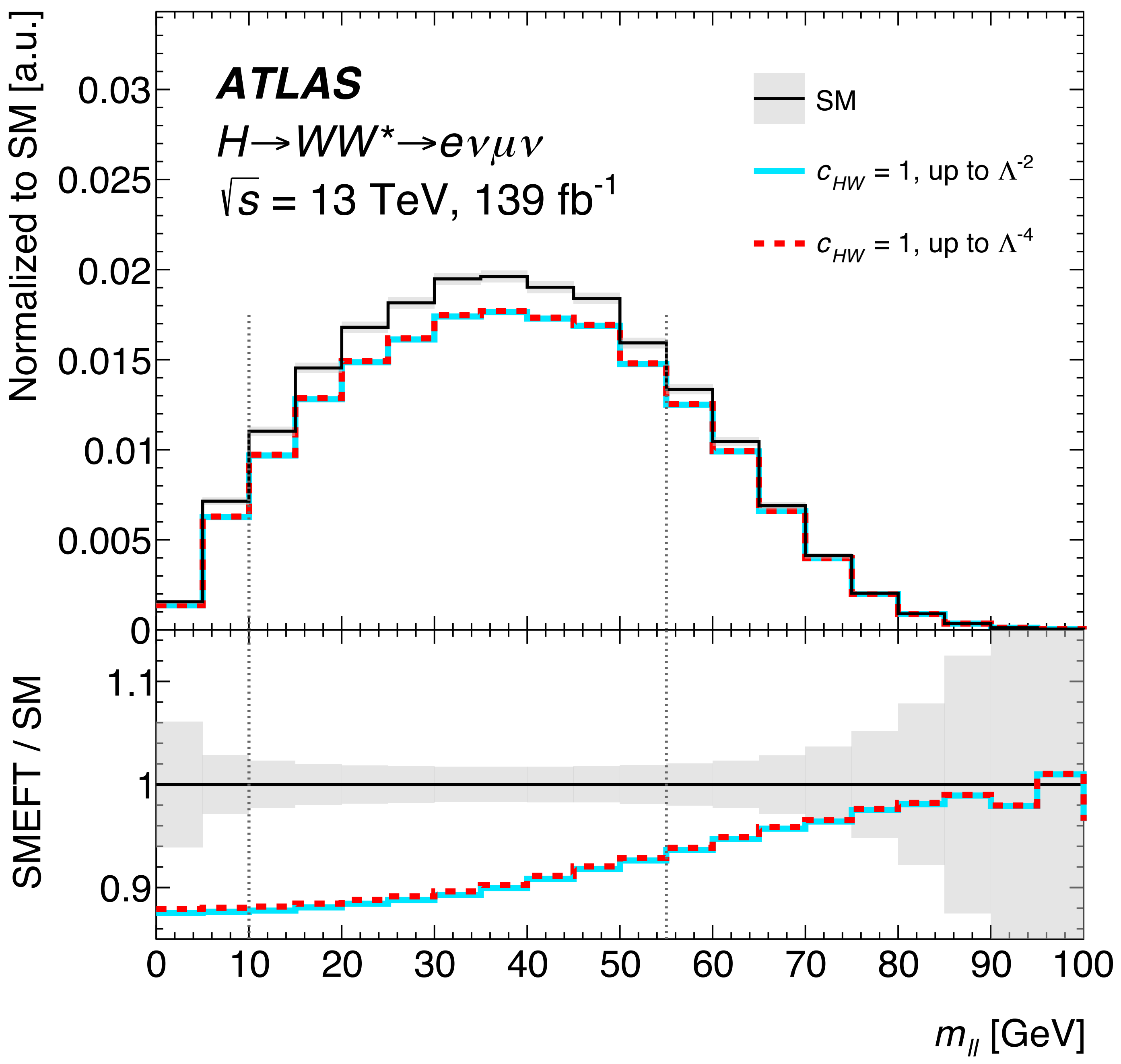

Taken into account the non-negligible acceptance effects for operator C_{HW}, C_{HB}, C_{HWB} and $C^{(3)}_{Hl}$ in the $H \to WW^*$ and $H \to ZZ^*$ decay modes

Fit basis for SMEFT interpretation

- Definition of the fit basis coefficients in terms of the Warsaw basis Wilson coefficients.
- Achieves both fit stability and fit-parameter interpretability.

arXiv:2402.05742 submitted to JHEP

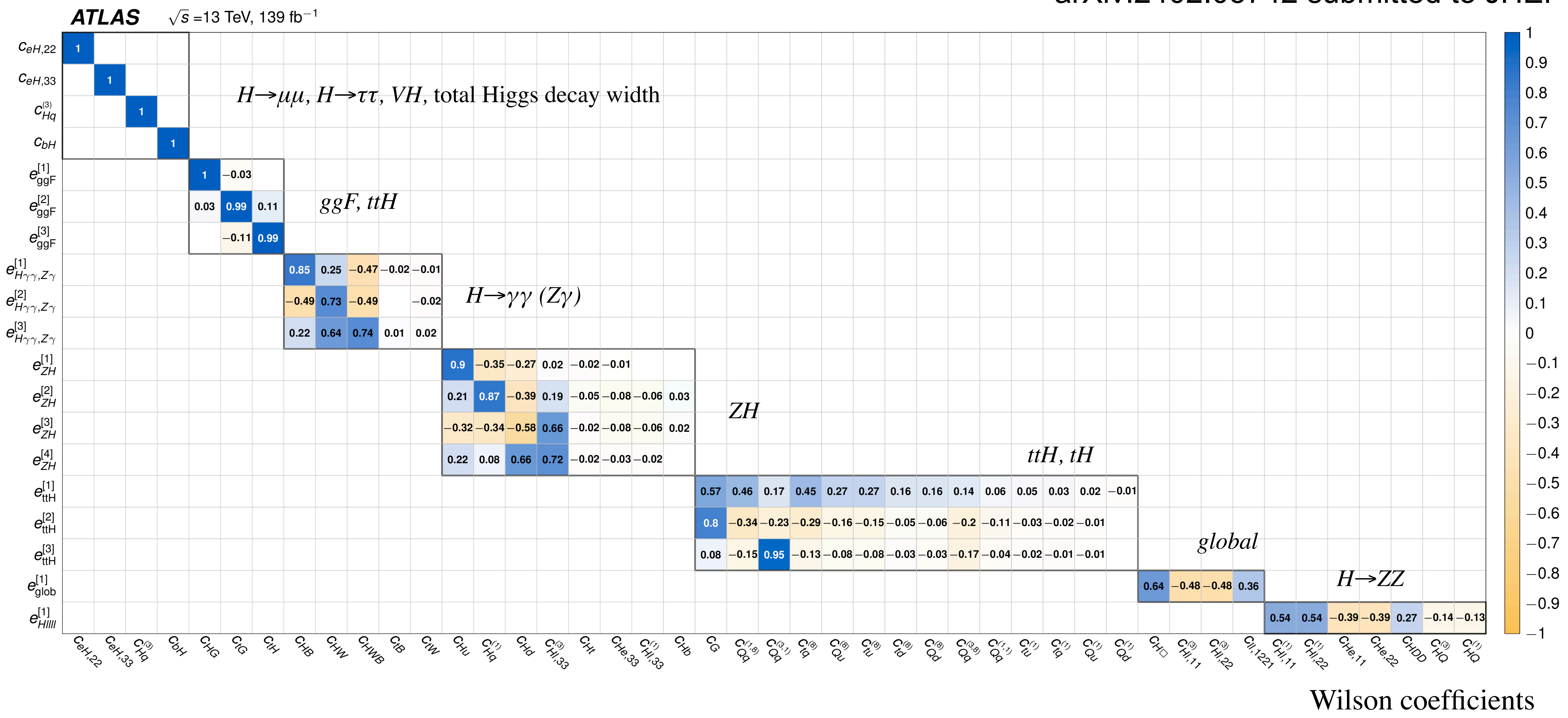

SMEFT interpretation of STXS combination

arXiv:2402.05742 submitted to JHEP

- SMEFT linear model vs SMEFT linear+quadratic results
- Linear+quadratic *p*-value **98.2%**, stronger constraints with linear+quadratic

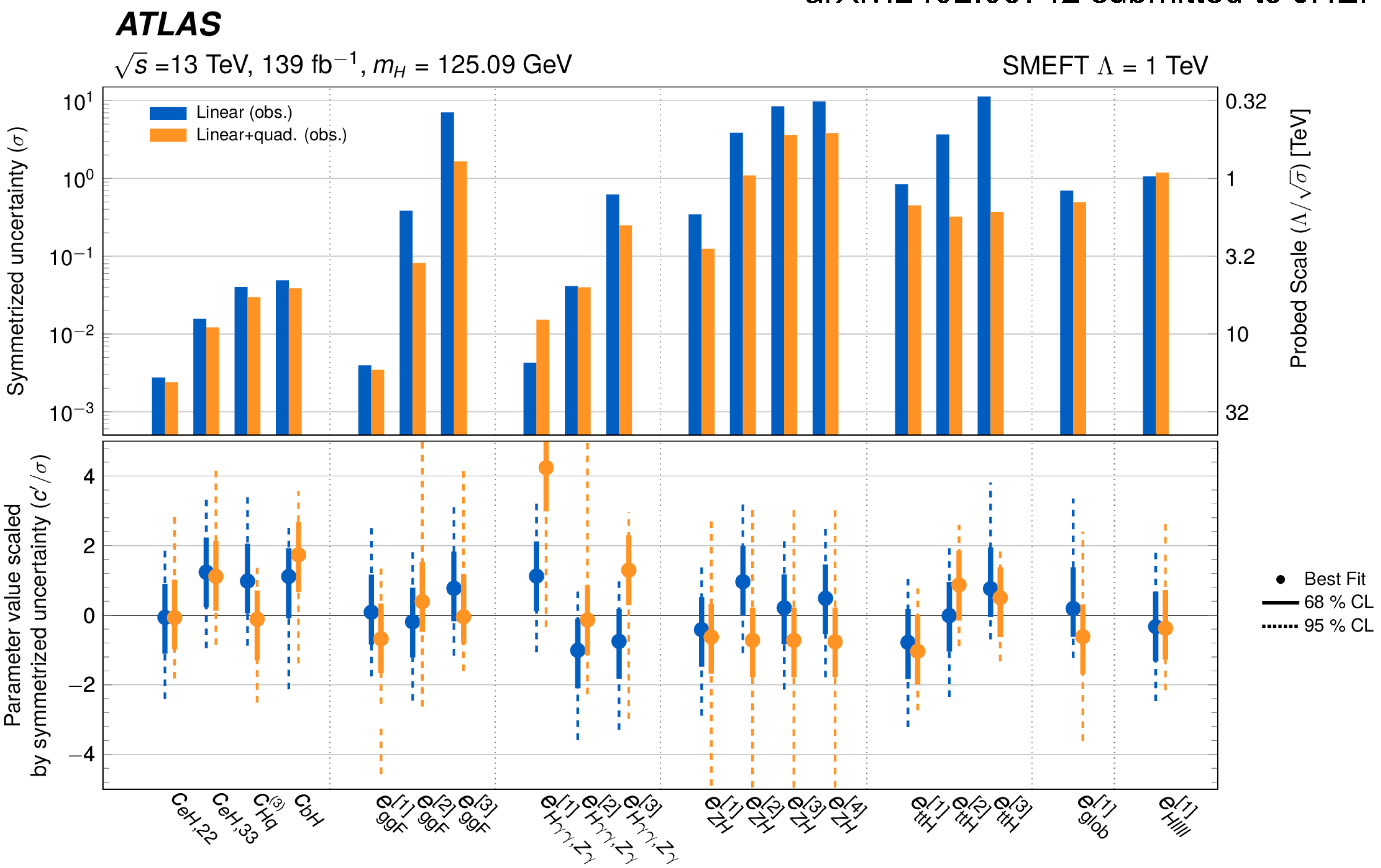

UV-complete models：2HDM

arXiv:2402.05742 submitted to JHEP

Comparison of the constraints in tanβ, cos(β-α) plane, from the κ- and EFT-interpretations of Higgs boson production and decay rates.

The κ_λ constraint is included in the Type-I model interpretation.

Type-I model

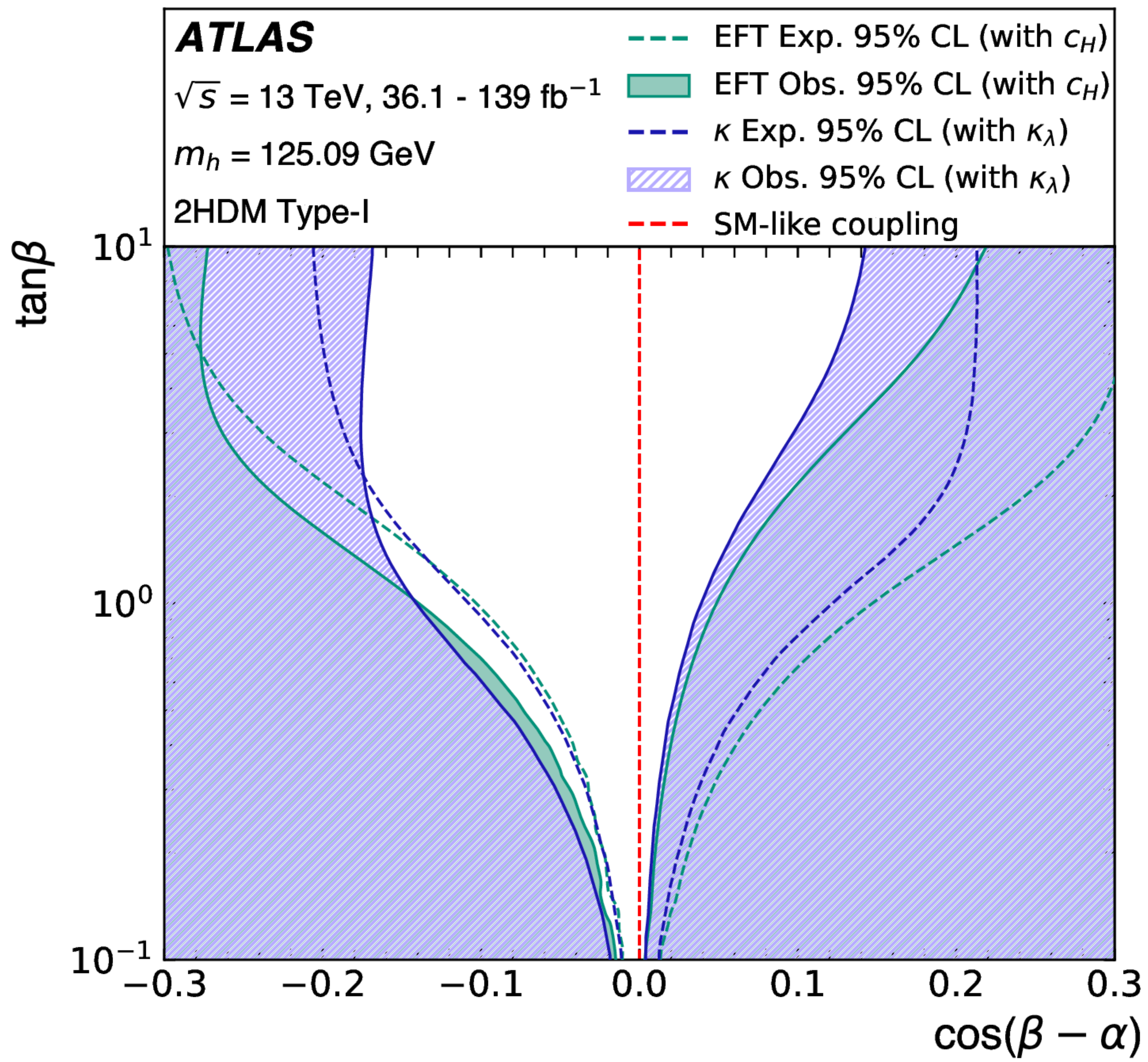

Type-II model

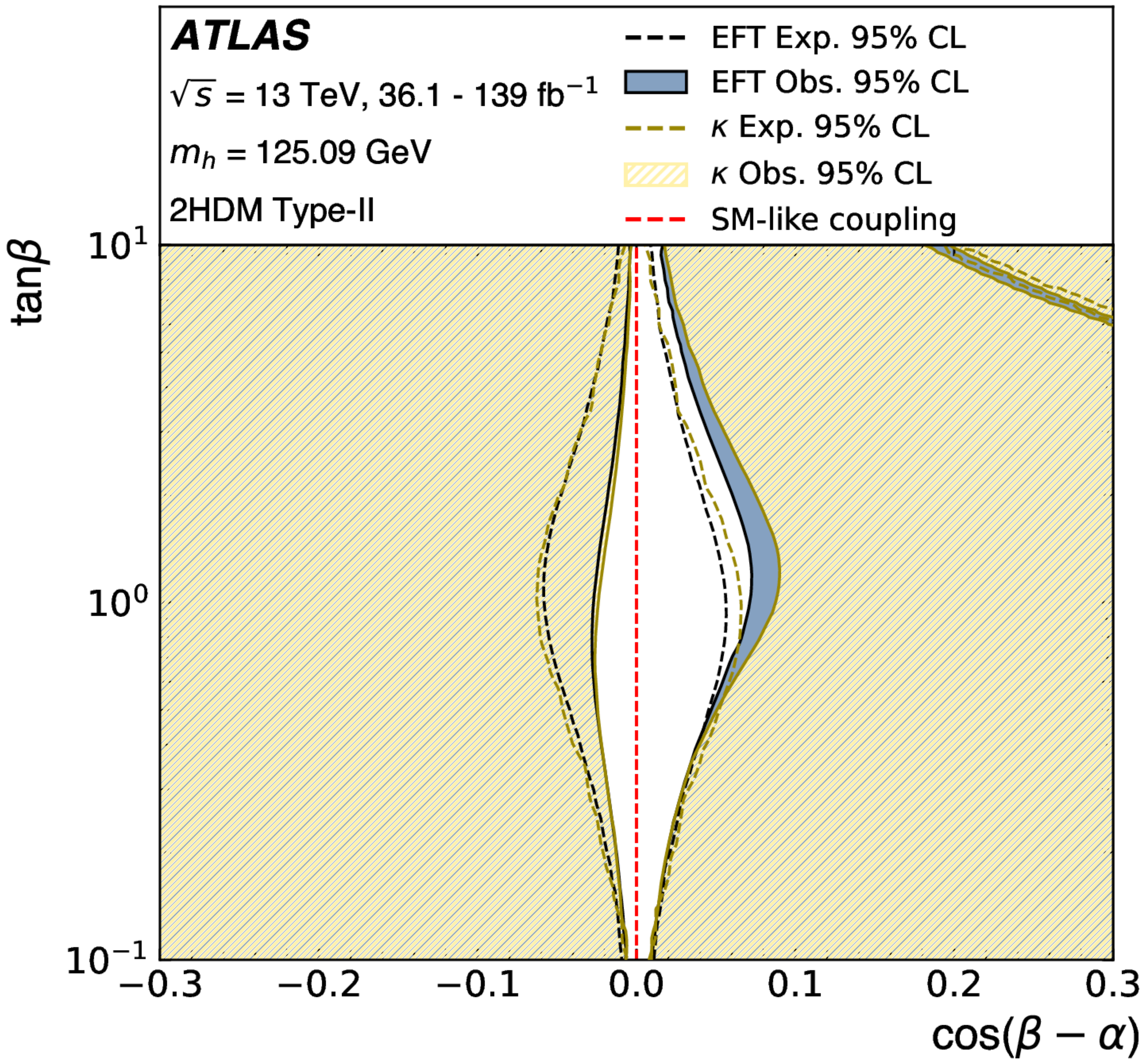

UV-complete models: hMSSM

arXiv:2402.05742 submitted to JHEP

$$\mu^{i,X}(m_A, \tan\beta) = \frac{\sigma^i_{\mathrm{(h)MSSM}}(m_A, \tan\beta)}{\sigma^i_{\mathrm{SM}}} \cdot \frac{\mathcal{B}^X_{\mathrm{(h)MSSM}}(m_A, \tan\beta)}{\mathcal{B}^X_{\mathrm{SM}}} \equiv r^i(m_A, \tan\beta) \cdot r^X(m_A, \tan\beta)$$

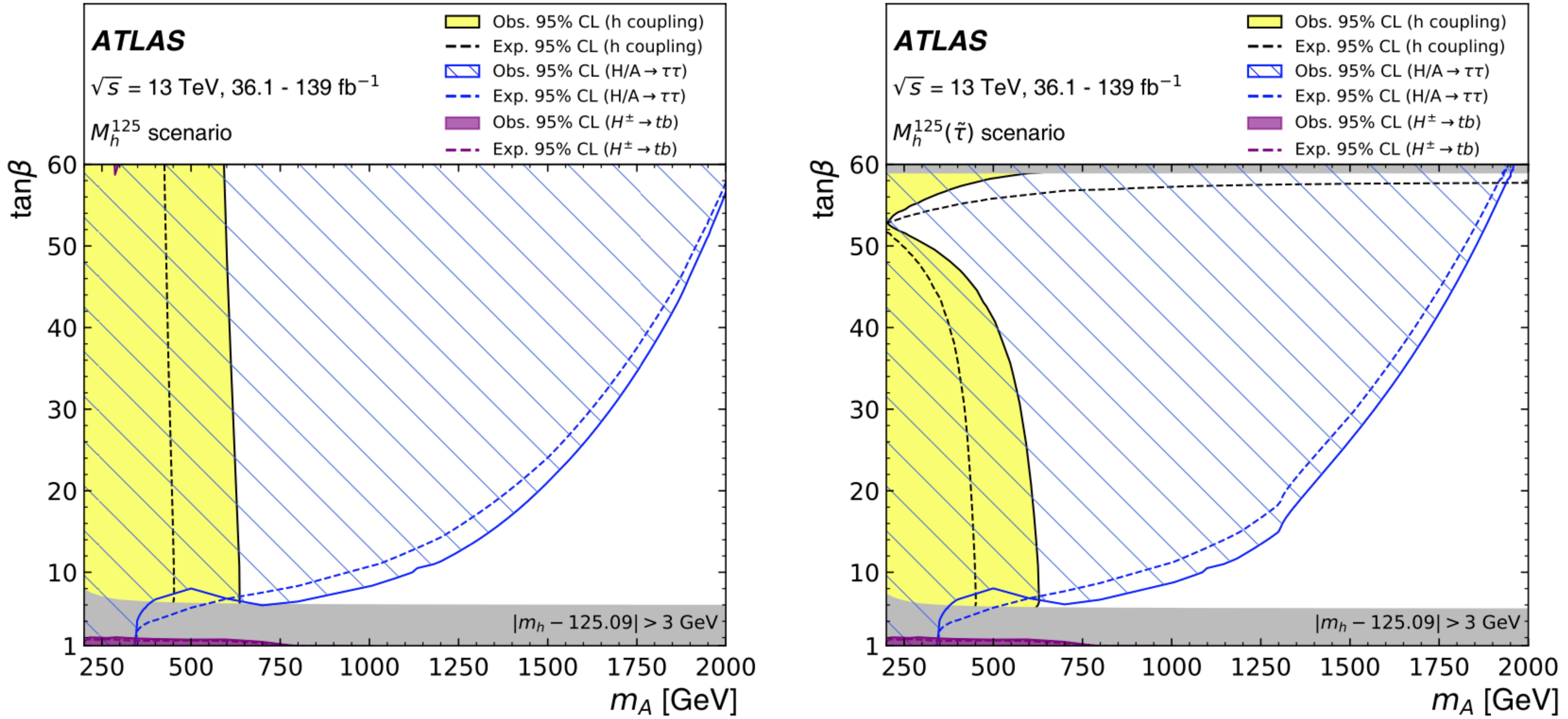

Higgs boson differential measurements combination and interpretation

Differential distributions are sensitive to Higgs couplings through distortions in the SM predicted spectra. Two interpretations: κ-framework and SMEFT

Higgs p_T sensitive to many BSM effects: physics in the ggF loops, perturbative QCD calculations, Higgs couplings to charm and bottom quarks, …

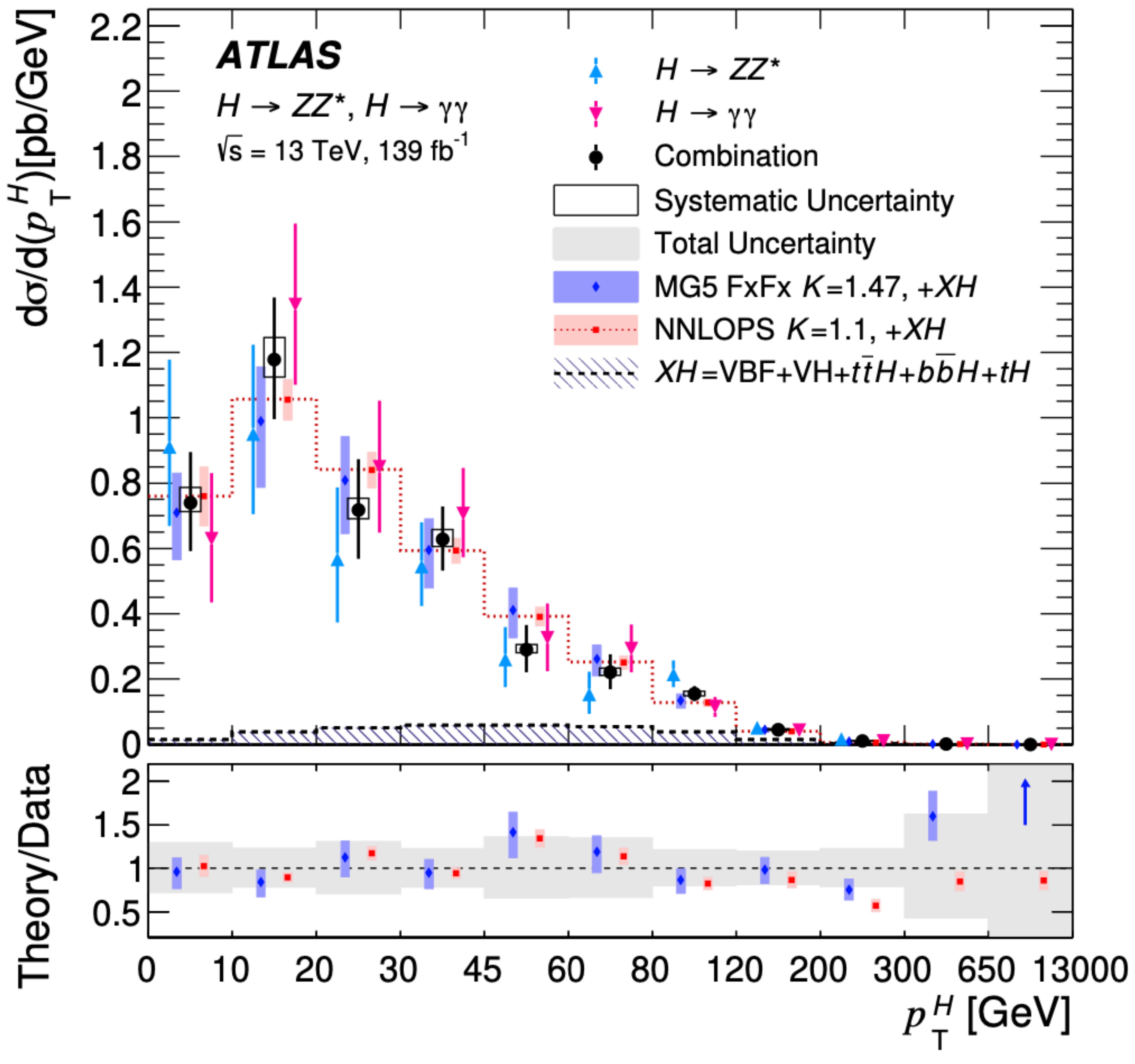

arXiv:2402.05742 submitted to JHEP

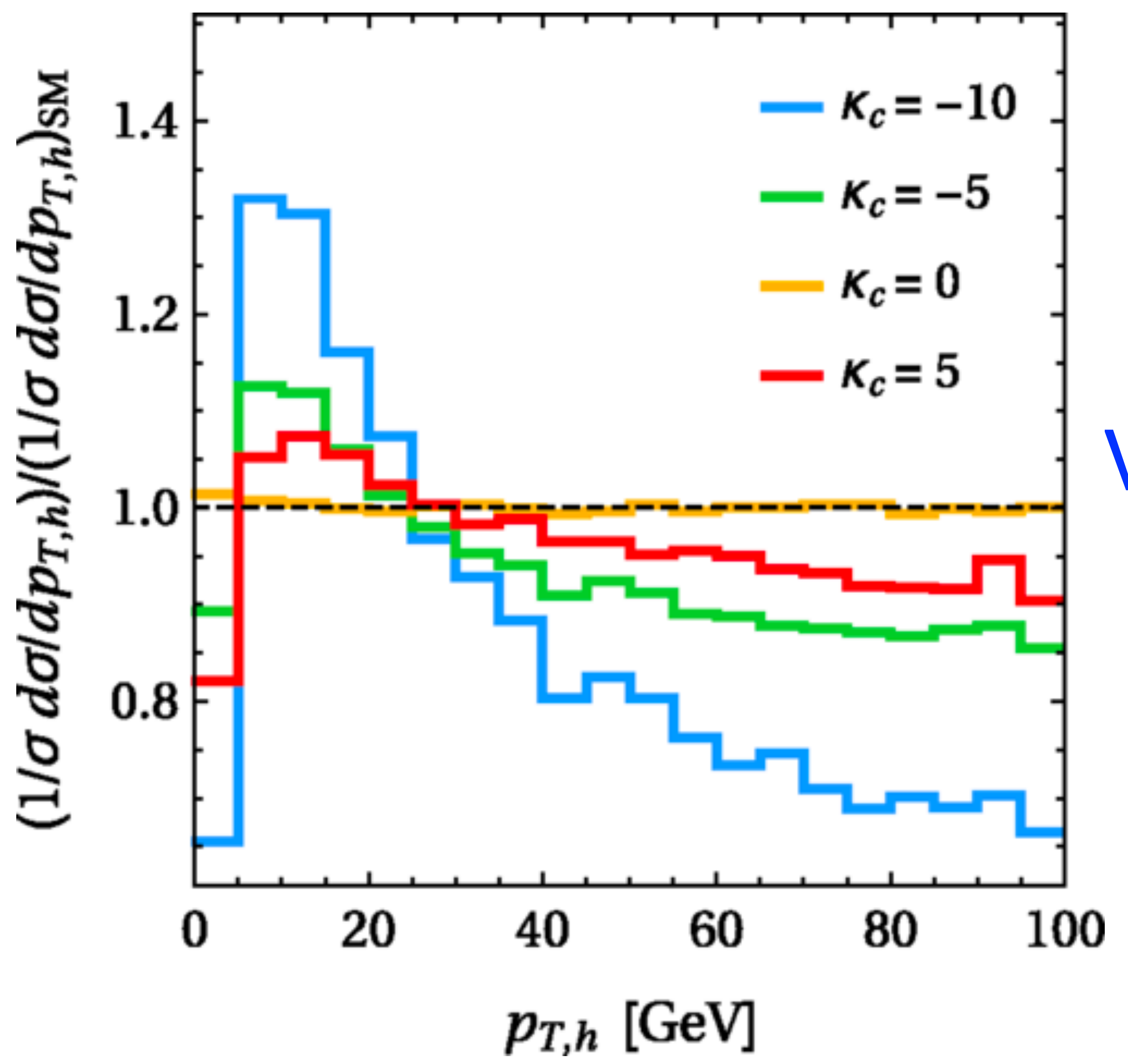

Variations in $p_T(H)$ with κ_c

Phys. Rev. Lett. 118 (2017) 121801

κ_c vs κ_b constraint from $p_T(H)$ shape

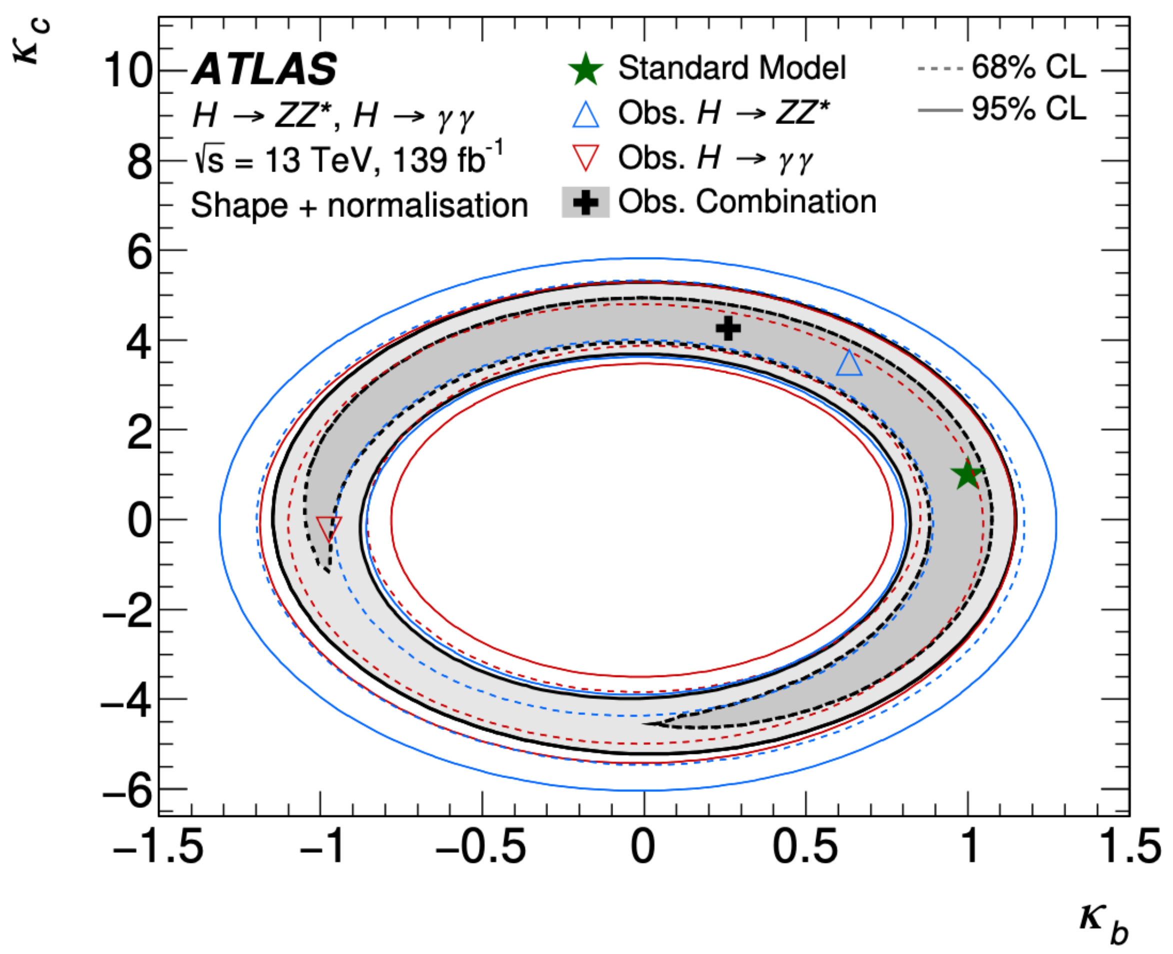

Higgs boson combined differential measurements

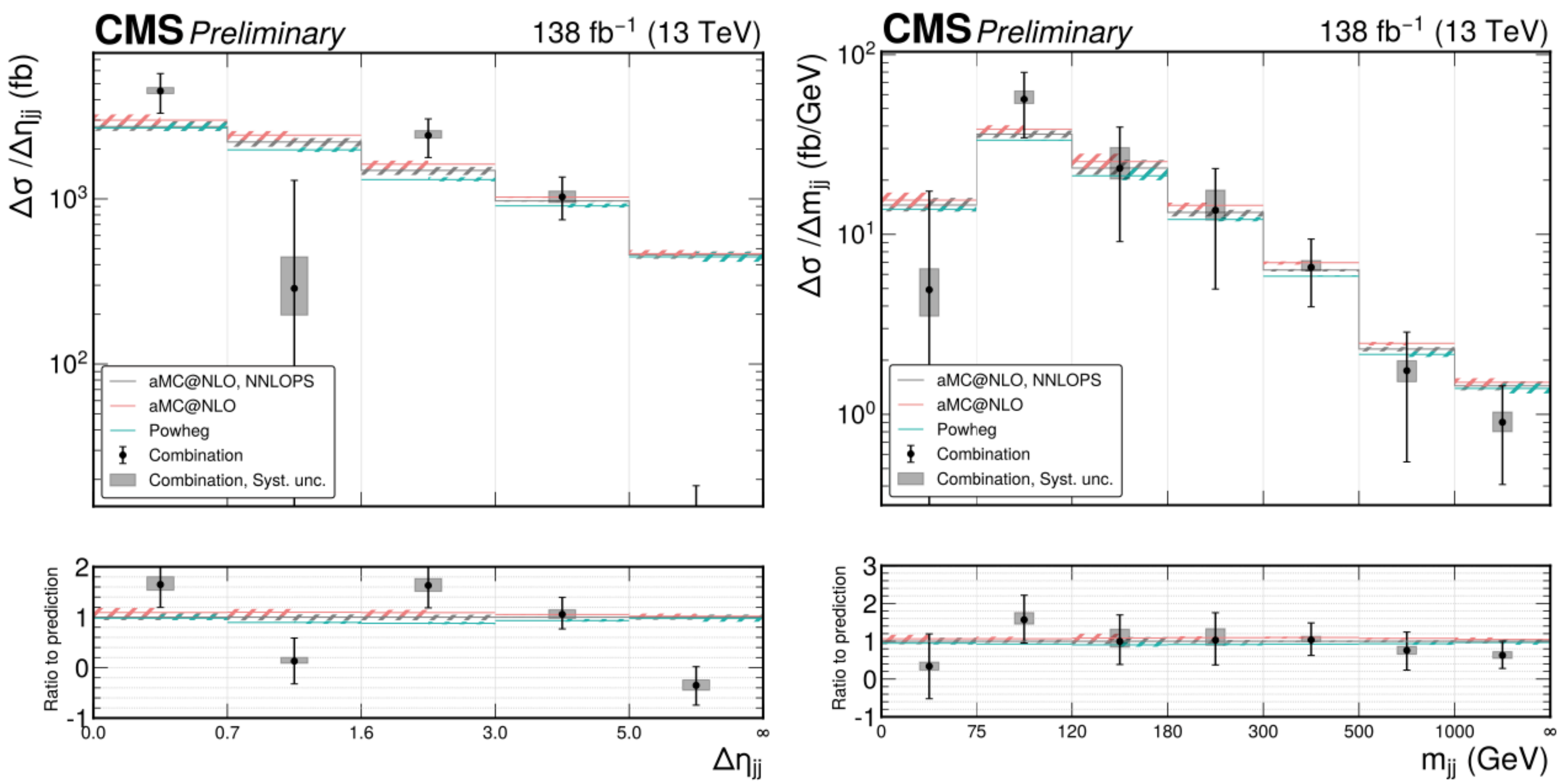

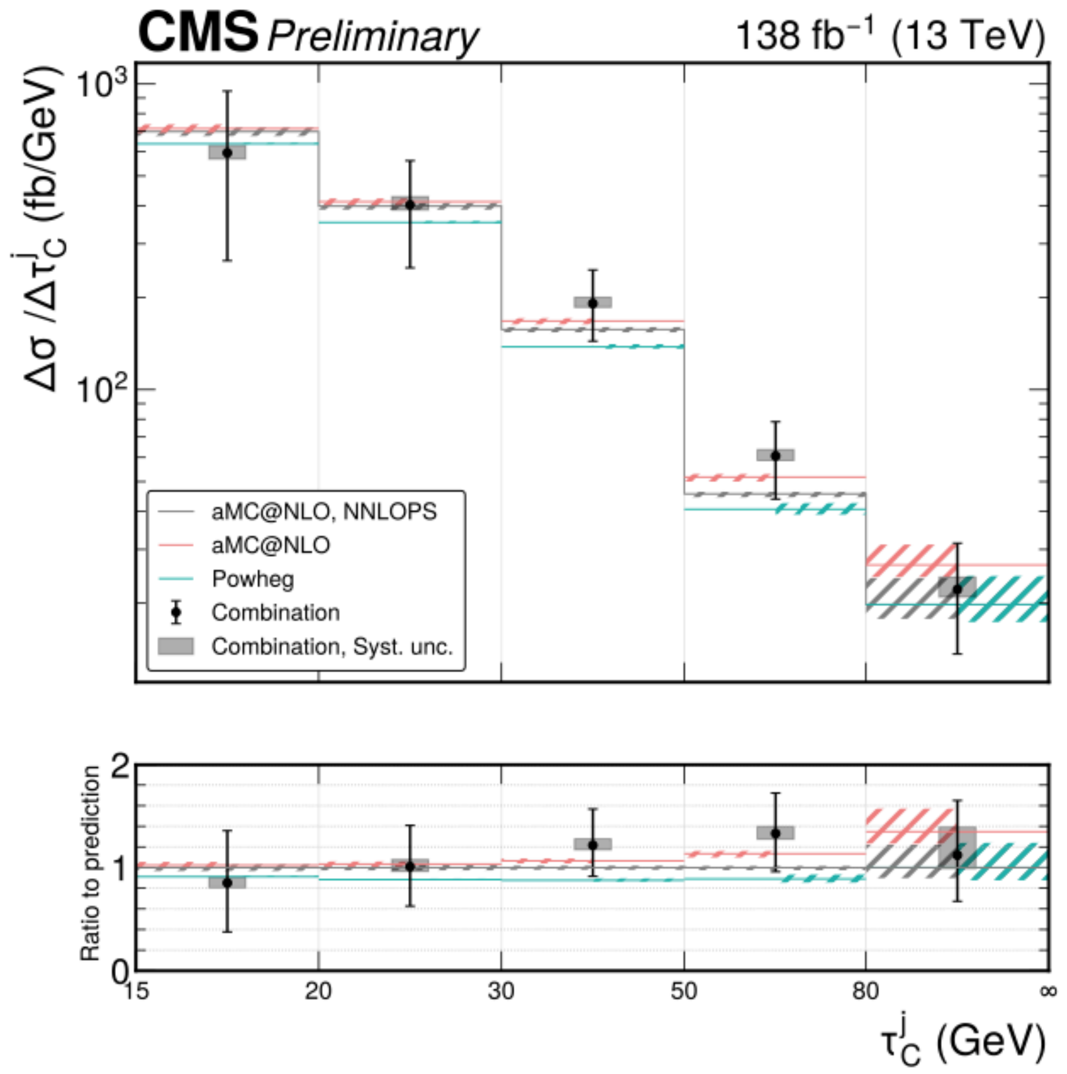

$$\tau_{\mathrm{C}}^{\mathrm{j}} = \max_{k \in \mathrm{jets}} \left(\frac{\sqrt{E_{\mathrm{k}}^2 - p_{\mathrm{z,k}}^2}}{2\cosh\left(y_{\mathrm{k}} - y_{\mathrm{H}}\right)} \right)$$

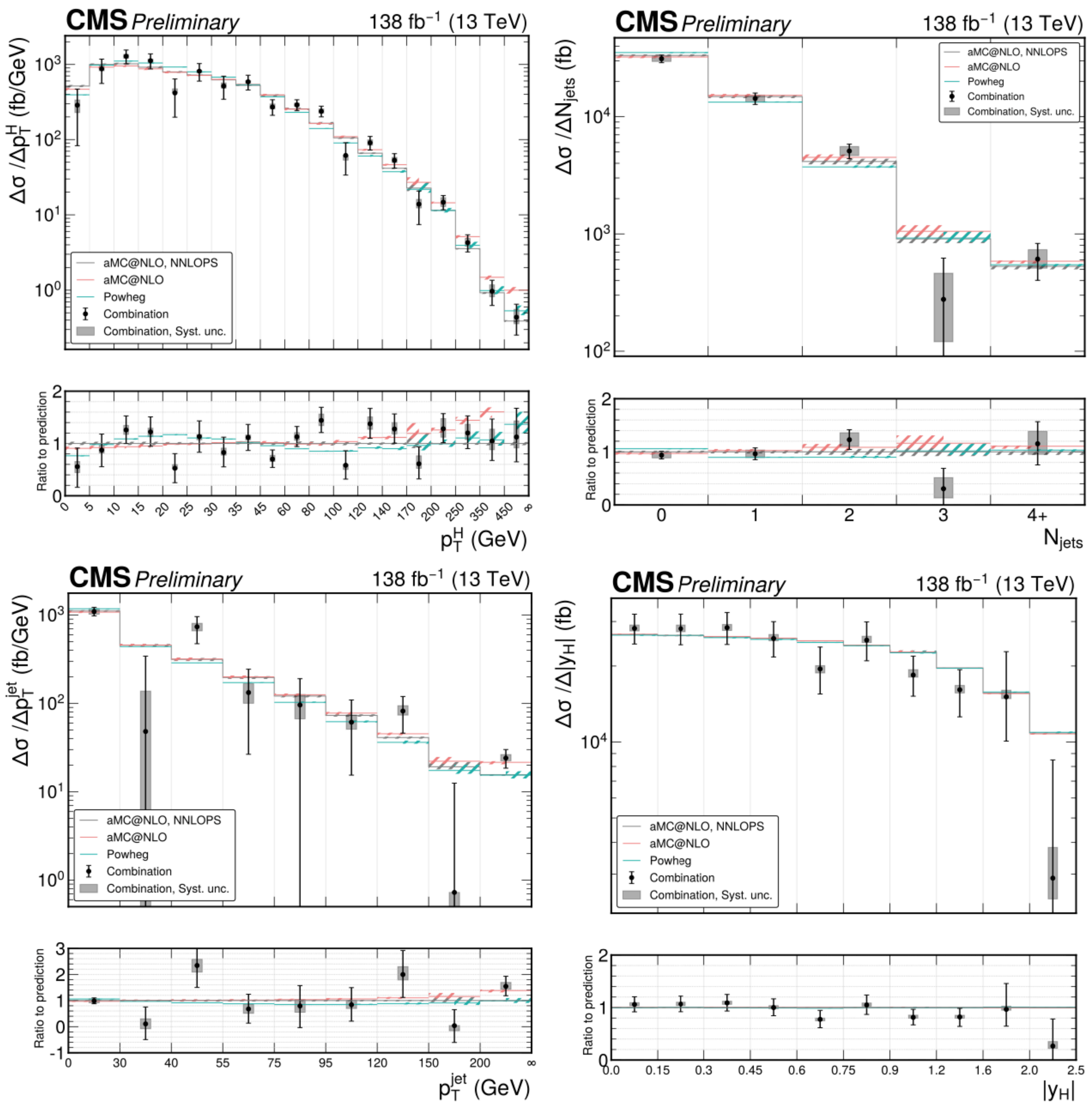

CMS-PAS-HIG-23-013

κ-framework interpretation of combined differential measurements

CMS-PAS-HIG-23-013

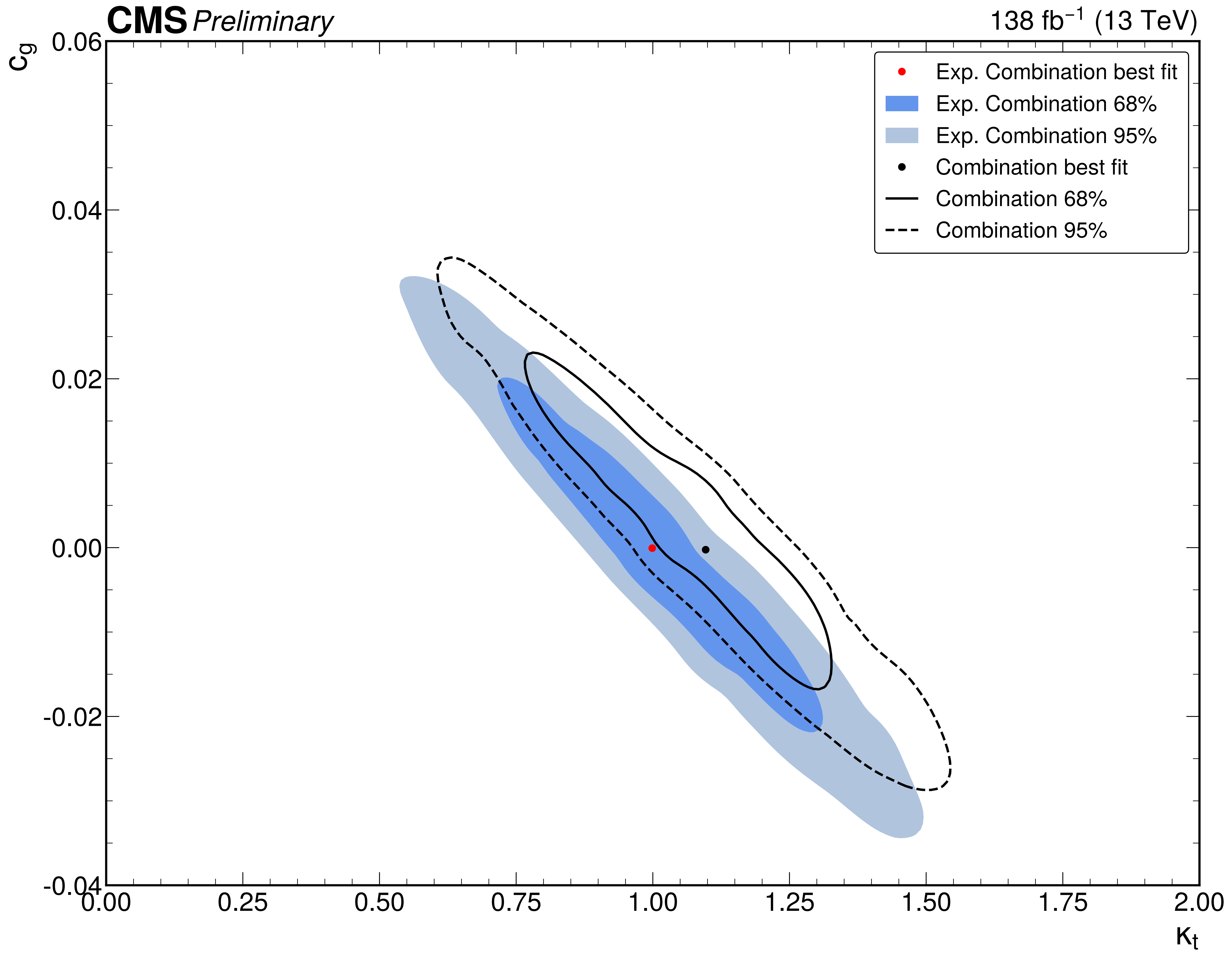

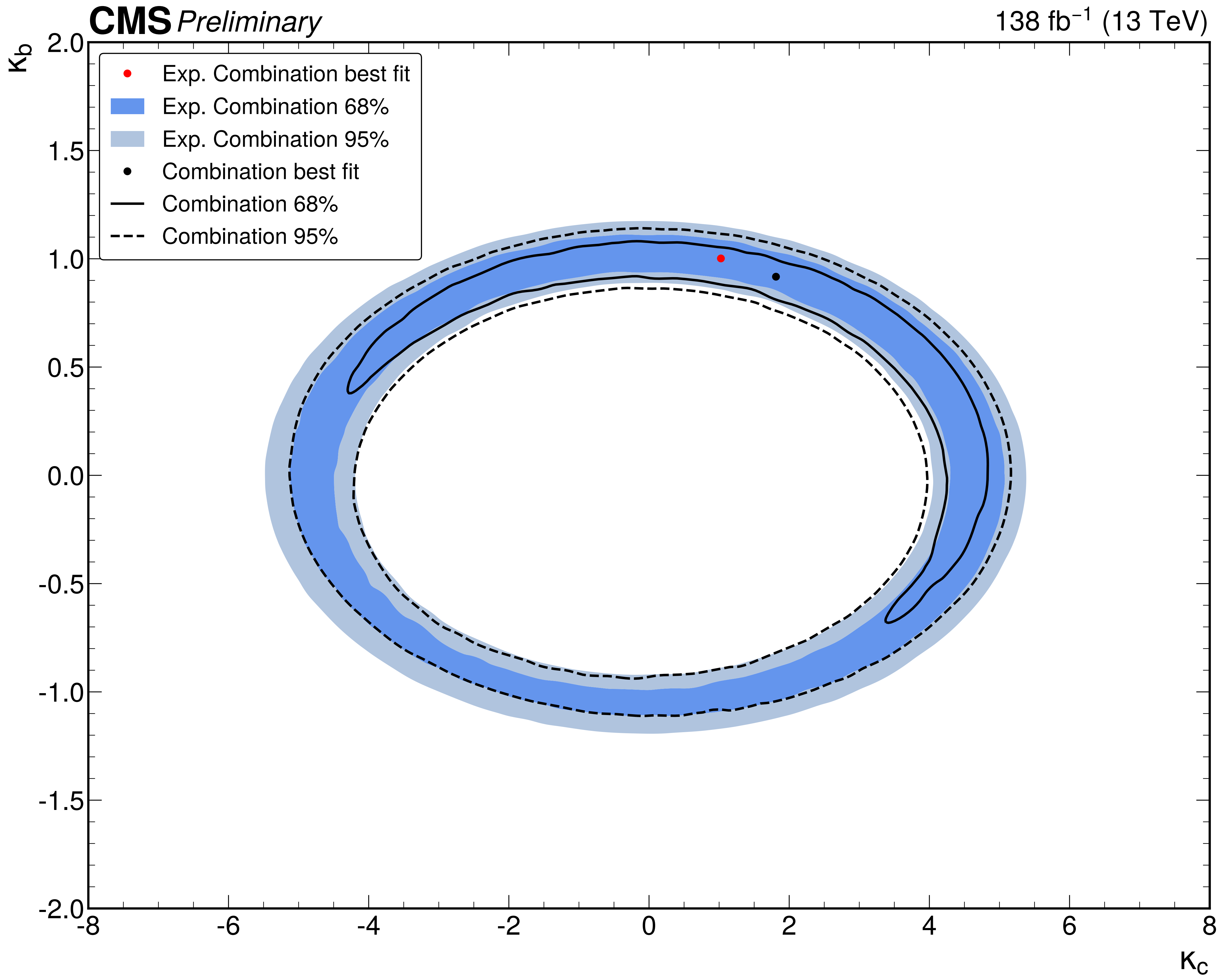

SMEFT interpretation of combined differential measurements

pT(H) 2D scans of Wilson coefficients

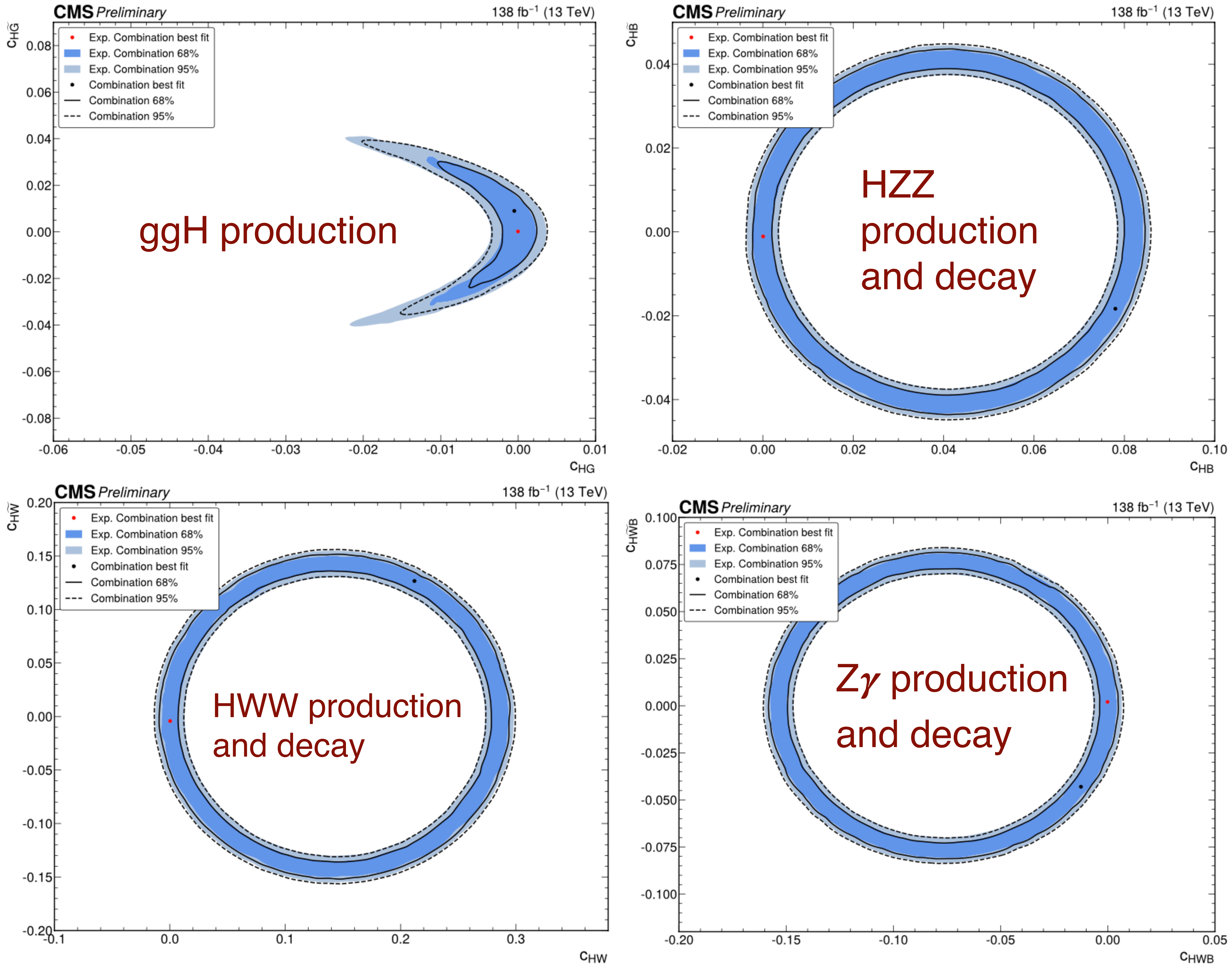

Class	Operator	Wilson coefficient	Example process
$\mathcal{L}_6^{(4)} - X^2H^2$	$H^\dagger H G^a_{\mu\nu} G^{a\mu\nu}$	c_{HG}	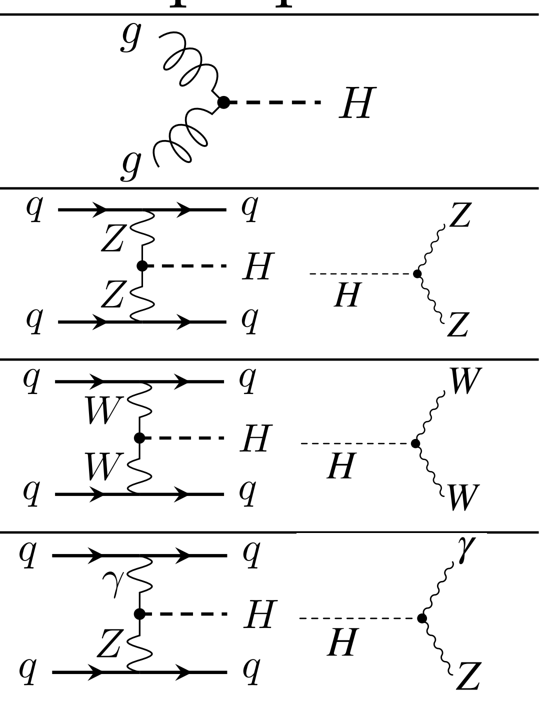
	$H^\dagger H \tilde{G}^a_{\mu\nu} G^{a\mu\nu}$	$\tilde{c}_{HG}$	
	$H^\dagger H B_{\mu\nu} B^{\mu\nu}$	c_{HB}	
	$H^\dagger H \tilde{B}_{\mu\nu} B^{\mu\nu}$	$\tilde{c}_{HB}$	
	$H^\dagger H W^i_{\mu\nu} W^{i\mu\nu}$	c_{HW}	
	$H^\dagger H \tilde{W}^i_{\mu\nu} W^{i\mu\nu}$	$\tilde{c}_{HW}$	
	$H^\dagger \sigma^i H W^i_{\mu\nu} B^{i\mu\nu}$	c_{HWB}	
	$H^\dagger \sigma^i H \tilde{W}^i_{\mu\nu} B^{i\mu\nu}$	$\tilde{c}_{HWB}$	

Fit pairs of CP-even and CP-odd Wilson coefficients to assess their impact on Higgs production and decay, all other coefficients set to their SM values of zero.

CMS-PAS-HIG-23-013

SMEFT interpretation of combined differential measurements

CMS-PAS-HIG-23-013

Summary of observed and expected confidence intervals at 68% and 95% CL for the first ten eigenvectors.

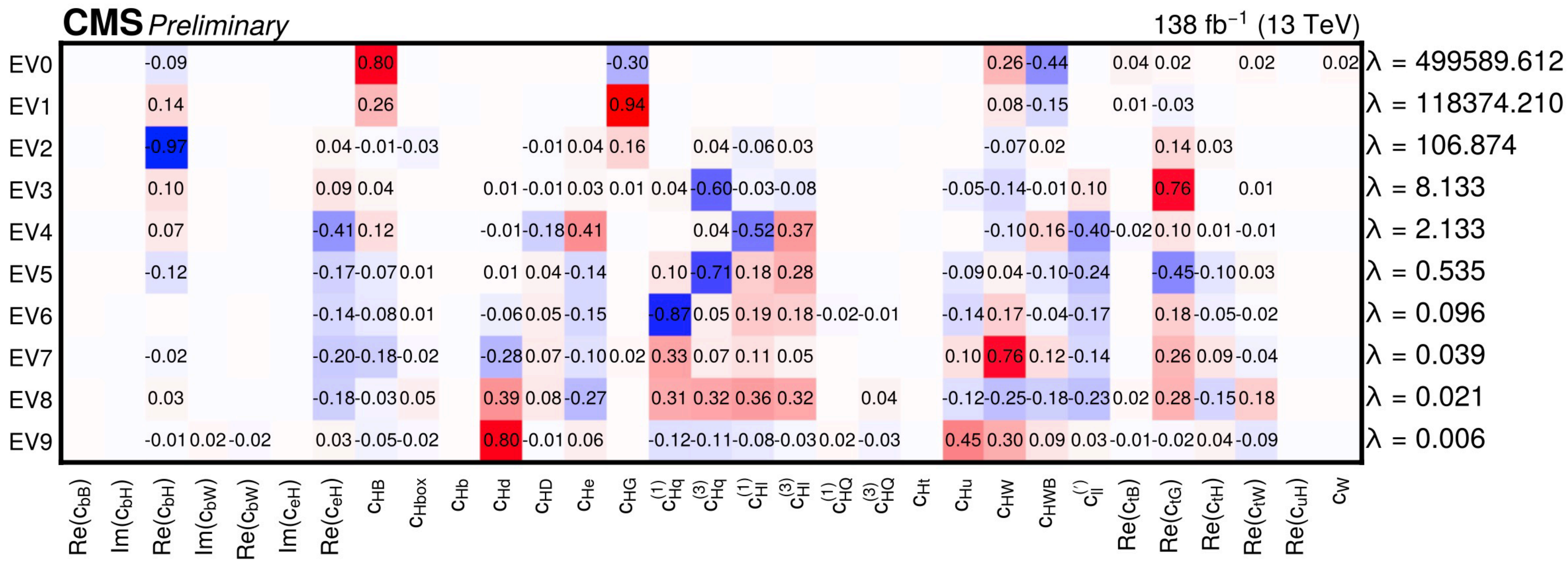

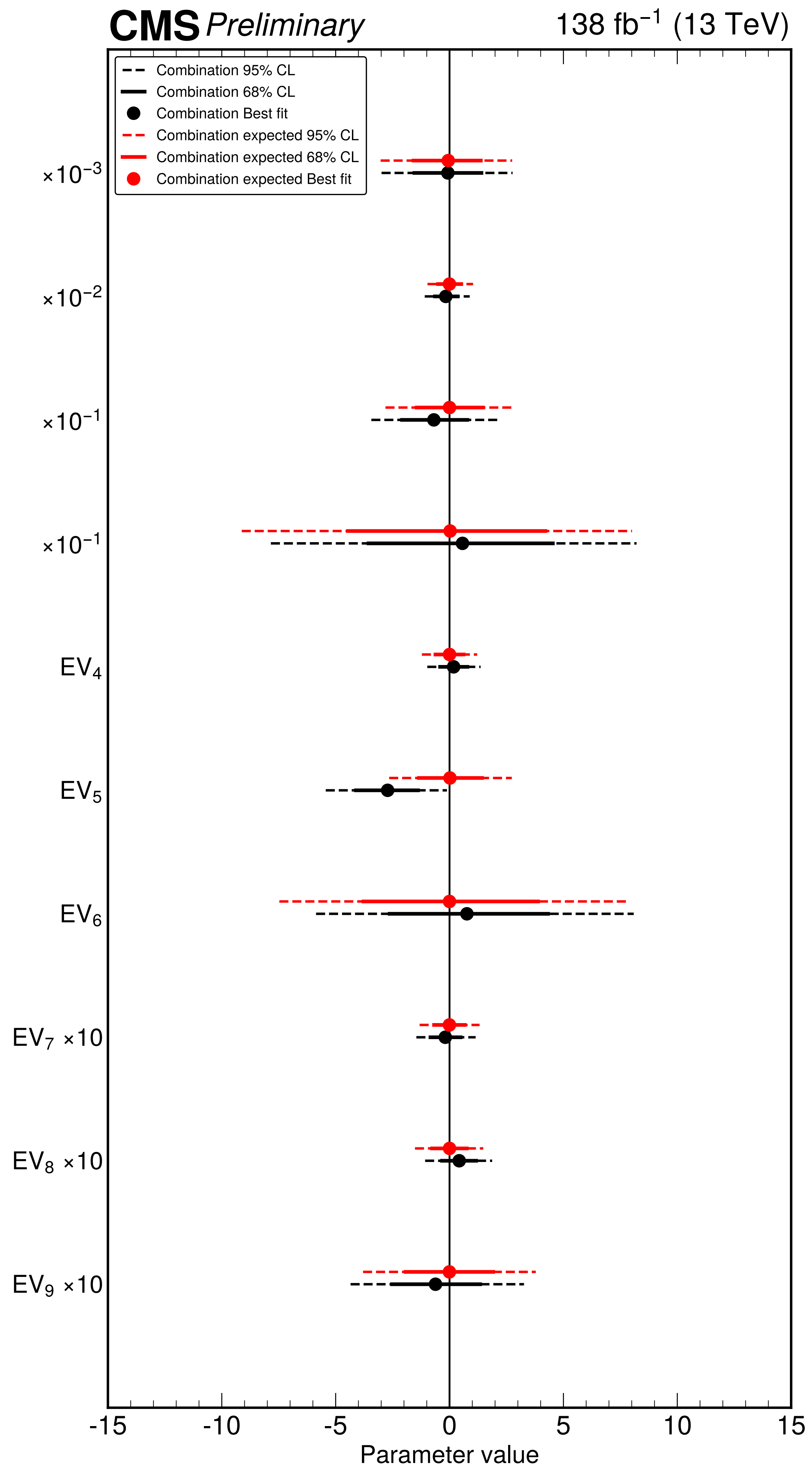

Determine orthogonal linear combinations of the most constrained Wilson coefficients from the data to simultaneously constrain 10 directions (EV) in parameter space.

SMEFT interpretation of combined differential measurements

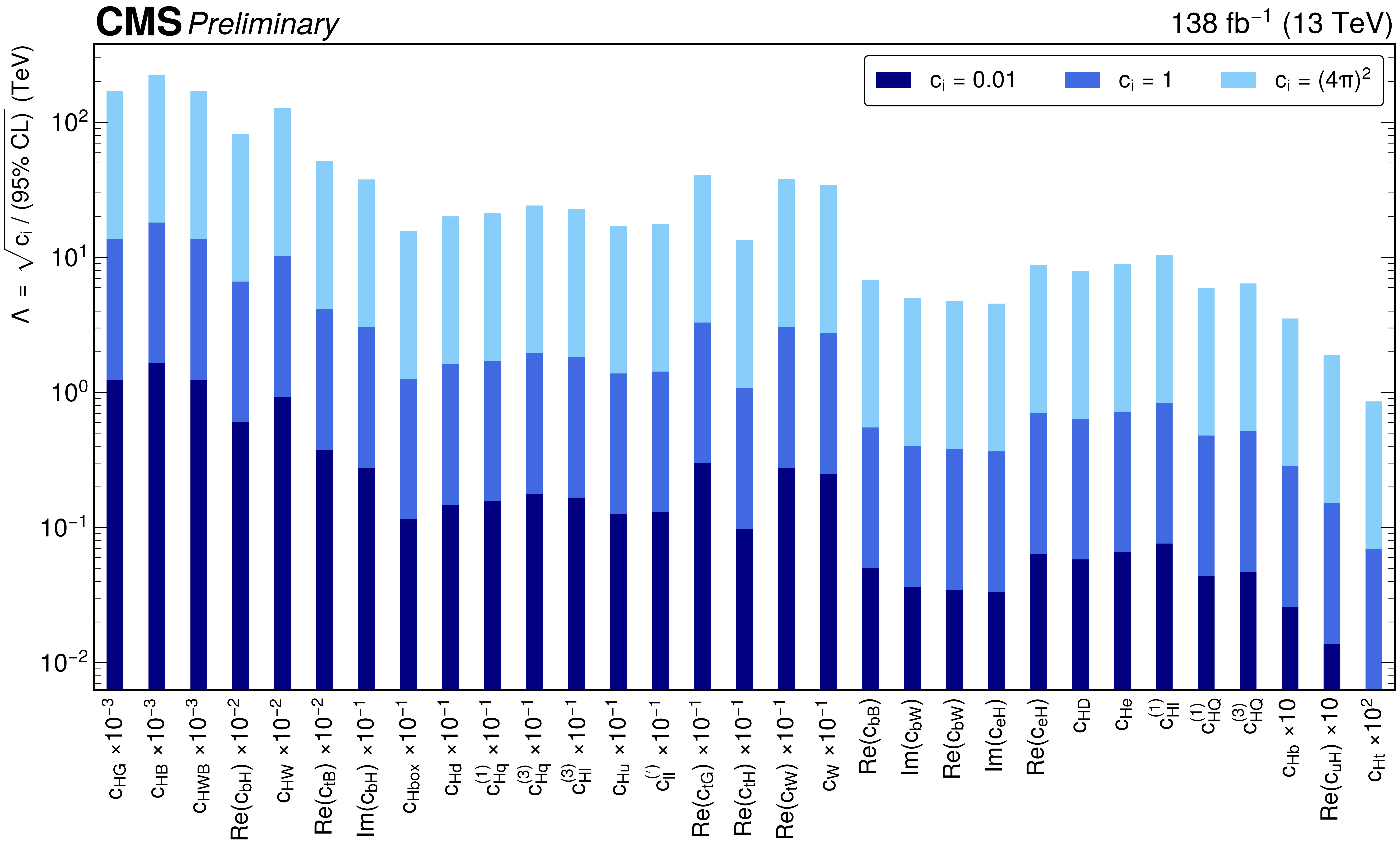

CMS-PAS-HIG-23-013

95% CL limits for each Wilson coefficient, others fixed to their SM value of zero, interpreted in terms of the energy scale Λ for three different assumptions for the value of the coefficient

Comparison of SMEFT interpretation: STXS vs differential combination

arXiv:2402.05742 submitted to JHEP

$$ev^{[1]} = 0.999c_{HG} - 0.035c_{tG} - 0.003c_{tH}$$
$$ev^{[2]} = 0.035c_{HG} + 0.978c_{tG} + 0.205c_{tH}$$
$$ev^{[3]} = -0.005c_{HG} - 0.205c_{tG} + 0.979c_{tH}$$

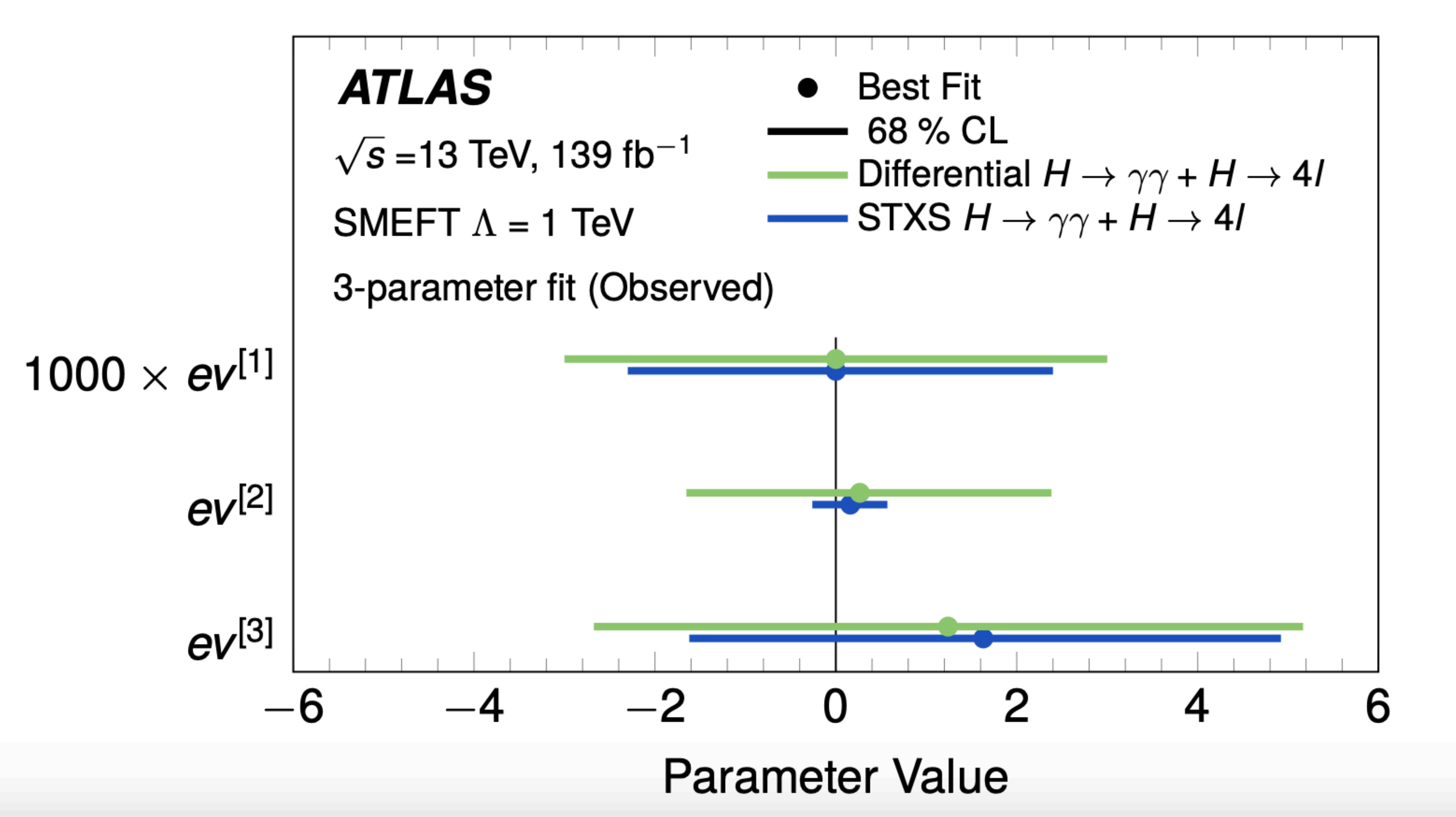

The large sensitivity difference observed for $ev^{[2]}$ originates from the separate measurements of ggF and ttH production in the STXS framework

Run 3: HH→ZZ*→4l at 13.6 TeV

- Measurements of inclusive and differential cross sections
- Using 34.7 fb^{-1} from 2022, dominated by data statistics

$$H \rightarrow ZZ$$
$$\sigma_{\text{fid}} = 2.94^{+0.53}_{-0.49}\ (\text{stat.})^{+0.29}_{-0.22}\ (\text{syst.})\ \text{fb}$$

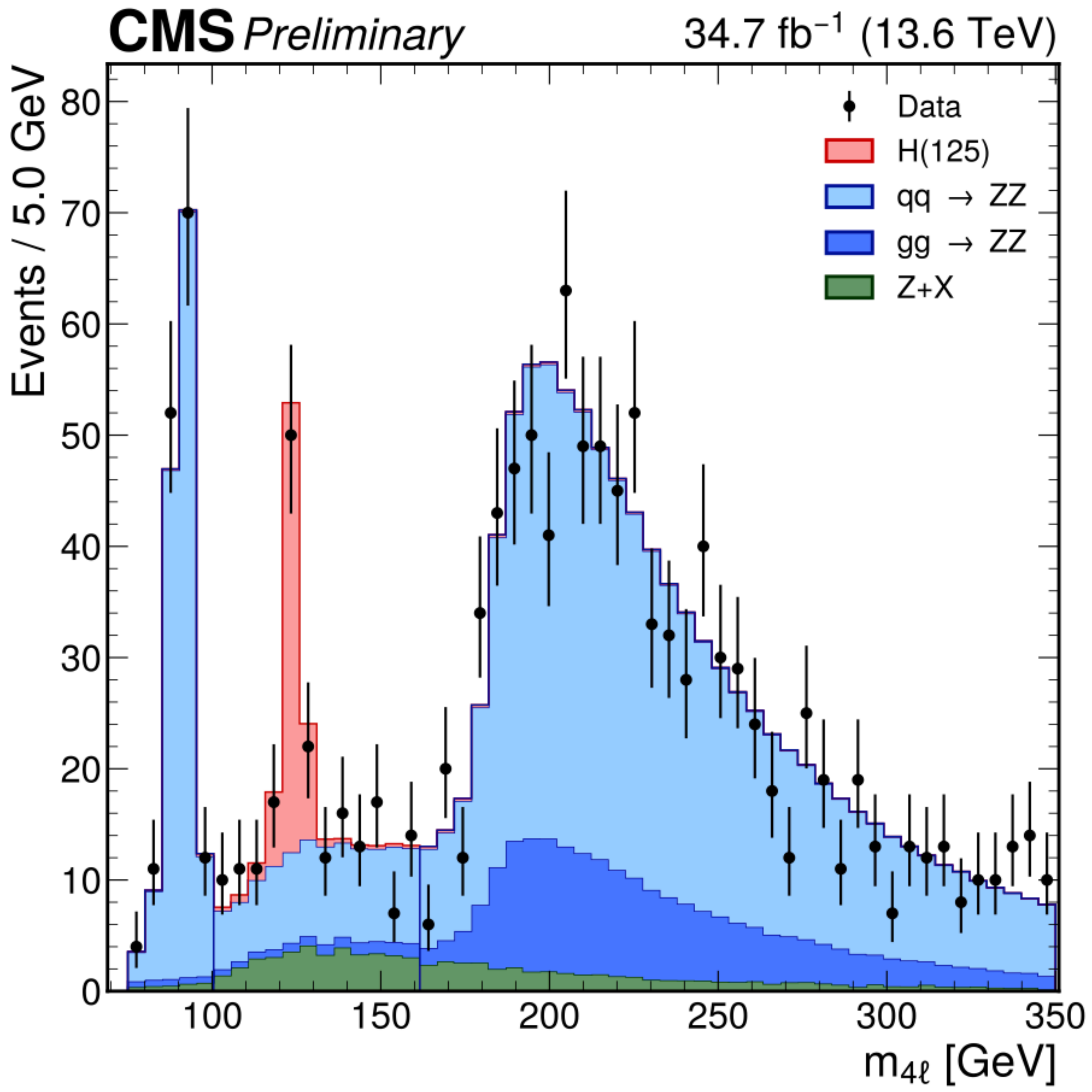

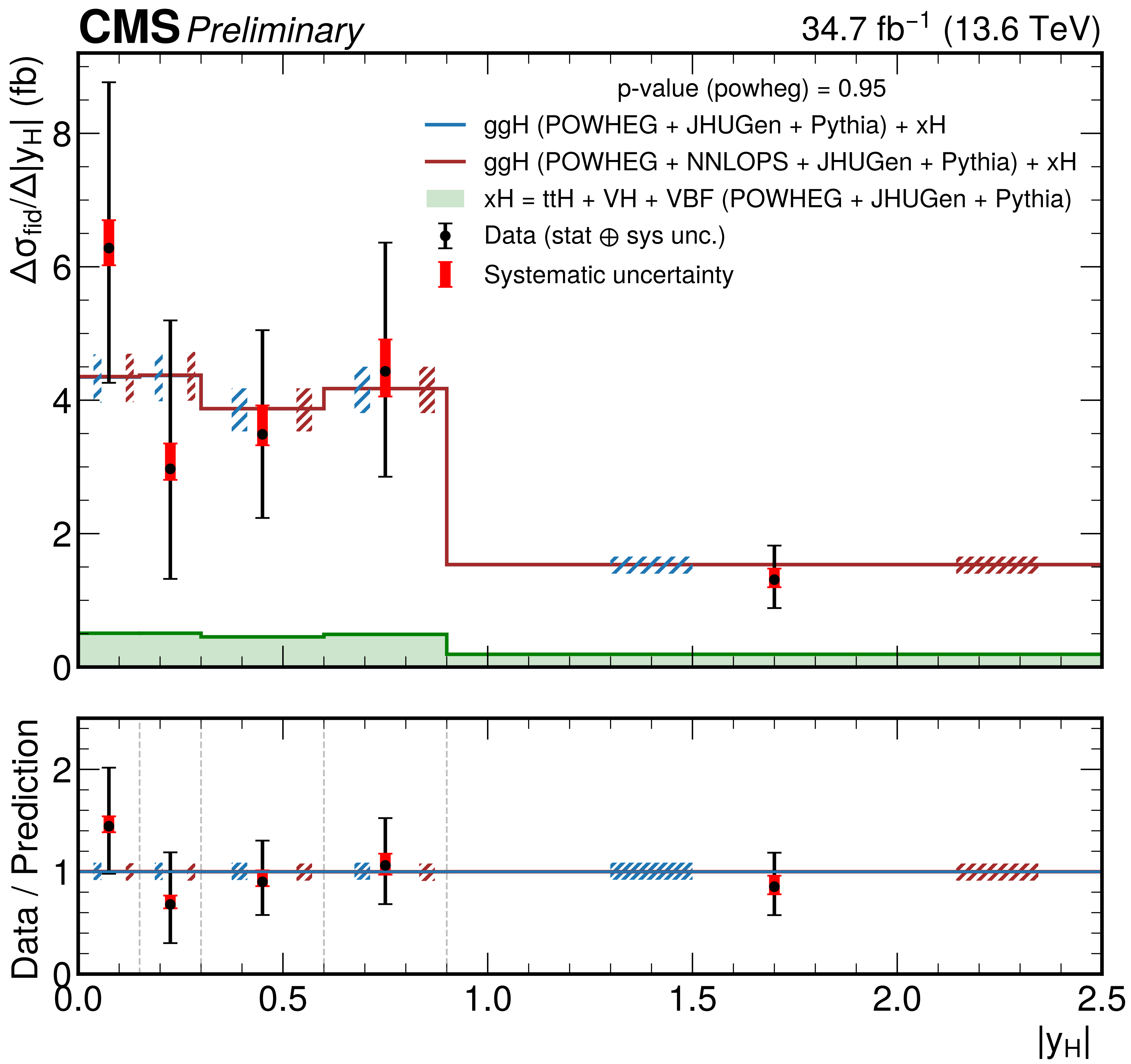

Run 3: $H\to\gamma\gamma$ at 13.6 TeV

- Using 34.7 fb^{-1} from 2022, dominated by data statistics
- Measurements of fiducial and differential cross sections

$$H \to \gamma\gamma \quad \sigma_{\mathrm{fid}} = 78 \pm 11\ (\mathrm{stat.})^{+6}_{-5}\ (\mathrm{syst.})\ \mathrm{fb}$$

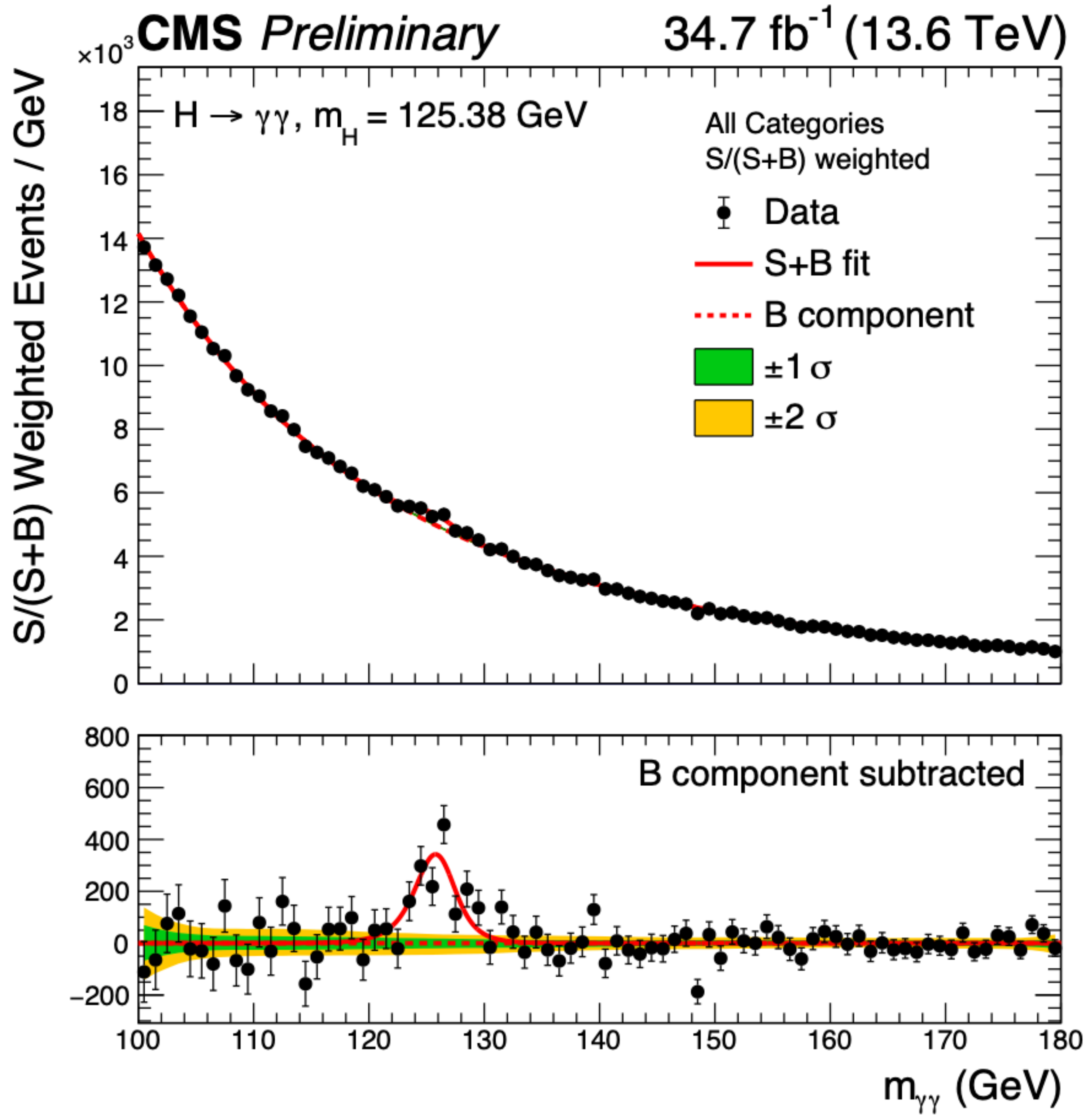

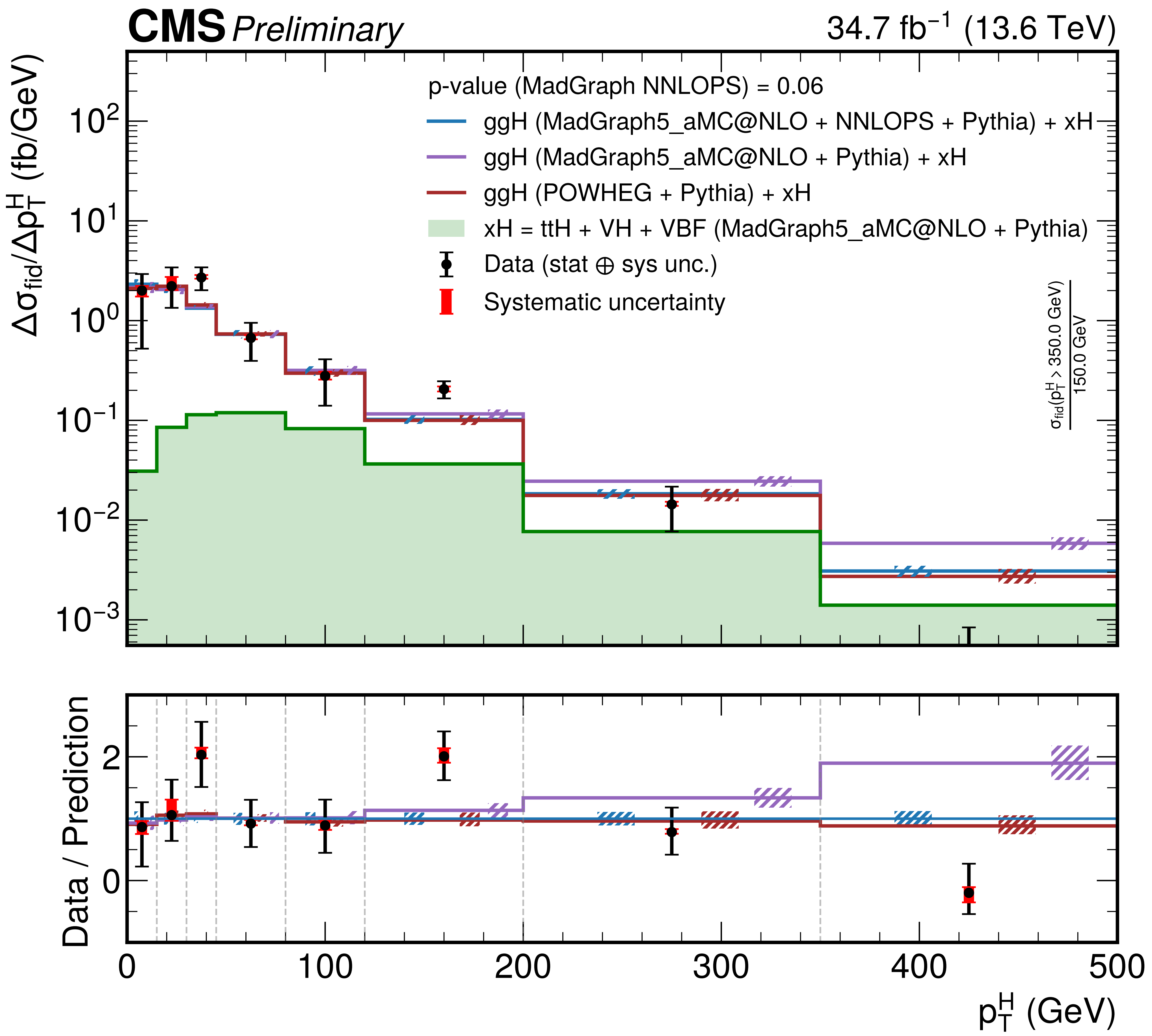

Run 3: $H\to\gamma\gamma$ and $H\to ZZ$ at 13.6 TeV

Eur. Phys. J. C 84 (2024) 78

- Fiducial cross section measurements.
- Using 13.6 fb^{-1} from 2022, dominated by data statistics

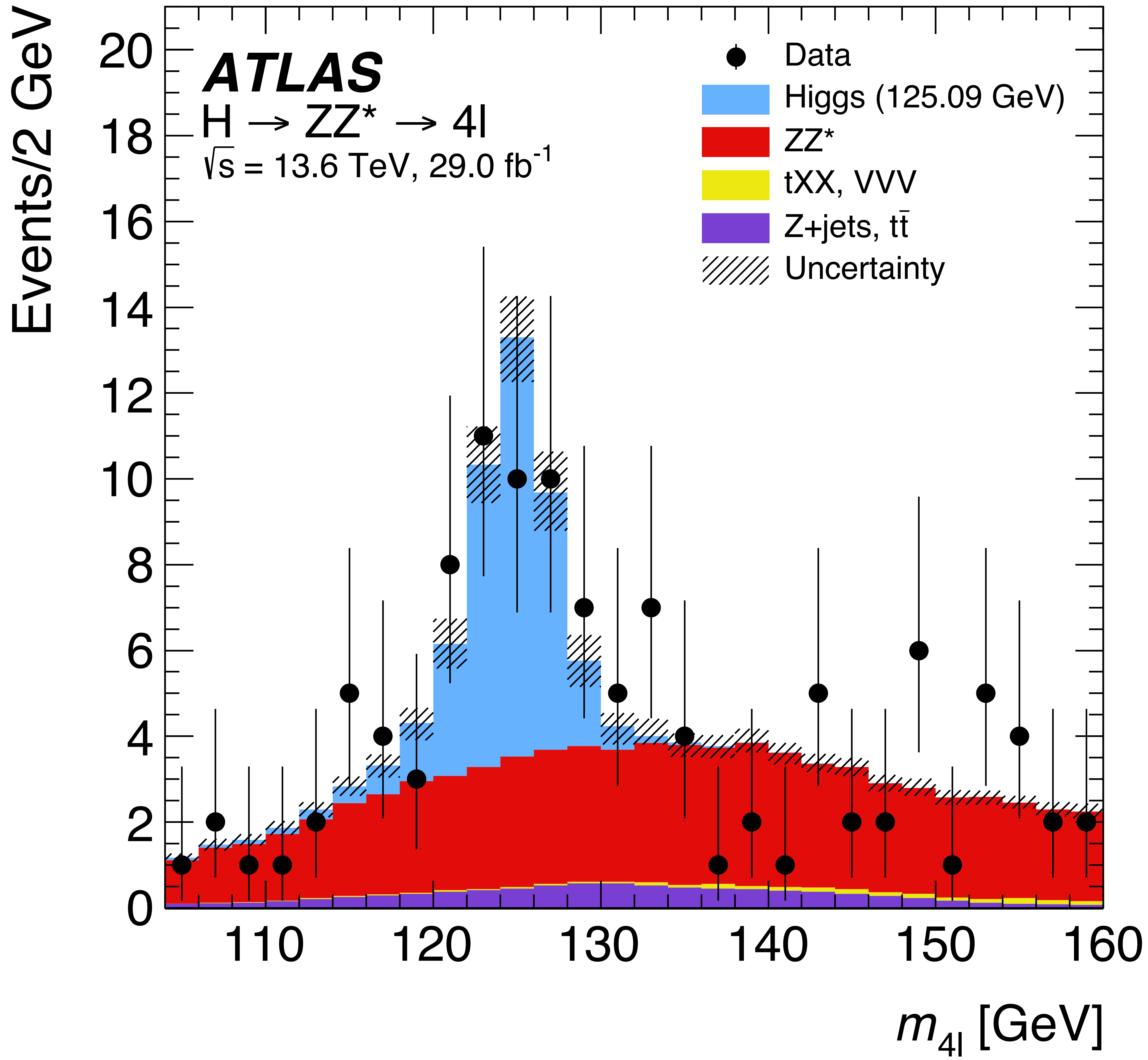

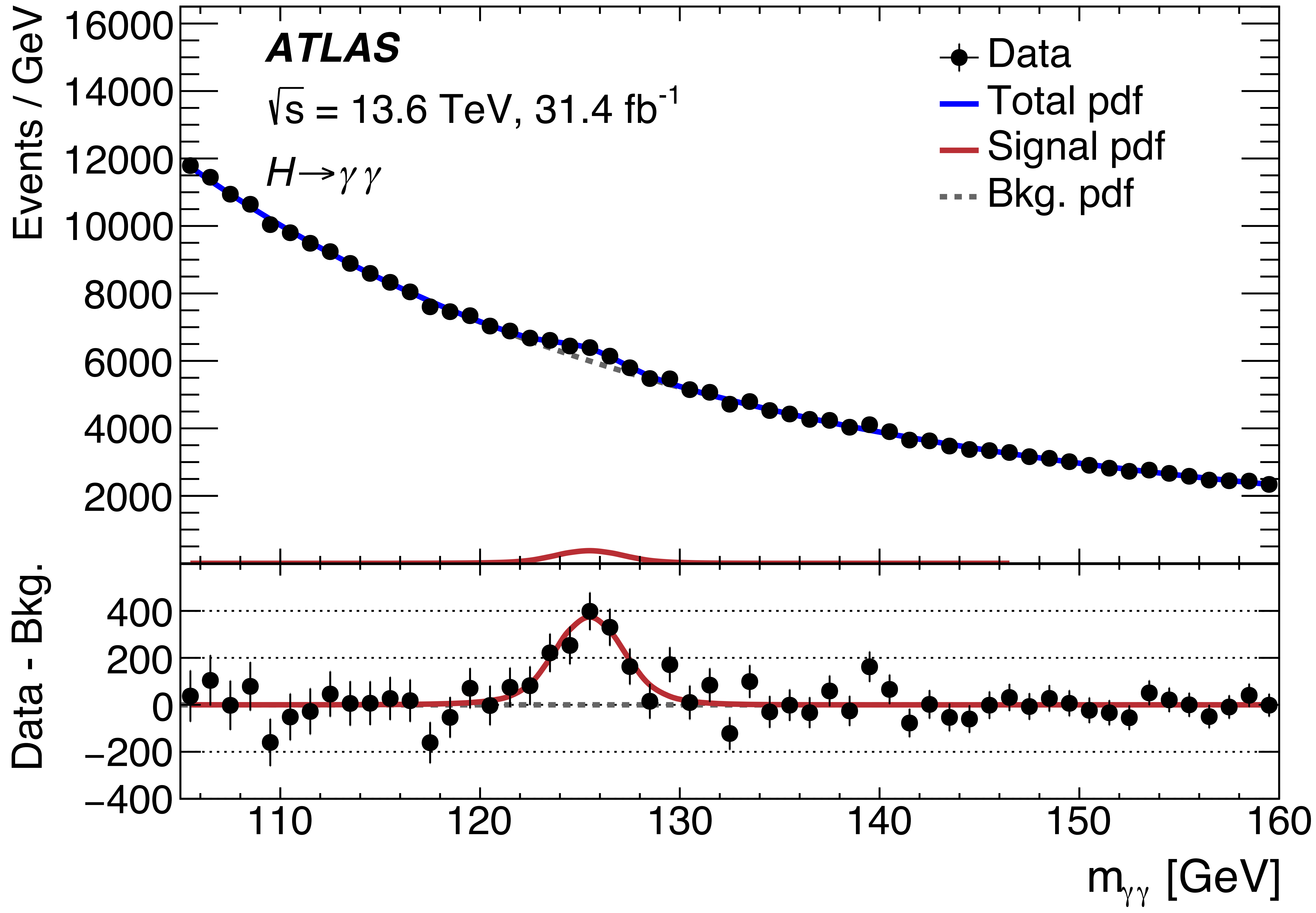

Run 3: combination of $H\to\gamma\gamma$ and $H\to ZZ$ at 13.6 TeV

- Total and fiducial cross-section measurements
- Using 13.6 fb^{-1} from 2022, dominated by data statistics

Eur. Phys. J. C 84 (2024) 78

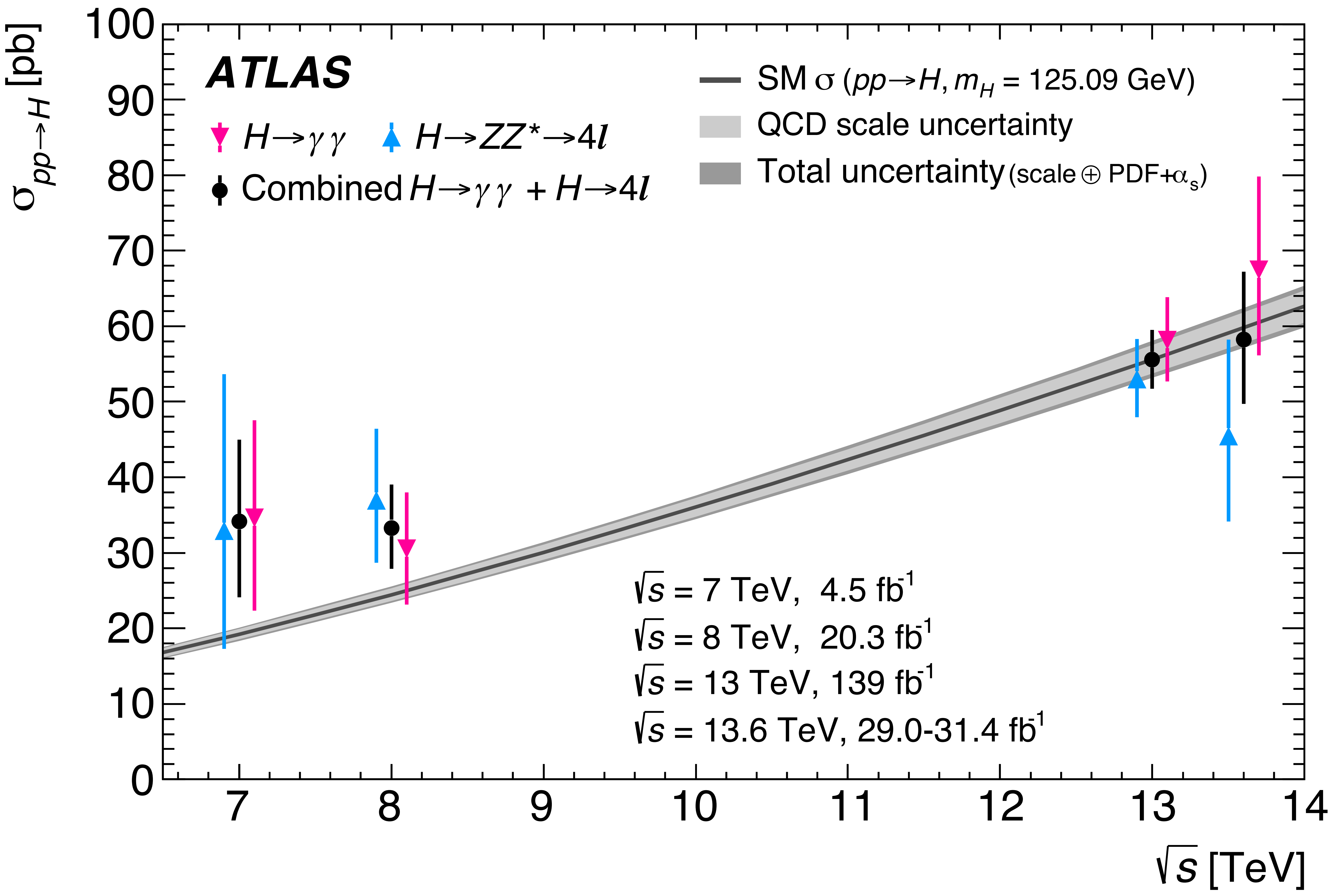

Total cross-section measurement:

$H\to\gamma\gamma$: 67^{+12}_{-11} pb,

$H\to ZZ$: 46 ± 12 pb

combined: of 58.2 ± 8.7 pb

to be compared with the Standard Model prediction of 59.9 ± 2.6 pb.

Conclusion and outlook

- Precision measurements of Higgs boson properties so far agree with SM, hints for new physics could be unravelled as data accumulates and analysis advance
  - Higgs boson mass 0.1% precision
  - Significant progress in fiducial/differential and STXS measurements and reinterpretation in κ-framework and SMEFT
  - significance progress in partial Run 3 results
- Looking forward to LHC Run 3 and beyond

Projection for HL-LHC: arXiv:1902.00134

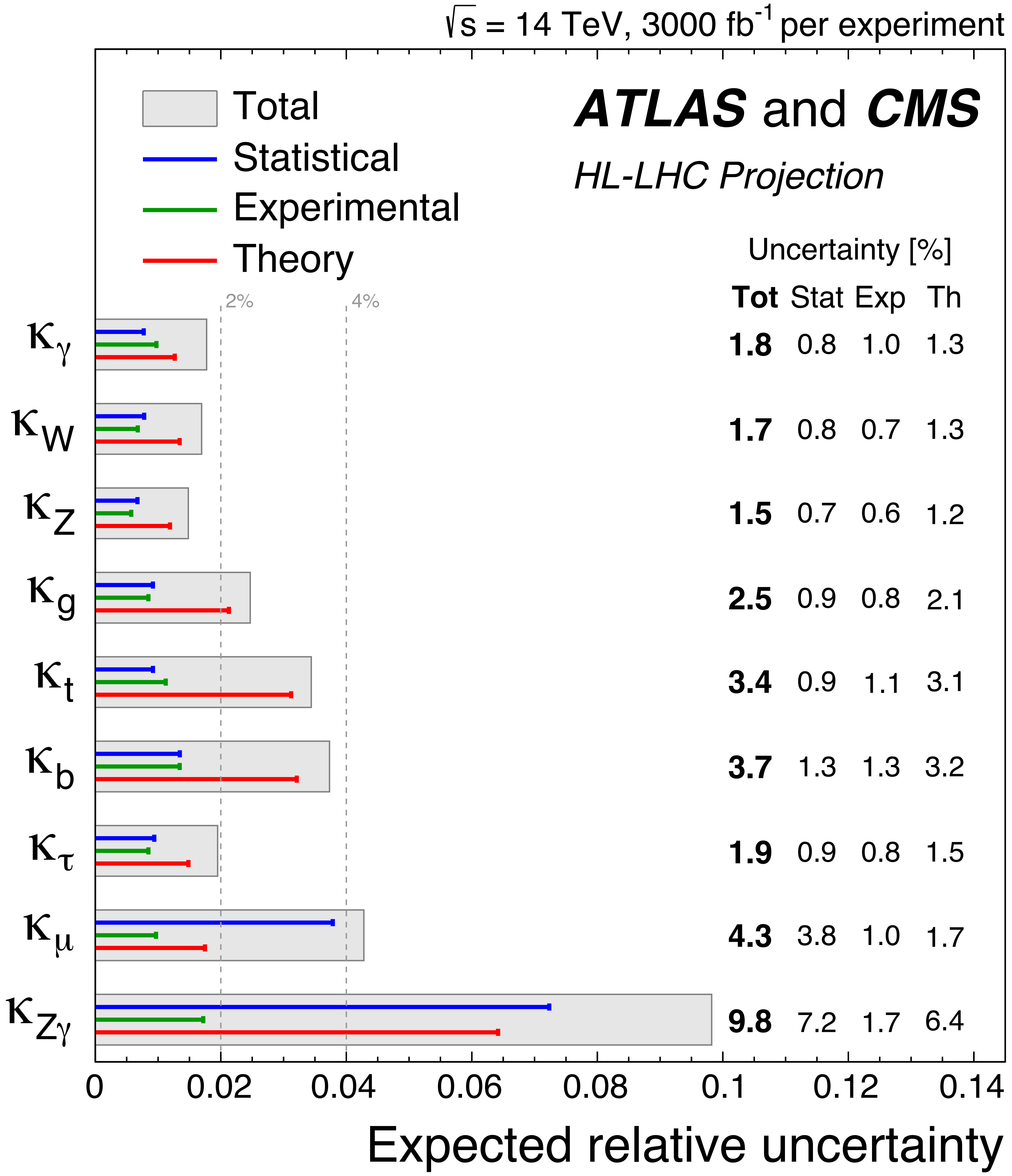

Apologies for all I could not cover

Thank you!

Higgs boson production and decay rates

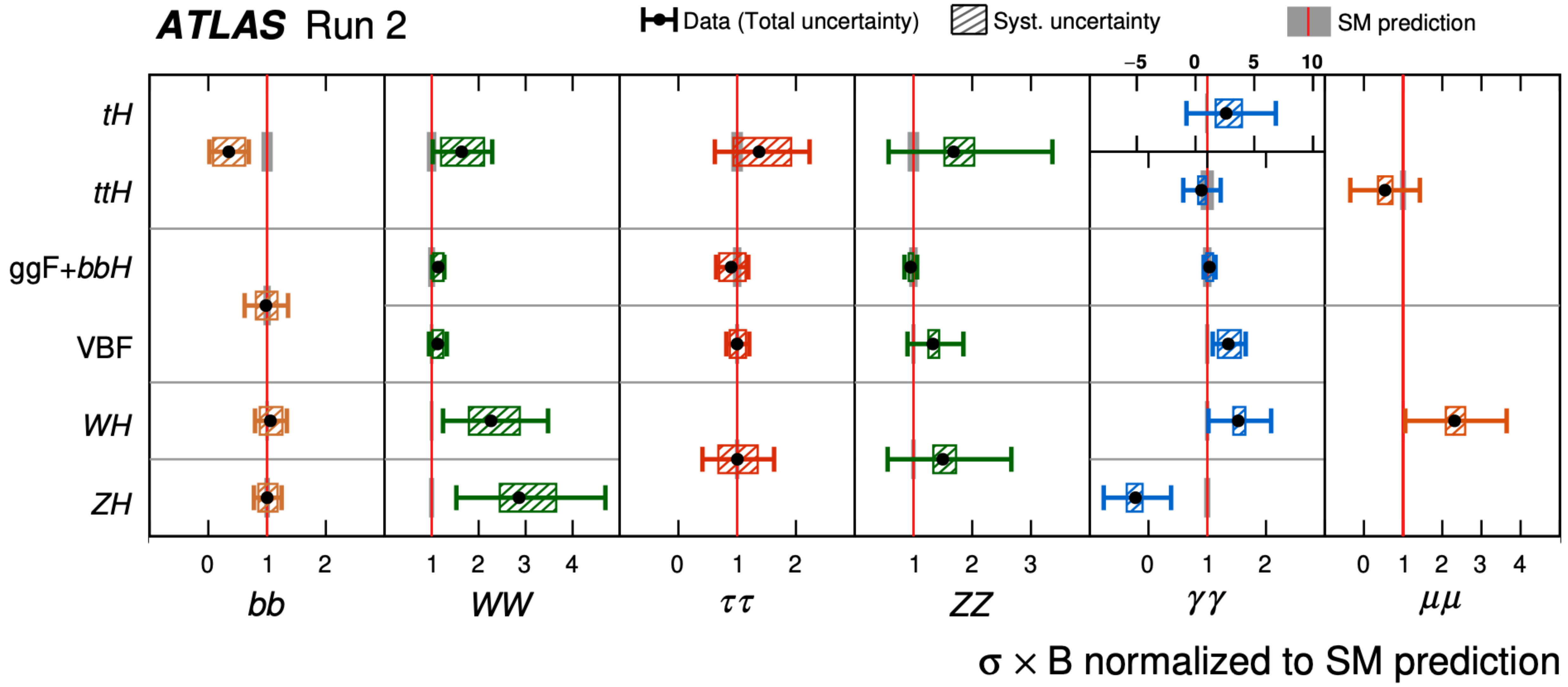

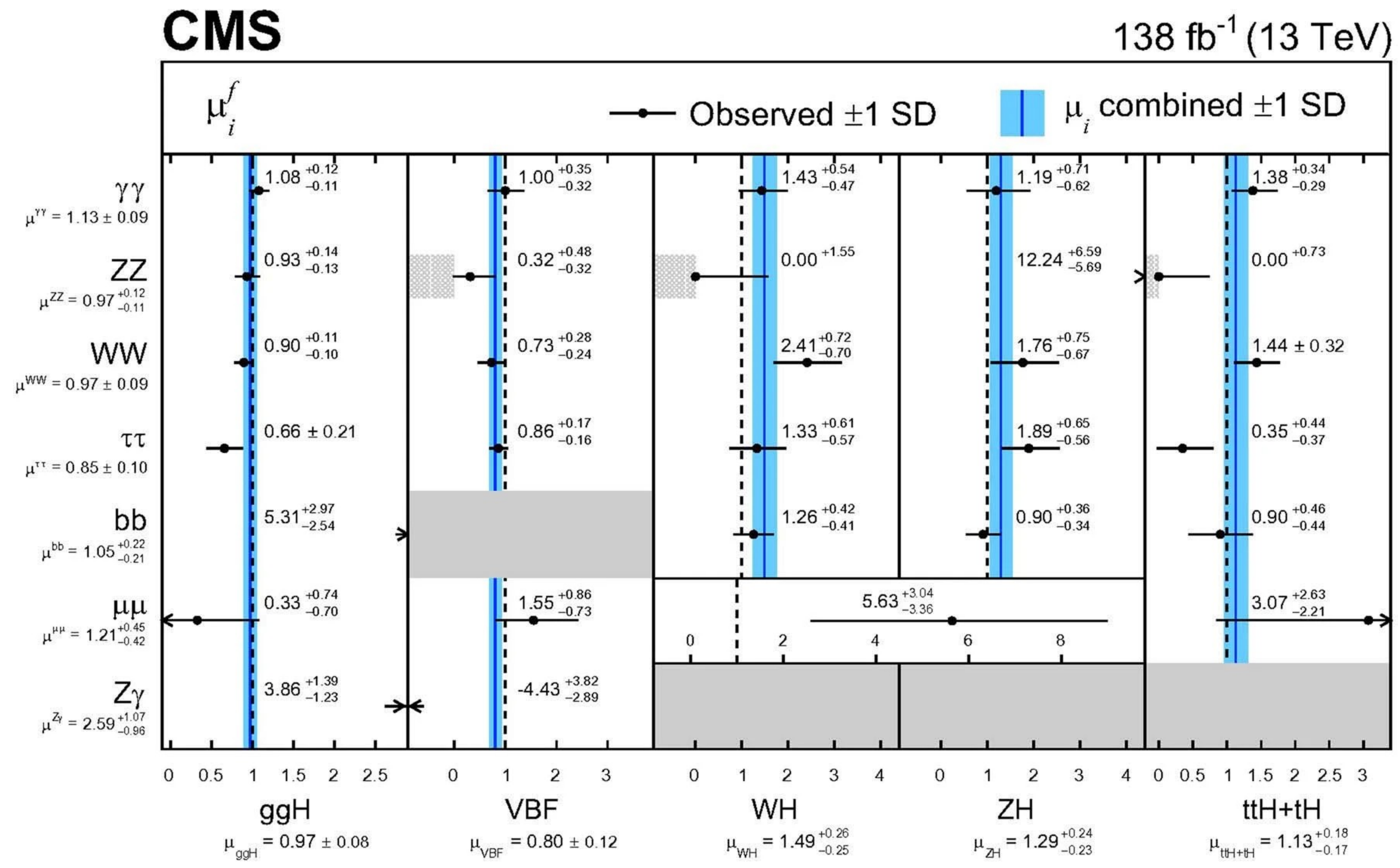

Production cross section	Effective coupling	Parametrization in terms of coupling strength modifiers
$\sigma(\text{ggF})$	κ_g^2	$1.040\,\kappa_t^2 + 0.002\,\kappa_b^2 - 0.038\,\kappa_t\kappa_b - 0.005\,\kappa_t\kappa_c$
$\sigma(\text{VBF})$	-	$0.733\,\kappa_W^2 + 0.267\,\kappa_Z^2$
$\sigma(qq/qg \to ZH)$	-	κ_Z^2
$\sigma(gg \to ZH)$	-	$2.456\,\kappa_Z^2 + 0.456\,\kappa_t^2 - 1.903\,\kappa_Z\kappa_t - 0.011\,\kappa_Z\kappa_b + 0.003\,\kappa_t\kappa_b$
$\sigma(WH)$	-	κ_W^2
$\sigma(t\bar{t}H)$	-	κ_t^2
$\sigma(tHW)$	-	$2.909\,\kappa_t^2 + 2.310\,\kappa_W^2 - 4.220\,\kappa_t\kappa_W$
$\sigma(tHq)$	-	$2.633\,\kappa_t^2 + 3.578\,\kappa_W^2 - 5.211\,\kappa_t\kappa_W$
$\sigma(b\bar{b}H)$	-	κ_b^2
Partial decay width		
Γ^{bb}	-	κ_b^2
Γ^{WW}	-	κ_W^2
Γ^{gg}	κ_g^2	$1.111\,\kappa_t^2 + 0.012\,\kappa_b^2 - 0.123\,\kappa_t\kappa_b$
$\Gamma^{\tau\tau}$	-	κ_τ^2
Γ^{ZZ}	-	κ_Z^2
Γ^{cc}	-	$\kappa_c^2\ (=\kappa_t^2)$
$\Gamma^{\gamma\gamma}$	κ_γ^2	$1.589\,\kappa_W^2 + 0.072\,\kappa_t^2 - 0.674\,\kappa_W\kappa_t$ $+0.009\,\kappa_W\kappa_\tau + 0.008\,\kappa_W\kappa_b - 0.002\,\kappa_t\kappa_b - 0.002\,\kappa_t\kappa_\tau$
$\Gamma^{Z\gamma}$	$\kappa_{Z\gamma}^2$	$1.118\,\kappa_W^2 - 0.125\,\kappa_W\kappa_t + 0.004\,\kappa_t^2 + 0.003\,\kappa_W\kappa_b$
Γ^{ss}	-	$\kappa_s^2\ (=\kappa_b^2)$
$\Gamma^{\mu\mu}$	-	κ_μ^2
Total width ($B_{\text{inv.}} = B_{\text{u.}} = 0$)		
Γ_H	κ_H^2	$0.581\,\kappa_b^2 + 0.215\,\kappa_W^2 + 0.082\,\kappa_g^2 + 0.063\,\kappa_\tau^2 + 0.026\,\kappa_Z^2 + 0.029\,\kappa_c^2$ $+0.0023\,\kappa_\gamma^2 + 0.0015\,\kappa_{Z\gamma}^2 + 0.0004\,\kappa_s^2 + 0.00022\,\kappa_\mu^2$

Nature 607, 52–59 (2022)

Higgs boson production and decay rates

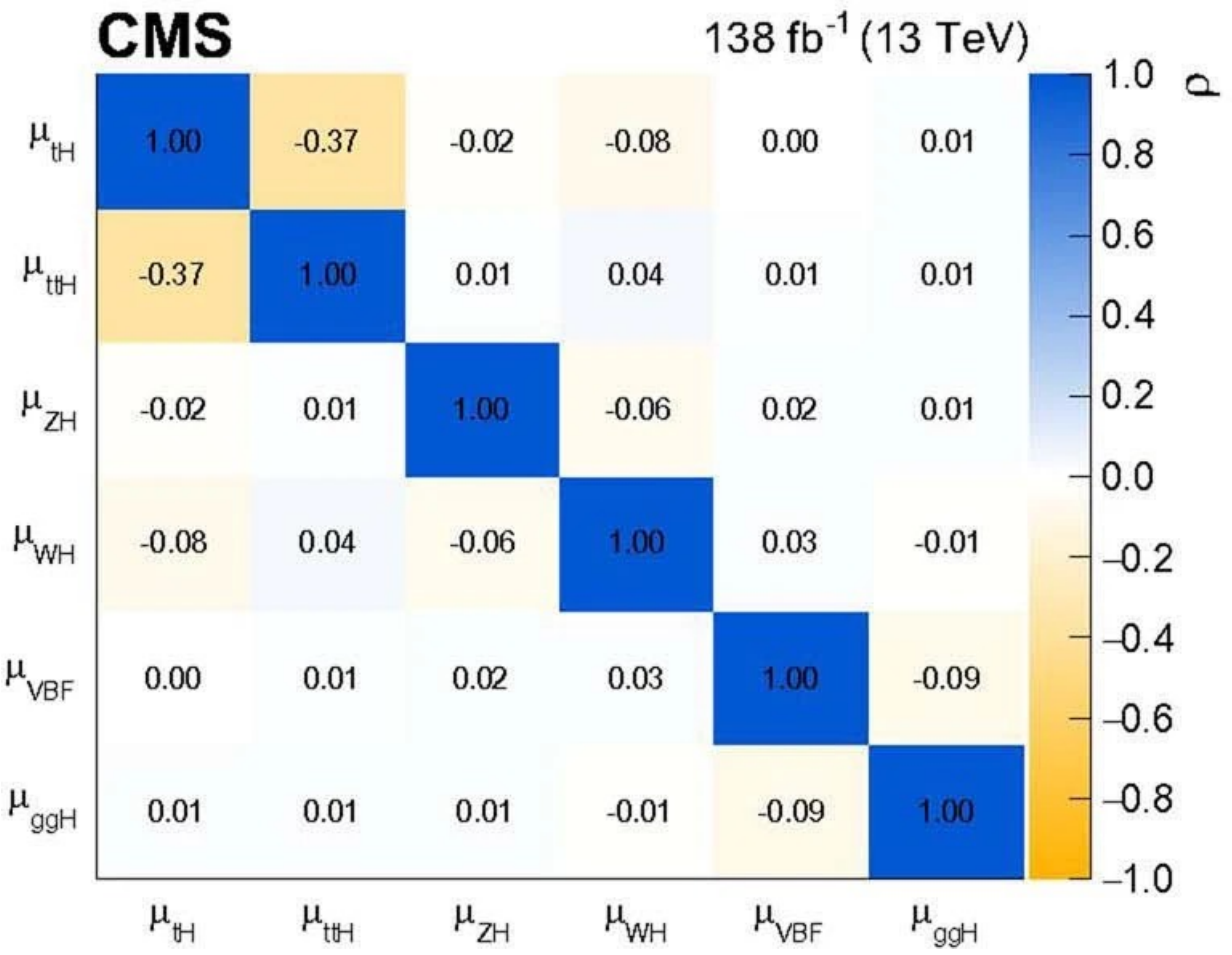

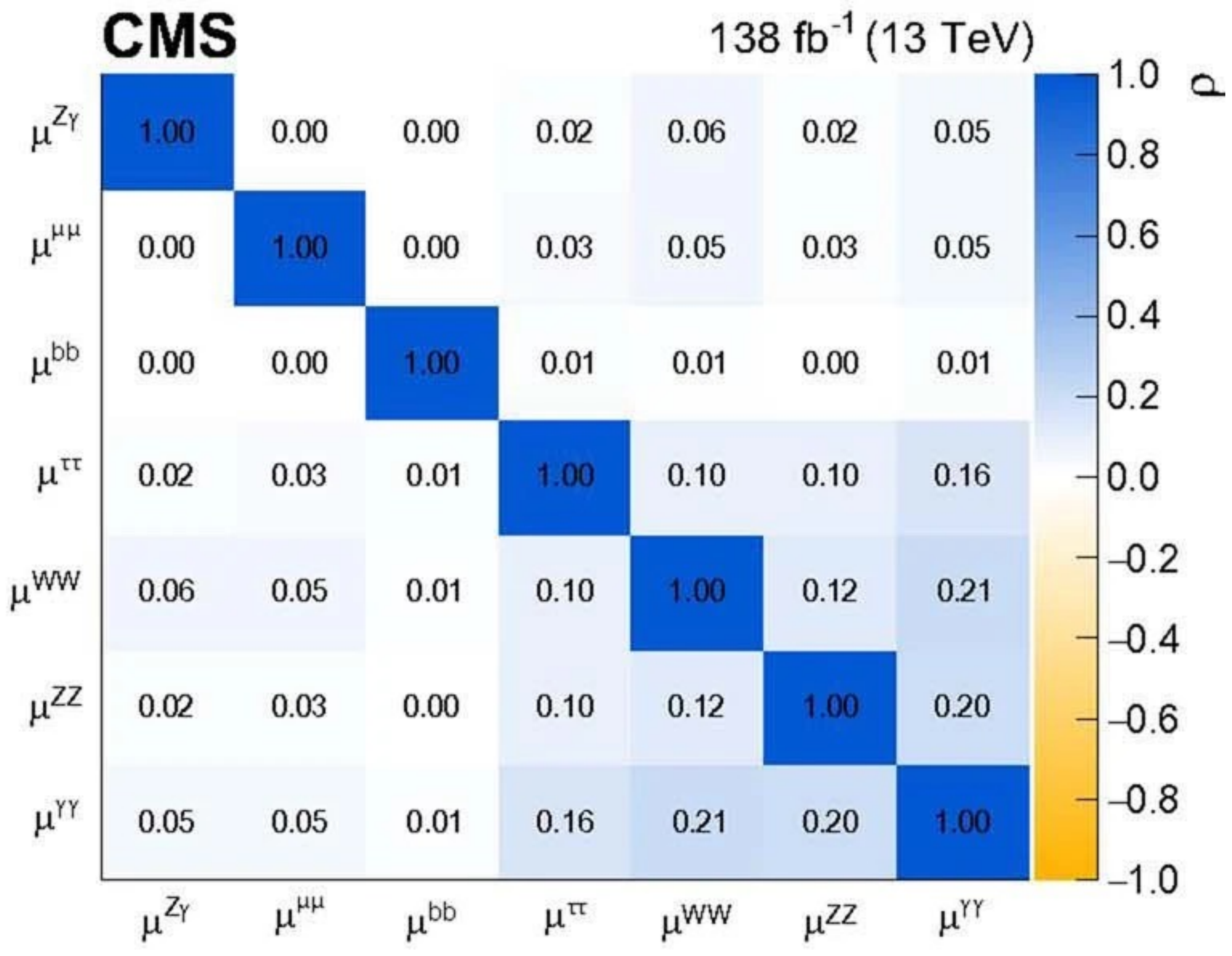

CMS STXS: recent result H→bb

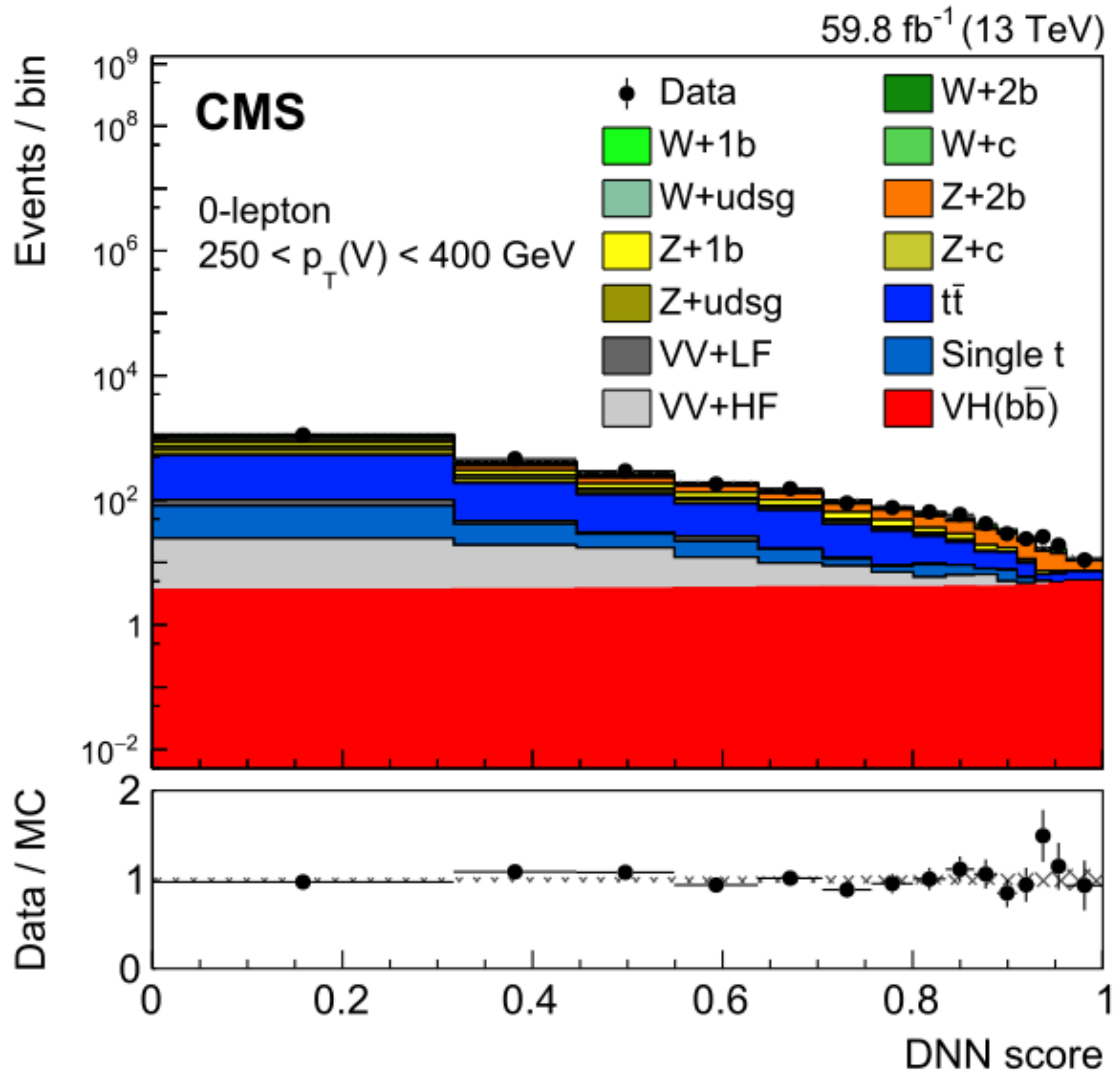

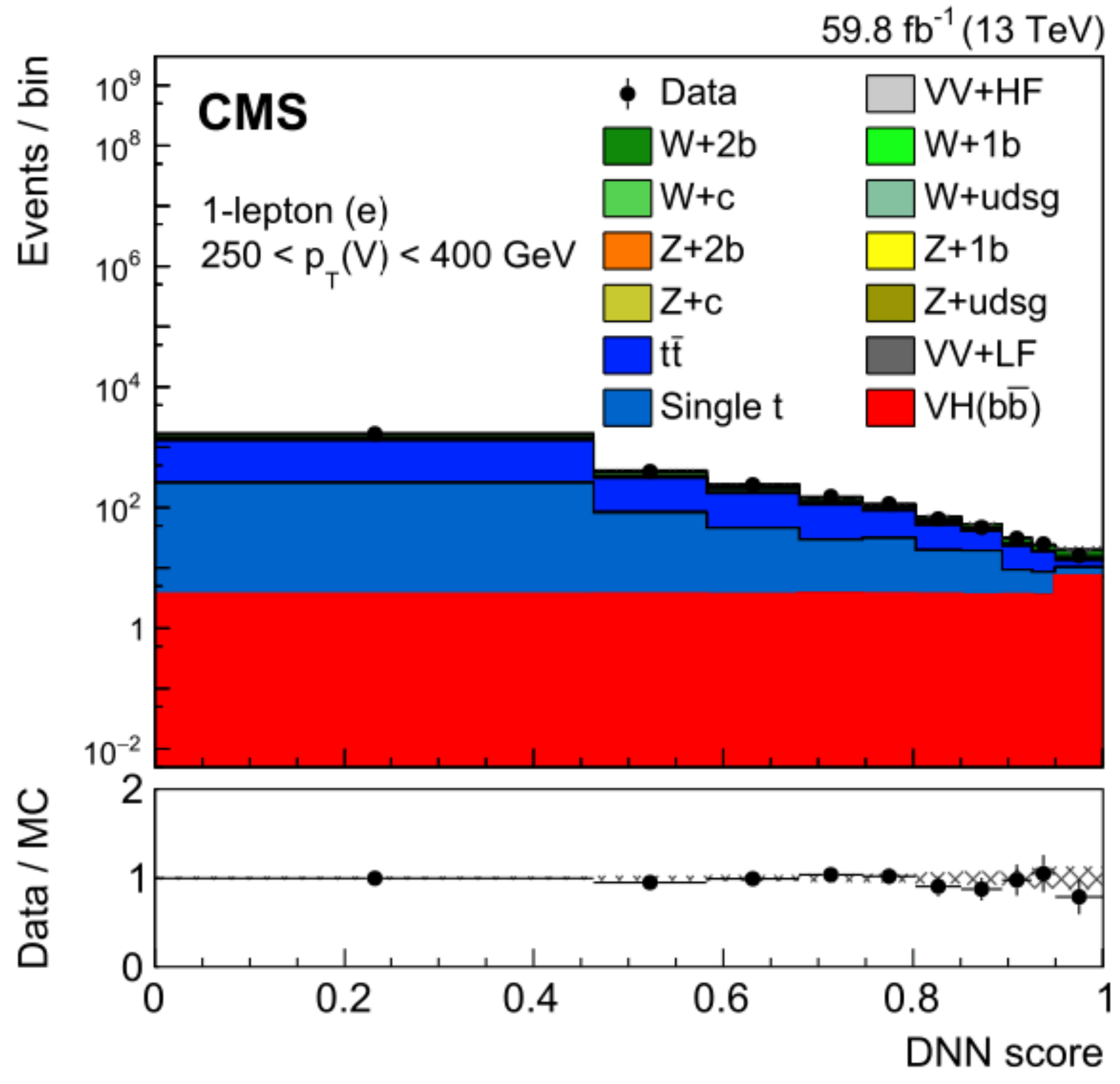

STXS bin	Expected $\sigma\mathcal{B}$ [fb]	Observed $\sigma\mathcal{B}$ [fb]	Best-fit μ
ZH $75 < p_T(Z) < 150$ GeV	50.0 ± 5.3	71 ± 38	1.4 ± 0.8
ZH $150 < p_T(Z) < 250$ GeV 0 jets	9.0 ± 1.4	3.8 ± 4.1	0.4 ± 0.5
ZH $150 < p_T(Z) < 250$ GeV ≥ 1 jets	10.1 ± 2.2	<0	-0.6 ± 1.0
ZH $250 < p_T(Z) < 400$ GeV	4.5 ± 0.9	6.9 ± 2.2	1.5 ± 0.5
ZH $p_T(Z) > 400$ GeV	0.9 ± 0.1	1.6 ± 0.6	1.8 ± 0.8
WH $150 < p_T(W) < 250$ GeV	24.9 ± 1.8	6 ± 16	0.2 ± 0.7
WH $250 < p_T(W) < 400$ GeV	6.3 ± 0.5	11.9 ± 3.8	1.9 ± 0.6
WH $p_T(W) > 400$ GeV	1.4 ± 0.1	2.7 ± 1.1	1.9 ± 0.8

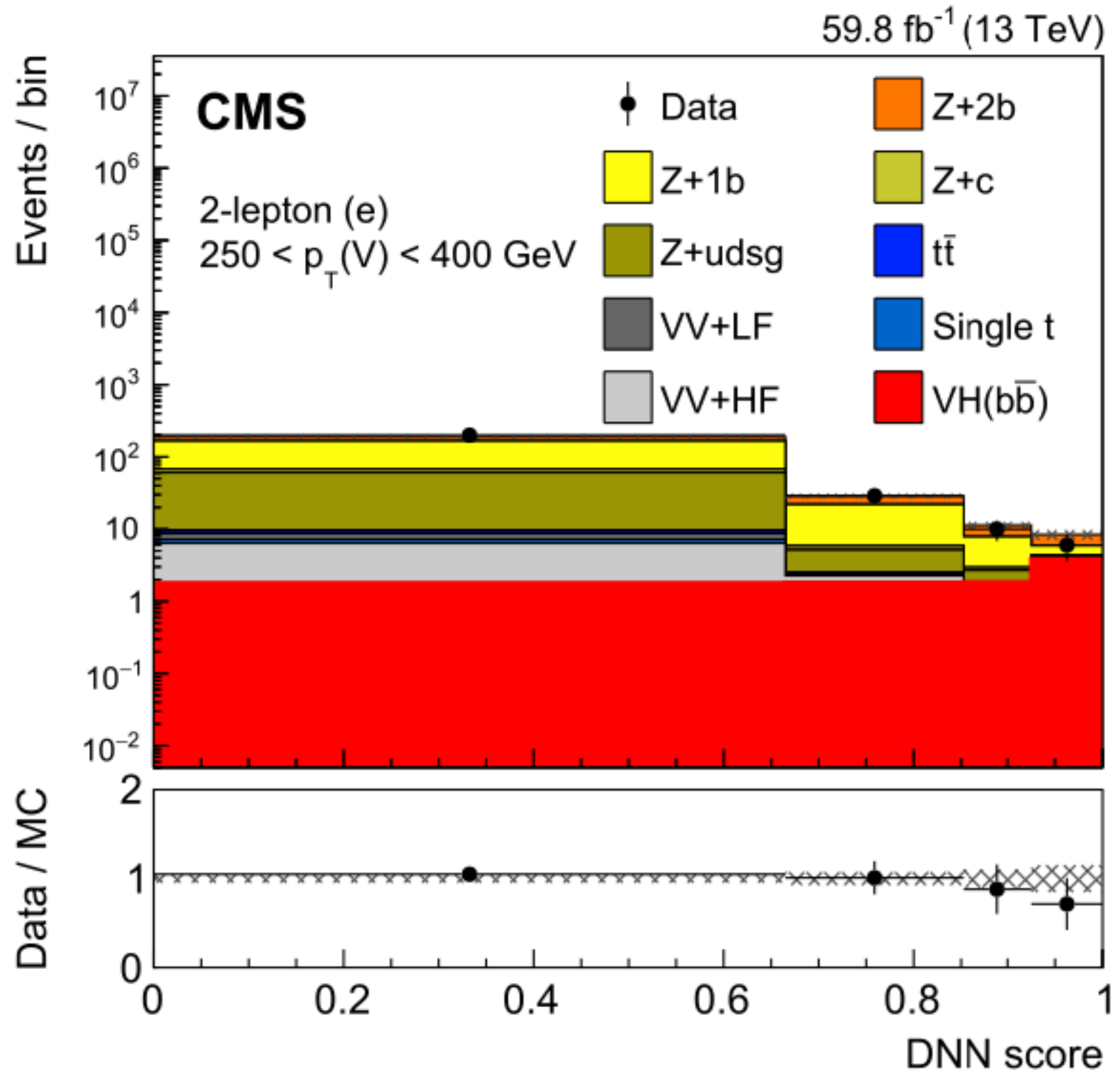

SMEFT interpretation of STXS combination

arXiv:2402.05742 submitted to JHEP

SMEFT linear model result *p*-value: corresponding to **94.5%**

Statistical uncertainty dominates.

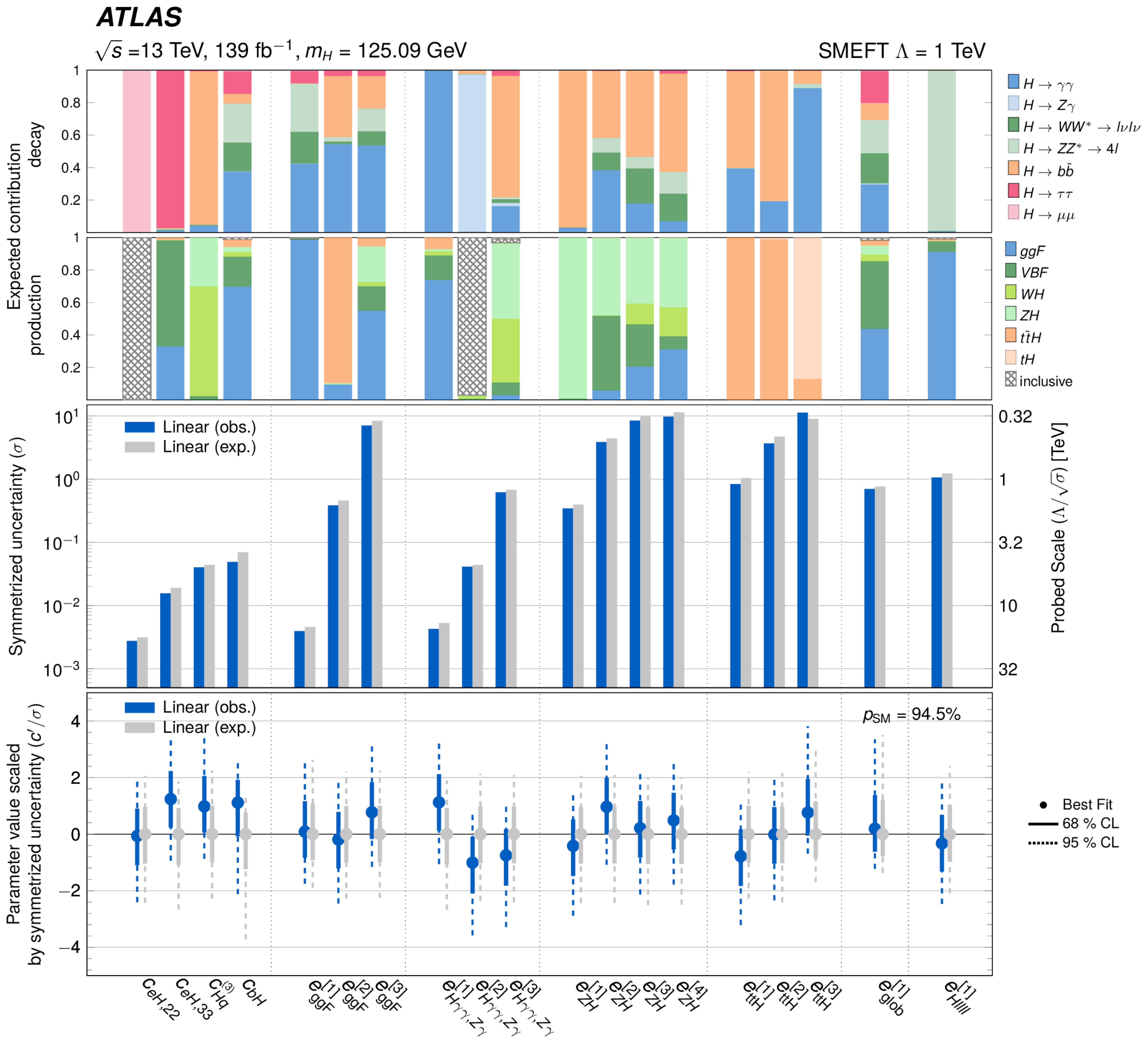

UV-complete models

arXiv:2402.05742 submitted to JHEP

Comparison of the constraints in tanβ, cos(β-α) plane, from the κ- and EFT-interpretations of Higgs boson production and decay rates.

The κ_λ constraint is included in the Type-I model interpretation.